Chemostratigraphic and Mineralogical Examination of the Kilwa Group Claystones, Coastal Tanzania: An Alternative Approach to Refine the Lithostratigraphy

Ross McCabe [a, b*], Christopher J. Nicholas [b], Bill Fitches [c], David Wray [d], Tim Pearce [a]

[a] Chemostrat Ltd, Unit 2 Ravenscroft Court, Buttington Cross Enterprise Park, Welshpool, Powys, UK.

[b] Department of Geology, Trinity College, University of Dublin, Dublin 2, Ireland.

[c] Leeds, W. Yorkshire, UK.

[d] School of Science, University of Greenwich, Chatham Maritime, Kent, UK.

[*]Corresponding author. Tel: +44 (0) 1938 555 330. Email: McCaber2@tcd.ie.

Abstract

The Cretaceous and Paleogene marine sedimentary rocks that crop out along southern coastal Tanzania have been the focus of the Tanzanian Drilling Project (TDP) since 2001. The comprehensive lithological and chronostratigraphic examination of over forty shallow cores by the TDP culminated in the formal definition of the Kilwa Group: a claystone-dominated succession comprising five formations deposited in middle to outer shelf and upper slope marine environments along a passive continental margin. Onshore, the TDP has cored important palaeoclimatic events within the Kilwa Group. Offshore, the group forms the reservoir and seal of several gas fields discovered in southern Tanzania.

The formations of the Kilwa Group cored onshore, have been differentiated from each other largely by variations in subsidiary lithologies (sandstones and limestones), rather than by diagnostic characteristics of their dominant lithology (olive grey claystone). To test and refine the lithostratigraphy of the Kilwa Group, a forensic examination of the claystones using whole-rock inorganic geochemistry, mineralogical analysis and detailed biostratigraphy, is employed in this study.

1210 core samples collected from 20 onshore TDP boreholes and 185 cutting samples acquired from three wells located in offshore in Blocks 1 and 4 are examined by inductively-coupled plasma optical emission spectroscopy and mass spectrometry, whole-rock and clay fraction X-ray diffraction analysis and heavy mineral analysis using Raman spectroscopy. The different methodologies are used to produce a claystone-based chemostratigraphic framework for the Kilwa Group that comprises three sequences, five packages and six units, and links the shallow subsurface rocks onshore to the deep subsurface stratigraphy offshore.

The multidisciplinary geochemical and mineralogical approach reveals that variations in detrital quartz, feldspars (K and Na), heavy minerals, phosphatic minerals and clay minerals (particularly illite, smectite and kaolinite) are key for defining the claystone-based stratigraphy of the Kilwa Group. The variation in the abundance of these mineral through time highlight mostly temporal changes in depositional environment, chemical weathering and sediment provenance that occurred in Tanzania during the Cretaceous and Paleogene.

Integration of the chemostratigraphic framework with detailed biostratigraphic information from the study sections and comparison with the published lithostratigraphy of the Kilwa Group onshore reveals that all three stratigraphic schemes are in broad agreement. Nevertheless, refinements are proposed based on the new chemostratigraphic results. It is suggested here that the top and base of the Kilwa Group is older than previously reported (base–Albian and intra-Rupelian, respectively, rather than the end of both stages) and in most cases, the geochemical data suggests that most of the Kilwa Group formations, as cored onshore, are thinner than formerly proposed. Only the Masoko and Lindi Formations are interpreted to be thicker than previously defined by the TDP.

Key words:

Chemostratigraphy; Lithostratigraphy; Kilwa Group; Provenance; Environment; Climate.

1. INTRODUCTION

Cretaceous and Paleogene (Albian to Oligocene) rocks that were deposited in middle to outer shelf and upper slope marine environments, crop out along stretches of coastal Tanzania, south of Dar es Salaam (**Figures 1** and **2**). The Mandawa and northern Ruvuma coastal basins in which these rocks were deposited, began to form during breakup of Gondwana in the late Triassic and Jurassic Periods (e.g., Kent *et al.,* 1971; Mbede, 1991; Salman & Abdula, 1995; Geiger *et al.,* 2004; Nicholas *et al.,* 2007; Davison & Steel, 2017). The marine rocks examined in this study were deposited during a period of tectonic stability, when a widespread marine transgression advanced across the East African passive continental margin and brought about the deposition of a thick succession of claystones (Pearson *et al.,* 2004 & 2006; Nicholas *et al.,* 2006 & 2007; Berrocoso *et al.,* 2010, 2012 & 2015).

Since 2001, these rocks have attracted the attention of geoscientists interested in understanding climate change over the past 120 million years because of the discovery of exceptionally well-preserved planktonic foraminifer shells in the claystones (Pearson *et al.*, 2001, 2004, 2007, 2008; Nicholas *et al.,* 2006; Berrocoso *et al.,* 2010, 2012, 2015). According to Pearson *et al.* (2004), the shells appear glassy under the reflected light microscope and, under scanning electron microscope, have retained their microgranular textures. Pearson *et al.* (2004) attributed the excellent preservation of the shells to their encasement within claystones whose impermeability inhibited movement of diagenetic fluids. With little or no diagenetic alteration, these shells are considered to have retained their original seawater-derived C and O isotopic composition so are excellent candidates for the accurate determination of palaeoclimate during the Late Cretaceous and Paleogene (Pearson *et al.,* 2001).

Whilst the quality of the foraminifer shells is excellent, the present-day outcrop exposures along the coastal margin are poor and restricted to the shoreline and roadsides (Pearson *et al.*, 2004, 2008). Consequently, the Tanzanian Drilling Project (TDP), an international collective of geoscientists, was assembled in 2001. One of the main objectives of the TDP was to conduct shallow coring of these Cretaceous and Paleogene marine sediments, on which more detailed palaeoclimatic, stratigraphic and palaeoceanographic studies could be based (Pearson *et al.,* 2004).

In total, 40 shallow boreholes have been drilled by the TDP in three main areas between the administrative centres of Kilwa and Lindi (**Figures 1** and **2**). The first 20 boreholes, drilled between 2002 and 2005, retrieved core from Late Cretaceous and Paleogene rocks (see Nicholas *et al.*, 2006, for a comprehensive review). The succeeding twenty TDP boreholes, drilled between 2007 and 2009, retrieved core from progressively older sections (Berrocoso *et al.*, 2010, 2012, 2015; Mweneinda, 2014), though most were drilled to core the Cenomanian-Turonian boundary. The boreholes have penetrated sediments as old as the Barremian-Aptian and possibly older in the basal sandstones of TDP-40A (**Figure 2**).

Among its many achievements, the TDP has cored rare onshore sedimentary successions that span the Paleocene-Eocene Thermal Maximum (PETM) event at the Paleocene-Eocene boundary (c.55.8 Ma - Nicholas *et al.*, 2006; **Figure 2**). The PETM lasted approximately 170 Ka (Röhl *et al.*, 2007), during which time sea temperatures increased abruptly by 5ºC globally and 8ºC locally (Handley *et al.*, 2012). Compared to the other successive hyperthermal events during the Eocene, such as the Eocene Thermal Maximum 2 (ETM2) that occurred around 53.7 Ma and lasted approximately 100 Ka (Stap *et al.*, 2010; **Figure 2**), the PETM experienced the greatest warming sustained over the longest time and, as such, has been extensively studied to understand better the impact of `greenhouse' gas-induced global climate change. Additionally, the Kilwa Group contains the Eocene-Oligocene boundary, which according to Pearson *et al.* (2008), records an episode of global cooling, marking the end of the extended period of predominantly 'greenhouse' conditions on Earth that extended back into the Mesozoic.

The bulk of the sedimentary succession cored onshore corresponds with what was formally defined by the TDP as the Kilwa Group (Nicholas *et al.*, 2006). The group consisted of four formations: Nangurukuru (Santonian to upper Maastrichtian), Kivinje (upper Paleocene to lower Eocene), Masoko (middle Eocene) and Pande (upper Eocene to lower Oligocene). Based on evidence from the more recent cores, Berrocoso *et al.* (2015) considered the group to be as old as Albian and defined a fifth formation at the base called the Lindi Formation (Albian to Coniacian - see **Table 1**).

Claystones are the dominant lithology of all five formations and all were deposited in middle to outer shelf and upper slope marine environments. Nicholas *et al.* (2006) separated the upper four formations by variations in their subordinate and sporadic intercalations of sandstones and carbonates, both of which are rarely more than a metre thick. In contrast, Berrocoso *et al.* (2015) considered that the Lindi Formation is distinguishable from the Nangurukuru Formation by subtle differences in the sedimentary features and colour of the predominant claystones (**Table 1**).

As reflected in **Table 1**, the lithological differences between the formations of the Kilwa Group are subtle and the claystones themselves (with the probable exception of the Lindi Formation claystones) are all broadly similar. This study seeks to test, improve and refine the division of the Kilwa Group claystones using bulk rock elemental chemostratigraphy.

Table 1. Lithological characteristics of the stratigraphic units of the Kilwa Group (after Nicholas *et al.*, 2006 and Berrocoso *et al.*, 2015)

Formations of the Kilwa Group	Main Lithology	Secondary Lithologies	Minimum Thickness (m)
Pande Fm. (upper Eocene to lower Oligocene: Nicholas *et al.*, 2006)	Soft, light olive grey or blue-grey clays, mottled with yellowish orange sandy clays[a]	White, massive, micritic limestones and/or calcarenites, with benthic foraminifera and clay rip-up clasts	202
Masoko Fm. (middle Eocene: Nicholas *et al.*, 2006)	Soft, light olive grey clays, mottled with yellowish orange sandy clays[a]	Orange-brown limestones cemented by sparry calcite, with large *Nummulites*, well-rounded coarse quartz grains, normal grading and cross lamination	173
Kivinje Fm. (upper Paleocene to lower Eocene: Nicholas *et al.*, 2006)	Hard/blocky, olive grey claystones, mottled with yellowish orange, sandy clay[a]	Common sandy partings throughout, occasionally developing into thin, partly cemented calcarenites with small bioclasts	401
Nangurukuru Fm. (Santonian to upper Maastrichtian: Nicholas *et al.*, 2006)	Hard/blocky, olive grey claystones, mottled with yellowish orange, sandy clay[a]	Sporadic, massive, carbonate-cemented, turbiditic sandstones, centimetric to metric in thickness	385
Lindi Fm. (upper Albian to Coniacian: Berrocoso *et al.*, 2015)	Interbeds of dark grey to black claystones and siltstones, with common finely-laminated, possibly organic-rich intervals[b]	Minor occurrences of cm-thick brownish grey, fine to coarse sandstone, generally massive and occasionally top-laminated	194

[a] Colour of weathered sediments

[b] Colour of fresh sediments

Minimum formation thickness calculated from TDP cores

Chemostratigraphy is an interpretative methodology that employs whole-rock inorganic geochemical data to characterise rock units. Chemostratigraphy has long been utilised in the oil and gas industry to address regional and reservoir-level stratigraphic issues (e.g., Pearce *et al.*, 2005; Ratcliffe *et al.*, 2006, 2010, 2012; McCabe *et al.*, 2012, 2018, 2019; Craigie, 2015, 2016; Craigie & Rees, 2016; Craigie *et al.*, 2016; McCabe, 2021; Tansell *et al.*, 2021). The temporal and spatial changes in the geochemical characteristics of clastic sedimentary rocks detected within the framework reflect changes in mineralogy that, themselves, are governed by changes in provenance, climate, depositional environment and diagenetic history. One of the principal advantages in using chemostratigraphy is that variations in chemistry can be detected in successions of otherwise apparently uniform sedimentary rocks, thus making it ideal for studies of the Kilwa Group claystones.

Most TDP boreholes pass through short lengths of the stratigraphy that have, in general, only been correlated locally. As well as being hampered by outcrop quality, demonstration by the TDP of the extent to which the Kilwa Group could be correlated was hindered by the fact that, at the time, there were few hydrocarbon wells drilled in the area that intersected the group. Moreover, it was not the objective of the TDP to tie the onshore stratigraphy to continuous and potentially more complete sedimentary successions encountered in the subsurface. Nicholas *et al.* (2006) noted that the Kilwa Group forms part of the seal rock in the Songo Songo gas field and it is now understood that the group constitutes reservoir and seal rocks in the deep water exploration wells drilled outboard of the TDP study area (Sansom, 2018). Thus, a better understanding of the development and interrelationships of the group between the onshore and offshore areas will contribute to the understanding of the hydrocarbon geology in the region.

To demonstrate these interrelationships, the chemostratigraphic results of three deep water exploration wells, Pweza-1, Taachui-1 and Taachui-1ST, are included in this study (**Figure 3**). These wells, and several others, were analysed by Chemostrat Ltd (2015, 2016 unpublished reports) for BG Group in Blocks 1, 3 and 4 (**Figure 1**) and permission has been granted by Shell, the present operator, to show the results here. Pweza-1 is located within Block 4, approximately 90km NW of Kilwa town and is selected because it intersects a succession of clastic rocks deposited throughout the Paleogene and Cretaceous (Rupelian to Albian). Taachui-1 and -1ST are located within Block 1, approximately 20km from the mainland between the Pande and Lindi areas (**Figure 1**). These wells are included because

they intersect a thick Cretaceous succession (Berriasian to Campanian). For Taachui-1 and -1ST, different parts of the Cretaceous stratigraphy were sampled in each well. Late Cretaceous samples were only available from the Taachui-1 pilot borehole, whereas older rocks were intersected (and sampled) by the side-track. In this study, Taachui-1 and -1ST are spliced together at the Cenomanian-Turonian boundary and treated as one well (see **Figure 3**). A comprehensive biostratigraphic (combined palynology, nannopalaeontology and micropalaeontology) examination of the study wells was conducted by CGG Services UK Ltd (CGG, 2017) and some of the results are incorporated here. Prior to this study, and as far as is known, these wells had not been placed within a formal lithostratigraphic framework. The completeness of the Palaeogene and Cretaceous sedimentary succession encountered in these wells ensures that a comprehensive chemostratigraphic framework for the Kilwa Group can be established between the onshore and offshore areas.

2. METHODS

2.1 SAMPLE COLLECTION

For this study, 1210 samples were collected for geochemical analysis. Samples have been taken from 15 of the first 20 boreholes cored by the TDP (**Figure 2**; **Table 2**). These cores penetrate much of the Paleogene succession, as well as the Campanian and Maastrichtian sedimentary rocks. The successions of Paleogene age are generally well represented in the cores, although there are two c.5 Ma uncored time gaps, one in the Late Eocene (Upper Bartonian and Lower Priabonian Stages) and the other in the Early Paleocene (Lower Selandian and Danian Stages) (**Figure 2**). Sediments deposited during the Late Eocene gap were recorded by Nicholas *et al.* (2006) at outcrop along Kitunda Shore, although the samples from this area were not collected and analysed as part of this study. Despite many attempts at coring them, Early Paleocene rocks have yet to be identified at outcrop or in the shallow subsurface of the Mandawa Basin (Nicholas *et al.*, 2006). A third c.5 Ma uncored time gap is also present in the sediments of lower Campanian age (**Figure 2**).

Samples have also been taken from 6 of the second set of 20 boreholes cored by Berrocoso *et al.* (2010, 2012, 2015; **Figure 2**). These cores are also from successions of Middle – Upper Cretaceous age (Barremian / Aptian to Campanian Stages). Few of the cores sample the Lower Cretaceous, and the Early-Middle Albian (c.7 Ma) is very poorly represented. Only a short (c.8m) interval of Middle Albian (*Ticinella primula* planktonic foraminifera zone) has been intersected, which is in TDP-40 (A&B; **Figure 2**).

The core samples have been collected approximately every metre but due to time constraints, samples from TDP-37 and TDP-39 were collected at approximately ten metre intervals. All the lithologies present in the core intervals were sampled. However, in this study, only the claystones are examined because: 1, claystones are the dominant lithology in the Kilwa Group; 2, unique physical / chemical characteristics of the Kilwa Group claystones have yet to be identified that would support the formation-level lithostratigraphic framework proposed by Nicholas *et al.,* (2006) and Berrocoso *et al.,* (2015); and 3, the subsidiary lithologies are few and unevenly distributed throughout the Kilwa Group sedimentary succession so are of little use for defining lithostratigraphic units and boundaries.

Table 2. Summary of TDP cores sampled for this study.

TDP Core	Sandstone	Claystone	Carbonate	Total
TDP-01	4	44	3	51
TDP-02	1	67	5	73
TDP-03	0	35	0	35
TDP-04	0	6	2	8
TDP-07B	0	99	8	107
TDP-08	1	19	0	20
TDP-09	1	73	0	74
TDP-10	1	90	6	97
TDP-12	2	100	9	111
TDP-13	0	81	4	85
TDP-14	0	20	0	20
TDP-17	8	60	7	75
TDP-18	0	23	1	24
TDP-19	0	38	5	43
TDP-23	1	79	0	80
TDP-24A	5	52	0	57
TDP-31	2	81	2	85
TDP-37	0	51	1	52
TDP-39	0	36	0	36
TDP-40A	16	61	0	77
GRAND TOTAL	42	1115	53	1210

185 ditch cutting samples have been collected and analysed from wells Pweza-1, Taachui-1 and Taachui-1ST (**Table 3**). In contrast to the high-resolution sampling of the cores, the cutting samples were taken approximately every 25 metres in each well (**Figure 3**).

Table 3. Summary of the wells sampled for this study.

Well	Sandstone	Claystone	Carbonate	Total
Pweza-1	17	53	1	71
Taachui-1	19	27	1	47
Taachui-1ST	9	58	0	67
GRAND TOTAL	45	138	2	185

Detailed biostratigraphic analysis of the TDP boreholes cores and study wells has been conducted by the TDP (Pearson *et al.*, 2004, 2006; Nicholas *et al.*, 2006; Mweneinda, 2014; Berrocoso *et al.*, 2015) and CGG (2017) and the zonations are plotted on **Figure 3**. The literature sources for the various planktonic foraminifera and calcareous nannofossil zones employed by the TDP and CGG are presented in **Table 4**. For ease of presentation, CGG converted the Cretaceous calcareous nannofossil zonation scheme of Sissingh (1977), used by them on Pweza-1, Taachui-1 and Taachui-1ST, to that of Burnett (1998), which was used by the TDP (A. Pardon, 2021, *pers. comm.*).

Table 4: Sources of Cretaceous and Paleogene planktonic foraminifera and calcareous nannofossil zonation schemes employed in Tanzania by the TDP (Nicholas *et al.*, 2006; Berrocoso *et al.*, 2015) and CGG (2017).

Period	TDP		CGG	
	Planktonic Foraminifera Zones	**Calcareous Nannofossil Zones**	**Planktonic Foraminifera Zones**	**Calcareous Nannofossil Zones**
Paleogene	Sliter (1989)	Martini (1971)	Blow (1979)	Martini (1971)
	Nederbragt (1991)			
	Gradstein *et al.* (1995)			
	Robaszynski & Caron (1995)			
	Huber *et al.* (2008)			
	Huber & Leckie (2011)			
	Petrizzio *et al.* (2011)			
Cretaceous	Berggren *et al.* (1995)	Burnett (1998)	Robaszynski *et al.* (1979 & 1984)	Sissingh (1977 & 1978)
	Berggren & Pearson (2005)			Perch-Nielsen (1985a&b)

2.2 SAMPLE ANALYSIS

All samples were analysed by inductively-coupled plasma - optical emission spectroscopy (ICP-OES) and inductively-coupled plasma - mass spectrometry (ICP-MS) at the laboratories of Origin Analytical, UK. The sample preparation and analytical protocols employed by Origin Analytical are given in **Appendix 1**. The ICP-OES and ICP-MS analyses yielded quantitative data for ten major elements (Al_2O_3, SiO_2, TiO_2, Fe_2O_3, MnO, MgO, CaO, Na_2O, K_2O, P_2O_5) and thirty-six trace elements (Ba, Be, Cs, Co, Cr, Cu, Ga, Hf, Mo, Nb, Ni, Rb, S, Sc, Sr, Ta, Th, U, V, Y, Zn, Zr) including fourteen rare earth elements (La, Ce, Pr, Nd, Sm, Eu, Gd, Tb, Dy, Ho, Er, Tm, Yb, Lu). For brevity, all the elements are referred to in the text by their appropriate chemical symbol, with the symbols for the major elements being taken to imply oxides, for example, K = K_2O, Al = Al_2O_3 and Mg = MgO.

To support the mineralogical and geological interpretations drawn from the elemental data, 12 claystone core samples were subjected to whole-rock (WR-) and clay fraction (CF-) X-ray diffraction (XRD) analysis and 11 samples have been subjected to heavy mineral analysis (HMA) by Raman spectroscopy (sample positions for each analytical method are presented on **Figure 3**). In both instances, sample selection was guided by the geochemical data and most chemostratigraphic zones are represented in the XRD and HMA datasets. For HMA, multiple claystone core samples had to be combined to obtain a volume of material (c.50g to 100g of rock) that would yield enough heavy minerals for analysis. Heavy mineral (HM) recovery was sufficient in all but two samples: the uppermost Maastrichtian of TDP-37 and the Priabonian of TDP-12 (see **Figure 3**).

XRD analysis and related sample preparations were conducted by X-Ray Minerals Ltd, UK following the procedures described in **Appendix 2**. XRD analysis yielded quantitative data for 14 minerals in the TDP core samples. The most common mineral species included: quartz, calcite, aragonite, orthoclase, plagioclase, muscovite, illite, mixed layer illite+smectite and kaolinite. Accessory minerals included: dolomite, siderite, pyrite, anatase, gypsum and chlorite.

The heavy minerals were separated from the claystone core samples at Origin Analytical, UK and analysed by Raman spectroscopy at the University of Greenwich, UK, following preparation and analytical procedures described in **Appendix 3**. Between 133 and 1103 transparent heavy mineral grains were analysed per sample. In the TDP claystones, recorded heavy mineral species include allanite, anatase, apatite, baryte, brookite, chloritoid, epidote, garnet, kyanite, monazite, pyroxene, rutile, spinel, staurolite, titanite, tourmaline, xenotime, and zircon.

2.3 KILWA GROUP COMPOSITE SECTION

Details of the lithostratigraphy, biostratigraphy and, in many instances, stable isotope chemistry for each of the forty cores taken by the TDP in the coastal Mandawa and Ruvuma Basins were described by Pearson *et al.* (2004, 2006), Nicholas *et al.* (2006), Berrocoso *et al.* (2010, 2012, 2015) and Mweneinda (2014). Nicholas *et al.* (2006) noted that there is no single stratotype section for any of the formations of the Kilwa Group (see also Berrocoso *et al.*, 2015). Consequently, the various formations have been defined by composite stratotype sections following guidelines of the International Subcommission on Stratigraphic Classification (1976). The composite stratotype for the entire Kilwa Group, developed by Nicholas *et al.* (2006) and Berrocoso *et al.* (2015), is illustrated in **Figure 2**.

Using the concept of the composite stratotype, a Kilwa Group composite section (KGCS) is created in this study to illustrate the inorganic geochemical evolution of the Kilwa Group through the Cretaceous and Paleogene Epochs (**Figure 3**). The KGCS consists of multiple TDP cores stacked on each other in chronostratigraphic order with no stratigraphic overlap (interpreted from the detailed biostratigraphic results of each TDP core). All the lithostratigraphic, chronostratigraphic and biostratigraphic information included on the KGCS is taken from Pearson *et al.* (2004, 2006), Nicholas *et al.* (2006) and Berrocoso *et al.* (2010, 2012, 2015). The benefit of this approach is that an appreciable weight of information is displayed simply and effectively. It allows for geochemical trends to be observed in the dataset that are broader than that of individual TDP cores and therefore enables testing of the validity of lithostratigraphic boundaries that are currently in place. The KGCS does not record subsurface depths, rather the cumulative thickness of the Kilwa Group, as currently cored.

A degree of caution is exercised when employing composite sections. Firstly, when stacking separate cores on each other, time breaks are inevitable, as it is unlikely that each successive TDP core in the composite will follow on from the previous one continuously and without any loss of time. Whilst chemostratigraphic boundaries may inadvertently coincide at the boundary between two cores (indicating that the chemostratigraphic boundary has not been cored by the TDP), real unconformities are picked only where they occur within a core.

Secondly, coring bias may have the undesired effect of over-, or under- emphasising the thickness and indeed the lithological composition of key (chemo-) stratigraphic zones. This issue is impossible to mitigate with the available core material collected by the TDP and improvements can only be made through additional shallow coring of key time intervals, particularly in the Paleocene and Early Cretaceous. The detailed biostratigraphic analysis conducted on the TDP cores (**Figures 2** and **3**) shows that most internationally recognised planktonic foraminifera and calcareous nannofossil zones are recorded. Thus, the chemostratigraphic characterisation presented on the composite section in this study is considered as a reasonably comprehensive representation of the Kilwa Group. Further mitigation of coring bias is achieved in this paper by comparison of the KGCS to wells Taachui-1ST and Pweza-1, which have intersected Paleocene and Cretaceous sedimentary successions that have not yet been cored onshore (**Figure 3**).

Finally, lateral variations in geochemical composition of the rocks caused by changes in depositional environment or sediment provenance may occur between cores situated in different localities. These variations may be strong enough to affect the geochemical composition of the sediments, obscuring subtle temporal geochemical trends in cores collected from the same locality. Lateral variations in the geochemical composition of the TDP claystones is not regarded as a strong control on the specific key elements and element ratios utilised to define the chemostratigraphic framework. Most of the cores were cut along the strike of the palaeo-shelf on a passive margin and encountered rocks deposited in closely similar environments (see **Figure 2**). Down - dip variations in the geochemical composition of the TDP claystones is not regarded as a strong control on the key element ratios employed in this study. As will be demonstrated through the integration of the chemostratigraphic framework with the detailed biostratigraphic zonations of the study sections, particularly the wells drilled outboard of the TDP cores (see **Section 4**), all but one of the chemostratigraphic boundaries represent synchronous events. These events, including those that define the top

and base of the Kilwa Group and its formations, are interpreted to reflect temporal variations in climate, depositional environment and / or provenance, rather than lateral changes.

2.4 SYNTHETIC GAMMA (CHEMGR)

In chemostratigraphic studies, a ChemGR trace is often calculated from the K, Th and U chemical data acquired from cuttings samples as a means of cross-checking the validity of material analysed (see Ratcliffe *et al.*, 2010 and Šimíček *et al.*, 2012). The operation involves superimposing the ChemGR on the wireline GR and determining how closely the two log traces match. The closer the match, the more likely it is that the data represents the *in situ* rocks in the subsurface and not contaminants (e.g., caved rock, drilling additive). The operation is demonstrated using the geochemical data acquired from the cuttings from wells Taachui-1, Taachui-1ST and Pweza-1 in **Figure 3**: the close match between the GR and ChemGR traces indicates that the data acquired is representative of the *in situ* rocks in the subsurface. In the Kilwa Group sedimentary rocks analysed (core and cutting samples), claystones have an average ChemGR API value of 102, whereas sandstones and carbonates have average API values of 61 and 35, respectively.

As all the TDP data were acquired from core samples, uncertainties regarding data validity with respect to caving or other contamination are not an issue. Nevertheless, the ChemGR is calculated for all samples to provide a visual representation of lithological variations throughout the KGCS. The ChemGR profile for the KGCS is displayed on **Figure 3**. The high API-equivalent values recorded throughout confirm that claystone is the dominant lithology, although layers with lower API-equivalent values do exist and correspond to limestone and sandstone interbeds. Whilst the equivalent aged sections in the two exploration wells are also generally clay-prone, thicker sand bodies have been intersected throughout the Cretaceous and Paleogene (**Figure 3**).

3. RESULTS & DISCUSSION

3.1 GEOCHEMISTRY & MINERALOGY

A comprehensive examination of all elements acquired by ICP analysis has been conducted and 23 index elements have been identified as key for defining the chemostratigraphic framework of the Kilwa Group. The index elements are Si, Al, Mg, K, Na, P, Zr, Th, Sc, the light rare earth elements (LREEs: La, Ce, Pr, Nd) and the heavy rare earth elements (HREEs: Ho, Er, Tm, Yb, Lu). To understand the geological controls acting on the key elements, their mineralogical affinities must be established (Ratcliffe *et al.* 2012, Craigie, 2015, Craigie & Rees, 2016). In this study, this objective is achieved through direct element-mineral comparisons and statistical modelling of the elemental dataset.

Direct comparison of key major elements to their likely dominant mineral hosts in the TDP claystones is presented as a series of binary diagrams on **Figure 4**. In general, a positive linear relationship is observed between Si and quartz, Ca and Ca-carbonates+gypsum, K and K-feldspar, Na and plagioclase, Al and kaolinite and Fe+Mg and illite+smectite. Craigie (2015) reports that direct comparison or major elements to framework and matrix minerals is usually possible only when the minerals occur in abundances >1% of the bulk rock (i.e., above the limits of analytical detection by XRD analysis). Moreover, comparison of major and trace elements to dominant HMs is less straightforward for several reasons, including differences in preparation and analytical procedures, different HMs having similar trace element chemistries, or chemistries that can be eclipsed by major minerals (e.g., Ca-silicates vs. Ca-carbonates and Al-HMs such as andalusite, sillimanite and kyanite vs. kaolinite, etc.) and the breakdown of chemically unstable heavy minerals to clay. Consequently, whilst HM data is utilised in this study, comparison of major and trace elements to dominant HMs is not attempted.

Sano *et al.* (2007) suggest that whilst direct comparison of elemental and mineralogical data can provide a basic understanding of which minerals are controlling some elements and element ratios, understanding can be enhanced by examining element-element relationships by using principal components analysis (PCA). PCA has been used widely in chemostratigraphic studies to improve understanding of element-element and element-

mineral relationships (Svensden *et al.*, 2007; Ratcliffe *et al.*, 2012; Sano *et al.*, 2013; Craigie, 2015 and references cited therein). PCA reduces the total variability in a dataset to a smaller number of variables known as principal components. Principal component scores, determined from the eigen vectors (EV), are assigned to each sample and can be plotted on a binary diagram. The closer the variables (i.e., elements) plot to one another on the diagram, the more closely they are related in the dataset. By identifying groups of clustered elements, it is possible to infer the minerals or mineral groups that may be controlling them.

The EV1 and EV2 scores for the claystones examined in this study, which account for 37.5% and 13%, respectively, of the total variance in the dataset, are plotted on **Figure 5**. Five broad element groups are observed and are discussed below. The interpretation of the likely mineralogical controls on the various element groups are based on the element-mineral relationships summarised by Salminen *et al.* (2005) and supported by the whole-rock, clay fraction and heavy mineral data acquired on the claystones in this study (see **Figures 4** and **8**).

Group 1: Includes Ca, Sr and Mn. The XRD data presented in **Figure 4** indicates that Ca is associated with Ca-carbonates and gypsum. The close association of Sr and Mn, suggests that these elements are controlled by similar mineral phases.

Group 2: Includes Zr and Hf. This cluster of elements is interpreted to be controlled almost exclusively by zircon, which commonly occurs in all the samples subjected to HM analysis (**Figure 8**).

Group 3: Includes Si only. As demonstrated in **Figure 4**, quartz is the likely dominant host of Si in the claystone dataset.

Group 4: Includes K, Na, Ti, Nb, Ta, Y, P, U, the HREEs and the middle rare earth elements (MREEs: Sm, Eu, Gd, Tb, Dy). This cluster of elements is interpreted to be controlled by a variety of minerals including K- and Na-feldspar, mica, garnet (Y, MREEs and HREEs), apatite (P and U) and rutile (Ti, Nb and Ta). All these minerals are commonly reported in the HM and XRD datasets (see **Figure 8**).

Group 5: Includes Al, Ga, Rb, Cs, Sc, Cu, Co, Be, Th, LREEs, Mg, Fe, Ni and Cr. This cluster of elements is likely controlled by the clay minerals (smectite, illite and kaolinite are common in the claystone XRD dataset) and fine grained REE-phosphate minerals (monazite, florencite, rhabdophane - Laveuf & Cornu, 2009; Berger *et al.*, 2008, 2014).

Based on the element-element relationships considered above and the mineralogical data presented in this study, the dominant key minerals controlling the index elements are presented on **Table 5**.

Table 5: Dominant mineral controls of the key index elements employed in this study.

Element	Dominant Minerals
Si	Quartz
Al	Clay minerals
Mg & Sc	Smectite
K	K-feldspar, mica, illite
Na	Na-plagioclase
Zr	Zircon
Ti	Rutile
P, Th & LREEs	LREE-phosphate minerals (apatite, monazite, rhabdophane)
HREEs	Zircon & garnet

The key elements have been combined to produce the following geochemical ratios: Si/Al, Zr/Th, Th/Sc, P/Al, LREE/HREE and Mg/Al. Element ratios are employed instead of the individual elements to demonstrate stratigraphic changes between minerals and to negate the effects of dilution by carbonates or quartz (Van der Weijden, 2002). The mineralogical significance of these ratios is considered in the following paragraphs and summarised on **Table 6**.

The chemical index of alteration (CIA) developed by Nesbitt & Young (1982) and McLennan *et al.* (1993) is also employed in the Kilwa Group chemostratigraphic framework. The CIA quantifies the degree of weathering of K, Na and Ca silicate minerals and concentration of residual Al in the form of alteration clays in sedimentary rocks relative to the unweathered upper continental crust. The CIA calculation is as follows:

$$CIA= Al_2O_3/(Al_2O_3+K_2O+Na_2O+CaO)x100$$

As presented in **Figure 4**, Ca abundance in the Kilwa Group claystones is overwhelmingly influenced by carbonate and sulphate minerals and not by Ca-silicates. Thus, for this paper, CaO is removed from the CIA calculation and the index reflects the weathering of only the Na and K minerals in the Kilwa Group claystones relative to the upper continental crust. On the relevant figures and in the text, the profile is referred to as CIA (-CaO).

Table 6: Key element ratios and indices employed in this study and their mineralogical interpretation.

Geochemical Ratio / Index	Mineralogical Interpretation: Abundance and Relative Abundance of Minerals
Si/Al	Quartz relative to clay
P/Al	All P-bearing minerals (detrital and/or authigenic) relative to clay
Zr/Th	Zircon relative to Th-bearing minerals (e.g., monazite, apatite, rhabdophane)
Th/Sc	Minerals derived from a felsic source relative to those derived from a ferromagnesian source (see McLennan, 1989; McLennan *et al.*, 1993; Nesbitt & Markovics, 1997)
LREE/HREE	LREE-phosphate minerals (e.g., apatite, monazite, rhabdophane) relative to HREE-rich varieties (e.g., garnet and zircon).
Mg/Al	All Mg-bearing minerals (e.g., smectite & ferromagnesian heavy minerals) relative to kaolinite

As discussed in **Section 3.3**, the chemostratigraphic framework proposed for the Kilwa Group claystones is interpreted to be controlled by a variety of geological factors acting on the sediments prior to, or during deposition. These include the mineralogy of the parent rocks, changes in sediment provenance, chemical weathering and depositional environment. Post-depositional diagenetic processes acting on the claystones is considered minimal in the study area, particularly in the successions cored onshore. These rocks have never been deeply buried and, as interpreted by Pearson *et al.* (2001), the claystones likely inhibited movement of diagenetic fluids, resulting in the excellent preservation of the foraminifer shells throughout the group.

3.2 CHEMOSTRATIGRAPHIC FRAMEWORK OF THE KILWA GROUP

The work presented in this paper builds upon that of McCabe (2021), who demonstrated the chemostratigraphic characteristics of the Kilwa Group, as cored by the TDP, but did not correlate the KGCS to broadly contemporary rocks encountered in the subsurface. McCabe developed a chemostratigraphic framework for the subsurface of the Mandawa Basin that comprised ten chemostratigraphic sequences: four of which are discussed in this paper (see

Table 7). The Kilwa Group itself is largely equivalent to the Middle-Late Cretaceous Sequence (MLC) and Paleogene Sequence (Pg; **Figure 6**).

Table 7: Chemostratigraphic sequences defined in the Mandawa Basin.
(Sequences in bold text are those examined in this paper).

Chemostratigraphic Sequence Name	Abbreviation
Late Paleogene to Neogene Sequence	**LPg-Ng**
Paleogene Sequence	**Pg**
Middle-Late Cretaceous Sequence	**MLC**
Early Cretaceous Sequence	**EC**
Late Jurassic to Early Cretaceous Sequence	LJEC
Middle Jurassic Sequence (a & b)	MJ (a&b)
Early-Middle Jurassic Sequence	EMJ
Early Jurassic Sequence	EJ
Late Triassic to Early Jurassic Sequence	LTEJ

Chemostratigraphic Sequences MLC and Pg are divided into higher resolution chemostratigraphic packages and some of the packages are divided into even higher resolution chemostratigraphic units. The various chemostratigraphic divisions recognised in the Kilwa Group claystones, as well as the key element ratios used to define them and observed minerals / mineral changes supporting the geological interpretations, are described in **Table 8**, and presented on **Figures 6, 7** and **8**.

Table 8: Geochemical and mineralogical characteristics of the claystone-based chemostratigraphic divisions examined in this study.

Sequence	Claystone Characteristics	Package	Claystone Characteristics	Unit	Claystone Characteristics
LPg-Ng	Low Th/Sc values and high CIA (-CaO) values				
	Highest epidote and lowest garnet percentages				
Pg	Highest Th/Sc values, high CIA (-CaO) values. Lowest Si/Al and Zr/Th values.	Pg3	Lower and upwardly decreasing LREE/HREE & Mg/Al values		
			Slight increase in quartz and decrease in kaolinite		
	Low apatite, plus low and upwardly decreasing garnet percentages. Elevated titanite. Presence of epidote	Pg2	High P/Al, Mg/Al and LREE/HREE values. Lower CIA (-CaO) values		
		Pg1	Low P/Al & Mg/Al values. High LREE/HREE values, highest CIA (-CaO) values	Pg1c	low and upwardly increasing P/Al & Mg/Al values
				Pg1b	Lowest P/Al and Mg/Al values
	Elevated kaolinite (kaolinite/K+Na minerals) values than MLC Sequence			Pg1a	low and upwardly decreasing P/Al & Mg/Al values
			Lowest apatite percentages		lowest apatite percentages
			Highest kaolinite values		
MLC	Low Th/Sc values, intermediate CIA (-CaO) values	MLC2	Intermediate LREE/HREE & CIA values		
			Lowest ZTi index		
			Highest calcite values		
	Garnet-dominated heavy mineral assemblage. Apatite percentages higher than Pg Sequence. Epidote is absent	MLC1	Low HREE/LREE & High P/Al values	MLC1c	High Mg/Al values & Low CIA (-CaO) values
	Lower kaolinite (kaolinite/K+Na minerals) values than Pg Sequence			MLC1b	Intermediate Mg/Al and CIA (-CaO) values
					Subtle increase in kaolinite values
				MLC1a	High Mg/Al values & lowest CIA (-CaO) values
EC	Highest Si/Al & Zr/Th values. Lowest CIA (-CaO) & LREE/HREE values				
	Highest apatite percentages. Low garnet percentages				
	Quartz and plagioclase-rich				

3.3 PALAEOGEOGRAPHIC, PALAEOCLIMATIC AND PROVENANCE CONTROLS ON THE CHEMOSTRATIGRAPHIC ZONES

The geochemical and mineralogical evolution of the Kilwa Group is discussed below using the various chemostratigraphic sequences, packages and units as the framework. The palaeogeographic, environmental and palaeoclimatic significance of the key element ratios employed to define the chemostratigraphic framework are also considered here.

3.3.1 EC Sequence

The EC Sequence is the oldest chemostratigraphic sequence discussed in this paper. It is present in TDP-40 and Taachui-1ST but has not been penetrated by Pweza-1 (**Figure 6**). When compared to the succeeding chemostratigraphic sequences, the high Si/Al and Zr/Th values and low LREE/HREE values that characterise the EC Sequence claystones are attributed to an overall abundance of detrital quartz; zircon and other HREE-bearing heavy minerals relative to LREE and Th-bearing minerals and clay minerals. The XRD data confirms that, when compared to all succeeding analysed samples, the claystone analysed from the EC Sequence is the most quartz-rich and clay mineral-depleted (**Figure 8**).

The geochemical and mineralogical composition of the EC Sequence claystones is interpreted to be indicative of a depositional environment of sufficiently high energy to deposit a higher proportion of silt-grade quartz and zircon than the claystones of the succeeding chemostratigraphic sequences and retain a higher proportion of the finer-grained mineral phases in suspension. Based on their geochemical and sedimentological examination of mudrock and siltstone cores from the Wolfcamp and Bone Springs Formations, USA, Driskill *et al.* (2018) offered a similar geological interpretation for the same elemental relationships. Driskill *et al.* demonstrated that siltstones generally had higher Si/Al and Zr values than the mudrocks and that, because of its strong relationship with Al, Th was likely associated with heavy minerals present in the clay size fraction. It is likely, therefore, that the EC Sequence rocks are siltstones that have a higher proportion of coarser grained terrigenous material, whereas the MLC rocks represent mudstones that have a higher proportion of clay minerals and clay-sized heavy minerals. The upward decrease in silt-grade terrigenous minerals observed between the EC and MLC Sequences probably indicates a change in depositional environment.

In the Mandawa Basin, a similar conclusion was reached by Berrocoso *et al.* (2015), who reported that the sediments encountered in TDPs 40A&B were deposited in a proximal marine setting with a relatively high terrigenous input. Indeed, Berrocoso *et al.* suggested that the sandstones encountered in the lower portion of TDP-40A may be indicative of a terrestrial setting, rather than the shallow-marine environments encountered in the middle and upper reaches of the borehole. Berrocoso *et al.* (2010) reported that the energy of deposition throughout most of the cored interval of TDP-24A (downwards from 11m; their 'lithofacies 2') is lower than that of the underlying sediments but still higher than that of younger sediments. Their interpretation is corroborated by the results acquired in this paper, because from the Albian to the end of the Cenomanian in both TDP-24 and the deep water wells, there is an upward decrease in Si/Al and Zr/Th values recorded in the claystones of the KGCS, which is indicative of a gradual decrease in energy leading to a reduction in the proportion of coarse grained detrital minerals (quartz and zircon) within the marine environment (**Figure 6**).

3.3.2 MLC Sequence

The MLC Sequence is the oldest complete chemostratigraphic sequence cored by the TDP boreholes and intersected by wells Taachui-1 & -1ST and Pweza-1. The MLC Sequence equates to the sedimentary rocks deposited during the Albian Stage and the Late Cretaceous. In contrast to the preceding chemostratigraphic sequence, detrital quartz and zircon are lower in abundance in the claystones of the MLC Sequence. This interpretation is supported by the geochemical data (lower Si/Al, and Zr/Th values - **Figure 6**) and XRD data (lower quartz and higher proportion of clay minerals and / or carbonate minerals - **Figure 8**). The geochemical and mineralogical composition of the MLC Sequence claystones is indicative of a depositional environment of sufficiently low energy to impede the transportation and deposition of silt-grade detrital minerals (quartz and zircon) to the outer shelf and upper slope environments and favour the deposition of finer-grained minerals out of suspension.

This environmental interpretation corroborates conclusions reached by Berrocoso *et al.* (2015) and Sansom (2018). Based on sedimentological analysis of the TDP cores, Berrocoso *et al.* reported that the depositional setting of the Lindi Formation claystones was low energy most of the time. Using 3D seismic and well data from the offshore areas covered by Blocks 1, 3 and 4, Sansom considered that a rapid increase in water depths and westward retreat of

continental clastic supply systems occurred during the widespread end-Aptian marine transgression. Thus, the study area rapidly transitioned from a proximal to a distal outer shelf marine environment between Sequences EC and MLC.

3.3.2.1 MLC Packages

Two chemostratigraphic packages are recognised in the MLC Sequence of the KGCS and the deep water wells. The Package MLC1 claystones were deposited during the Albian to early Campanian (calcareous nannofossil zone UC14; **Figure 14**), whereas the Package MLC2 claystones were deposited throughout the remainder of the Cretaceous. The claystones of Package MLC2 have LREE/HREE, CIA (-CaO) values and Mg/Al values between those in the claystones of the preceding package and the succeeding sequence (**Figure 7**). The difference in claystone chemistry is related to a change in the proportion of LREE-bearing minerals relative to HREE varieties and a decrease in felsic minerals and illite+smectite. The decrease in these minerals marks the start of an uninterrupted upward increase in the amount of chemically weathered material being deposited in the marine environment between the Campanian and Thanetian Stages. This weathering interpretation is supported by the XRD results presented in **Figure 8**. Sample TDP-37 (43.81m core depth, 801.87m composite depth) analysed from the Maastrichtian of Package MLC2 contains more kaolinite relative to feldspar (high kaolinite/K+Na mineral values) and illite+smectite than the analysed claystones in the preceding package.

Unlike the more substantial LREE enrichment relative to HREE that occurs in the claystones of Packages Pg1 and Pg2 (see below, this section) which is related to LREE enrichment, a comparison of the chondrite-normalised REE patterns of the TDP claystones with the chondrite-normalised REE patterns of the Post Archaean Australian Shale (PAAS) (Condie, 1993; **Figure 9**) reveals that the fractionation in the Package MLC2 claystones is mainly related to depletion of HREEs and, to a lesser extent, MREEs. The MREEs and HREEs are often enriched in chemically resistant heavy minerals, such as garnet and zircon (Salminen *et. al.*, 2006; Laveuf & Cornu, 2009). Consequently, the depletion in MREEs and HREEs relative to average shale may indicate that these heavy minerals are in low abundance in the Campanian and Maastrichtian rocks because of changes in hydrodynamic sorting, energy and / or sediment provenance.

Using 3D seismic data, Sansom (2018) reported that the high-energy north-flowing contour currents that influenced the depositional architecture of the Albian to Early Campanian sediments between the study area and the Seagap Fault shifted outboard of that structure during the Middle Campanian to Maastrichtian (i.e., during the deposition of the MLC2 claystones). This shift led to an overall decrease in energy in the study area that is likely to account for the change in REE composition of the Kilwa Group claystones during this time.

Based on the heavy mineral data acquired from the MLC Sequence claystones, there is little variation in the percentages of garnet and zircon relative to other recorded heavy minerals in the assemblage that could be used to support the interpretation of the LREE/HREE ratio variation in Package MLC2 (**Figure 8**). However, the zircon-tourmaline (ZTi) index (Morton, 2007) of the heavy minerals acquired from the Kilwa Group claystones, shows that the combined sample from the Maastrichtian interval of TDP-37 has the lowest recorded values in the study interval. According to Morton (2007), the ZTi index reflects differences in hydrodynamic sorting rather than provenance because zircon and tourmaline have different densities (4.7 vs. 3-3.25g/cm^3, respectively: Mange & Maurer, 1992). Thus, the higher proportion of less dense heavy minerals relative to denser species indicates that the energy of environment was probably lower during the deposition of the Package MLC2 claystones than that of the preceding chemostratigraphic package.

MLC1 Units

Package MLC1 is divided into three chemostratigraphic units (MLC1a-c), all of which are recognised in the Kilwa Group composite and the deep water exploration wells (**Figure 7**). The threefold division is based on up-section fluctuations in the Mg/Al and CIA (-CaO) values of the MLC1 claystones, with the lowest and highest values, respectively, encountered in Unit MLC1b. As with the more substantial change in values of these geochemical parameters that defines the package-level division of the MLC Sequence, the fluctuations in Mg/Al and CIA (-CaO) values recorded in the Package MLC1 claystones reflect more subtle changes in chemical weathering episodes during the earlier stages of the Late Cretaceous. The weathering interpretation is supported by the XRD data (**Figure 8**), which shows that kaolinite values are highest in the TDP-31 claystone analysed within Unit MLC1b.

From the chronostratigraphic information of the study intervals, the onset of this earlier (and shorter lived) episode of chemical weathering occurred around the end of the Cenomanian (top *Rotalipora cushmani* planktonic foraminifera zone; **Figure 14**). The decrease in chemical weathering that marks the top of Unit MLC1b is diachronous (the only diachronous chemical boundary observed in this study). In the KGCS and in well Pweza-1, the top of MLC1b is picked in the Santonian / Late Coniacian (base of the *Dicarinella asymmetrica* zone), whereas in well Taachui-1ST, the base of the unit is older and picked within the *Dicarinella concavata* zone (Late Turonian). The diachronous change in chemical weathering observed in the study area during the Late Cretaceous could be related to the location of Taachui-1ST away from the influence of the large Rufiji and Ruvuma river catchments (**Figure 1**). Accordingly, the smaller river systems that drained the Mandawa Basin directly may have transported and deposited less weathered material to the outboard area earlier than in the north and south of the study area. Regardless of the diachronous onset of recovery from chemical weathering, the highest Mg/Al values and lowest CIA (-CaO) values encountered in the claystones on Unit MLC1c occur within the Santonian / Late Coniacian (coincident with the *D. asymmetrica* zone).

3.3.3 Pg Sequence

The Pg Sequence equates to the sediments deposited during the Paleogene up to and including the early Oligocene (Rupelian). Compared to the previous chemostratigraphic sequences, the high(est) CIA (-CaO) values encountered in the claystones of the Pg Sequence (**Figure 6**) reflect a period of intense chemical weathering of rocks in the Tanzanian hinterland that resulted in the deposition of K- and Na-depleted minerals in the marine environment. The chemistry is supported by the XRD data, which shows that all analysed samples from the Pg Sequence have the highest kaolinite and kaolinite/K+Na mineral values (**Figure 8**). The increase in weathering during the greater part of the Paleogene occurs during a time when global marine temperatures were between 10^{o}C and 14^{o}C warmer than the present day (Zachos *et al.*, 2008; Pearson *et al.*, 2001; Handley *et al.*, 2012).

The high Th/Sc and LREE/HREE values of the Pg Sequence claystones correspond to an increase in the abundance of detrital Th-bearing minerals relative to Sc-rich minerals (e.g., pyroxene and smectite - Wilson, 2004; Salminen *et al.*, 2005). Th and Sc are useful for

determining variations in sediment provenance in sedimentary rocks due to their insolubility and immobile character during transport, diagenesis, weathering and metamorphism (e.g., Taylor & McLennan, 1985; McLennan, 1989; Condie, 1993; McLennan *et al.,* 1993; Hofer *et al.,* 2013). The Th/Sc ratio is particularly useful for distinguishing derivation from mafic and felsic source areas because Th is more abundant in felsic crustal rocks and Sc is generally more abundant in mafic rocks (McLennan, 1989). Most Pg Sequence claystones have Th/Sc values above 0.95 (baseline of the blue colour fill – **Figure 6**), maximum values of 1.5 and average values of 1.05, which are interpreted to mark an increase in the contribution of detrital material derived from a predominantly felsic crustal source area.

A change in sediment provenance across the Cretaceous – Palaeogene boundary is, in part, supported by the HM data acquired from the Kilwa Group claystones (**Figure 8**). Whilst garnet dominates the HM assemblage in the Cretaceous claystones of the MLC Sequence, it is generally lower in abundance in the Paleogene claystones of the Pg Sequence. Apatite is also less abundant in the claystones of the Pg Sequence. Conversely, titanite is generally more abundant in the Pg Sequence claystones and minerals such as epidote and kyanite are also present, although the latter two become more prominent in the assemblage during the Eocene.

Similar trends were observed in the HM assemblages of the TDP sandstones examined optically by Fossum *et al.* (2018; **Figure 8**). Based on their work, sandstones with a garnet-dominated heavy mineral assemblage were identified as the most common in the Mesozoic and Cenozoic successions of the Mandawa Basin. Using electron probe micro analysis (EPMA) they also suggested that the garnets indicate derivation from a wide range of sources, including amphibolite and granulite facies metamorphic rocks. Those authors proposed that the garnet-rich sands were likely eroded from parent rocks located in the interior of Tanzania and transported to the study area from the palaeo-Rufiji River to the north.

Fossum *et al.* (2018) also recognised an influx of garnet-depleted and epidote-dominated sandstones during the Eocene and Oligocene (**Figure 8**). As well as lower percentages of garnet in the overall HM assemblage, a reduction in chemical diversity of garnet species (as determined by EPMA) in these sandstones indicates derivation from fewer metamorphic localities. Fossum *et al.* suggested that the epidote-dominated sandstones were likely sourced

from the Masasi Spur and transported to the study area by the Matandu and Mbemkuru Rivers to the west.

The results of the heavy mineral analysis conducted on the Kilwa Group claystones in this study are broadly supportive of the results and conclusions of Fossum *et al.* (2018). However, it is suggested here that the change in provenance from garnet-dominated to epidote- (and titanite-) dominated rocks occurred during the Paleocene (Selandian Stage at least), rather than the Middle Eocene (**Figure 8**).

The chondrite-normalised REE data presented in **Figure 9**, demonstrate that the LREE/HREE fractionation in the Pg Sequence claystones is controlled as much by LREE enrichment as it is by HREE depletion. LREEs are often present in primary minerals that are susceptible to chemical weathering so the LREE-HREE fractionation may also be related to a change in climatic and environmental conditions that increased chemical weathering and erosion of LREE-rich sediments in the hinterland. In this instance, LREE enrichment as a function of weathering is favoured as a stronger control on the LREE/HREE ratio than HREE depletion triggered by changes in environment and provenance. According to Laveuf & Cornu (2009) and Babechuk *et al.* (2014), LREEs are retained (or more retained than MREEs and HREEs) in laterites during *in situ* chemical weathering and the MREEs and HREEs tend to be leached to deeper parts of the profile (Berger *et al.*, 2014). If a change in climatic and environmental conditions in the hinterland caused laterites to be partially eroded, then the resultant material deposited in the offshore area is likely to be LREE rich.

3.3.3.1. Package Pg1

The Pg Sequence is divided into three chemostratigraphic packages. The claystones of Package Pg1 have the lowest P/Al values encountered in the Kilwa Group study interval, indicating that they contain the fewest phosphatic minerals (**Figure 7**). The heavy mineral data acquired on the Kilwa Group claystones support the geochemical results, as they show that apatite values are lowest in Package Pg1 (**Figure 8**). The decrease in detrital apatite may be related to a change in sediment provenance during the Paleocene and Eocene. However, apatite is chemically unstable under some climactic and environmental conditions (Morton & Hallsworth, 1999) and it also possible that the decrease in this mineral is related to a change

in either sediment provenance or climate / environment during the Paleogene.

On balance, it is likely that the decrease in P/Al values observed in the Package Pg1 claystones is controlled by a change in climate and / or environment during the Early Paleogene. The decrease in P/Al values coincides with an increase in global sea level during the Paleocene, reaching a maximum during the early Eocene (**Figure 10**). Indeed, the global sea level curve presented by Miller *et al.* (2005) is largely the inverse of the Si/Al curve. The combination of the geochemical data and sea-level information strongly suggests that the Package Pg1 claystones were deposited in the most distal and / or deeper water environments than those of the preceding sequence and succeeding packages.

Pg1 Units

Package Pg1 is divided into three chemostratigraphic units (Pg1a-c). All three are recognised in Pweza-1, whereas only parts of Units Pg1a and Pg1c have been cored by the TDP (**Figure 7**). The threefold division is based on up-section fluctuations in the Mg/Al and CIA (-CaO) values of the Pg1 claystones. The lowest Mg/Al values and highest CIA (-CaO) values (and lowest and highest values in the entire study interval), are encountered in Unit Pg1b. As with the units of the MLC1 Package, the unit-level change in chemistry of the Kilwa Group claystones is interpreted to reflect a decrease in detrital K-, Na- and Mg-bearing minerals (feldspars and illite+smectite) in response to an increase in chemical weathering of the detrital clastic material prior to deposition in the marine environment.

The claystones from most weathered sources encountered in the Kilwa Group study interval do not coincide with the PETM at 55.5 Ma or the Early Eocene Climatic Optimum (EECO; 53.3 - 49.1 Ma; Inglis *et al.,* 2020; **Figure 2**) but occur during late Selandian (58 - 59 Ma) (**Figure 7**). Indeed, from the upwardly increasing Mg/Al values and upwardly decreasing CIA (-CaO) values throughout Unit P1b, it is argued that during the late Thanetian and early Ypresian (and including the PETM), the claystones of the Kivinje Formation were derived from progressively less weathered sources. Based on the heavy mineral data acquired in this study and by Fossum *et al.* (2018; **Figure 8**), it is likely that the observed upward decrease in chemically weathered material of the Package Pg1c claystones is related to a gradual change in drainage onshore.

These arguments do not imply that the influence of the PETM, EECO and other Eocene thermal maxima (ETM) cannot be observed in the geochemical data. Based on their work on TDP-14, Handley *et al.* (2012), noted an increase in Ti/Al and Si/Al values in the claystones at the PETM and interpreted the data to reflect a period of enhanced terrestrial input related to changes in the hydrological cycle. The same geochemical trends are recognised in the geochemical data acquired for this study (**Figure 11**) and thus support the interpretation of Handley *et al*. Additionally, from the heavy mineral data acquired from the TDP-14 claystones, there is an increase in the Ti-bearing minerals rutile and titanite within the PETM interval (**Figure 8**).

When the CIA (-CaO) and Mg/Al ratios are included and the TDP-14 interval studied by Handley *et al.* (2012) is expanded to include TDPs 7B and 8, several features are observed (**Figure 11**). Firstly, the Ti/Al and Si/Al excursions at the PETM are preceded by an increase in CIA (-CaO) values and a decrease in Mg/Al values, indicating that a weathering episode builds up to, and then terminates at the period of enhanced terrestrial input. Secondly, this trend is not unique and a similarly large increase in chemical weathering that terminates at a period of enhanced terrestrial input occurs within TDP-8 and may relate to the 'Eocene thermal maximum 2', which is the second major, but shorter-lived (<50,000 years), hyperthermal event that occurred around 53.5 million years ago (Sluijs *et al.*, 2009). Thirdly, a series of similar, but even shorter lived and less pronounced events occur throughout TDP-7B and may reflect cyclical oscillations in the hydrological cycle associated with the EECO. These short-lived geochemical features in the CIA (-CaO) and Mg/Al curves that may be influenced by Eocene climatic events are excursions that stand out against decreasing and increasing trends, respectively, which may be related to changes in drainage onshore (**Figure 11**). Indeed, the decrease in CIA (-CaO) values, increase in Mg/Al values, as well as highest proportions of titanite and epidote encountered in the Pg2 claystones that are diagnostic of the package (**Figures 7** and **8**), may represent the period of maximum contribution of detritus from greenschist and amphibolite facies metamorphic rocks during the Paleogene portion of the Kilwa Group.

3.3.3.2. Package Pg2

In the study area, the Package Pg2 claystones were deposited between the Ypresian and Priabonian Stages (**Figure 7**). As discussed in the **Pg1 Units** section above, the subtle decrease in CIA (-CaO) values and increase in Mg/Al and P/Al values of the Package Pg2 claystones, corresponds to an influx of minerals (feldspars, phosphates, illite+smectite) that were probably derived from a local metamorphic source area in the Tanzanian hinterland that is also rich in titanite and epidote but depleted in garnet (**Figure 8**).

3.3.3.3. Package Pg3

The decrease in LREE/HREE values in the Package Pg3 claystones is indicative of a change in climatic and / or environmental conditions that contributed to an overall reduction in chemical weathering, transportation and deposition of (L)REE-rich material from the hinterland to the study area. The decrease in LREE/HREE values coincides with the decrease in sea surface temperatures inferred by Pearson *et al.* (2007) in the late Eocene and early Oligocene, which further supports the argument that the REE fractionation in the Kilwa Group claystones is, at least in part, climate controlled. Additionally, Jacobs (2004) noted that, across many parts of Africa, palaeobotanical data suggests a re-establishment of forested areas during the late Eocene. That reforestation may have led to greater stabilisation of soil in the hinterland, leading to decreased soil erosion.

Throughout Package Pg3 in TDP-12, there is a general upward increase in Si/Al and Zr/Th values that, as mentioned above in this section, is likely to reflect an increase in energy of the marine environment favouring the deposition of silt-grade detrital minerals over finer-grained Al-silicate and clay minerals (**Figure 6**). The increase is probably related to a change to more shallow / proximal marine conditions triggered by eustatic sea level drop (Miller *et al.* 2005 - **Figure 10**). Indeed, Nicholas *et al.* (2006) attributed the Pande Formation claystones to a shallower marine environment than that of the claystones of the preceding formations.

A rapid but short-lived increase in Si/Al and Zr/Th values are recorded in the claystones of the upper 25m of TDP-12, throughout much of TDP-17 and may be represented by the only Package Pg3 claystone analysed in Pweza-1 (**Figures 6** and **12**). The change in chemistry is, again, related to an increase in silt-grade detrital quartz and zircon relative to finer-grained

Al-silicate and clay minerals and likely controlled by an increase in hydrodynamic energy of the marine environment. The change in energy occurs during the Rupelian and coincides with the early Oligocene glacial maximum that marks the transition from the Eocene into the Oligocene (Pearson *et al.*, 2008). Despite a sample gap in TDP-17 (**Figure 12**), the increase in Si/Al and Zr/Th values coincides with the second step in δ18O stable isotope values recorded by Pearson *et al.* (2008) and Lear *et al.* (2008), which they attribute to ice-sheet advance over the poles. Claystones with similarly high Si/Al and Zr/Th values are not present in TDP-1 (see the LPg-Ng Sequence of the KGCS on **Figure 6**), which suggests that the period of high energy was short-lived and did not continue later into the Rupelian Stage.

3.3.4. LPg-Ng Sequence.

The claystones of the LPg-Ng Sequence record low Th/Sc and LREE/HREE values that are interpreted to record a decrease in the abundance of detrital Th-bearing minerals during the late Paleogene and Neogene. This chemical signature highlights a change in sediment provenance, perhaps returning to something similar to that during the deposition of the MLC Sequence sediments. Although the LPg-Ng Sequence is poorly defined in the TDP cores, upper Oligocene and Miocene claystones with a similar chemical composition have been analysed by McCabe *et al.* (2012) in the Ruvuma Basin, which demonstrates that the LPg-Ng Sequence is both temporally and laterally extensive along the Tanzanian coastal margin. It is hypothesised here that the trigger for the change in provenance is the onset of tectonic activity associated with the East African Rift System (possibly the onset of the EARS 1 rifts described by Macgregor, 2014).

3.4 CHEMOSTRATIGRAPHY, LITHOSTRATIGRAPHY & BIOSTRATIGRAPHY

The chemostratigraphic framework has been integrated with the detailed biostratigraphic zonation schemes assigned to the TDP boreholes and deep water wells (**Figure 13**). The stratigraphic frameworks derived from these two approaches match at a biozone level and demonstrate that all but one of chemostratigraphic boundaries represent synchronous events in Tanzania during the deposition of the Kilwa Group sediments. The integration of the chemostratigraphic, biostratigraphic and lithostratigraphic schemes for the Kilwa Group are presented in **Table 9**.

Table 9: Comparison of the chemostratigraphic and lithostratigraphic framework for the Kilwa Group presented in this paper with the planktonic foraminifera and calcareous nannofossil zones identified in the study interval.

Lithostratigraphy		Chemostratigraphy			Top / Base	Planktonic Foraminifera Zone		Calcareous Nannofossil Zone	
Group	**Formation**	**Sequence**	**Package**	**Unit**					
Kilwa	Pande	Pg	3		T.	**T.** P18		**T.** NP21	
					B.	**T.** P15		NP18 (?)	
	Masoko		2		T.				
					B.	**T.** P6b		**T.** NP11	
	Kivinje		1	c	T.				
					B.	**T.** P4b (?)		**I.** NP9a	
				b	T.				
					B.	**T.** P4a(?)		**I.** NP6	
				a	T.				
					B.	**T.** *A mayaroensis*		**T.** UC20	
	Nangurukuru	MLC	2		T.				
					B.	**T.** *D. asymmetrica*		**B.** UC14	
	Lindi		1	c	T.				
					B.	**B.** *D. asymmetrica*	**B.** *D. concavata:* (Taachui)	**I.** UC10	**I.** UC9 (Taachui)
				b	T.				
					B.	**B.** *W. archaeocreta*		**I.** UC4	
				a	T.				
					B.	**B.** *M. Rischi*		**B.** BC22	

T. = Top, **B.** = Base, **I.** – Inter.

One of the objectives of this study is to compare the chemostratigraphic framework established here with the lithostratigraphy of the Kilwa Group and its associated formations proposed by Nicholas *et al.* (2006) and Berrocoso *et al.* (2015) on the TDP boreholes. **Figure 14** presents the comparison and reveals that overall, there is a good match between the chemostratigraphic and lithostratigraphic schemes. Even so, refinements to the lithostratigraphic scheme are proposed based on the chemostratigraphy and biostratigraphy.

Nicholas *et al.* (2006) proposed that the Kilwa Group spanned a c.55 Ma interval of time, covering the Santonian to Rupelian and Berrocoso *et al.* (2015) extended the base of the group to the Upper Albian. However, it is suggested that the Kilwa Group spans the whole of the Albian to middle Rupelian Stages (c.83 Ma.). Accordingly, the Kilwa Group is equivalent to chemostratigraphic Sequences MLC and Pg, the claystones of which are interpreted to have been deposited during the period of maximum transgression in the passive margin tectonic phase.

The base of the Kilwa Group is picked at c.8m in TDP-40, which corresponds to the Aptian – Middle Albian unconformity identified biostratigraphically by Mweneinda (2014) and Berrocoso *et al.* (2015). The revised interpretation, based on the inorganic geochemical data, suggests that the MC Sequence rocks encountered in TDP-40, Taachui-1 and -1ST correspond to the underlying Mavuji Group (Hudson, 2010; Fossum *et al.,* 2021; McCabe, 2021).

The suggested revision of the top of the Kilwa Group corresponding with the top of the Pg Sequence is closely comparable to that originally interpreted by Nicholas *et al.* (2006). Both the lithostratigraphic and chemostratigraphic results place the termination within the lower Oligocene. However, it is suggested here that the top is placed at the top of the NP21 calcareous nannofossil zone rather that the top of the NP23 zone. The revised interpretation, based on the inorganic geochemical data, would suggest that TDP-1 represents the earliest sediments of a new group of formations (the 'Songo Songo Group' of Hudson, 2010 and Fossum *et al.,* 2021) that continue through the remainder of the Oligocene Epoch and probably into the Neogene Period.

In this study, the Lindi Formation equates to Package MLC1. Based on the inorganic geochemical data, the top of the formation extends into the Campanian Stage (base of nannofossil zone UC15b – although in the deep water wells, the base occurs in the UC14 zone, which has not been cored by the TDP). The result of the proposed revision of the Lindi Formation is that the Nangurukuru Formation would equate to Package MLC2 and is restricted to most of the Campanian and Maastrichtian Stages only (**Figure 14**).

The placement of the top of the Lindi Formation into the Campanian conflicts with the interpretation of Berrocoso *et al.* (2015), who picked the boundary within the Coniacian-Santonian interval of TDP-39 (between core parts 28-30 and around the top of the *D. concavata* zone). Using carbonate data acquired from stable isotope analysis, Berrocoso *et al.* placed the formation top at the base of a sharp $CaCO_3$ increase in the TDP-39 claystones and argued that the Nangurukuru Formation is generally more calcareous than the Lindi Formation. Whilst the $CaCO_3$ data acquired for this study is broadly supportive of the interpretations made by Berrocoso *et al.,* the $CaCO_3$ trend is not consistent between the two formations in the TDP cores and in the deep water wells. The Campanian sediments encountered in TDP-23 (assigned to the Nangurukuru Formation by Berrocoso *et al.,* 2015) also have low $CaCO_3$ values (**Figure 15**). Additionally, McCabe (2021) reported that age-equivalent outcrops to the Lindi Formation in the Mandawa Basin are not consistently calcareous either but do have similar REE signatures that are consistently definitive of Package MLC1. Thus, it is argued here that the REEs provide a more consistent means of differentiating the Lindi and Nangurukuru claystones and not $CaCO_3$, which appears more variable.

Nicholas *et al.* (2006) placed the top of the Kivinje Formation within a 10m interval (between 53-62m) in TDP-2. The interval marks the first appearance of large benthic foraminiferal coquinas, which are characteristic of the Masoko Formation, and a change in hardness of the clay. In this study, the Kivinje Formation equates to Package Pg1 and is slightly thinner than that proposed by Nicholas *et al.* (2006). The geochemical data picks a strong boundary between TDPs 2 and 3 and suggests that the true chemostratigraphic boundary lies somewhere between nannofossil zones NP11 and NP14 (**Figure 14**). The integration of the chemostratigraphic and biostratigraphic results from well Pweza-1 support this lithostratigraphic assignment. In both the well and TDP boreholes, calcareous nannofossil zones NP12 and NP13 are absent. In addition, the boundary marks the change in depositional environment associated with the Kivinje (most distal marine) and Masoko (more proximal marine) Formations. Acceptance of Package Pg1 as representing the Kivinje Formation would make the formation slightly thinner than originally defined.

Finally, Package Pg2 is interpreted to correspond to the Masoko Formation, whereas Package Pg3 is interpreted to equate to the Pande Formation (**Figure 14**). The revised boundary between the two formations is picked within TDP-12, rather than the top of TDP-4 (i.e., within the Priabonian Stage, rather than at the Bartonian / Priabonian boundary). The proposed revision makes the Pande Formation half as thick as that proposed by Nicholas *et al.* (2006) (100m vs. 210m), whereas the Masoko Formation is approximately a third thicker (248m vs. 170m) than that inferred by Nicholas *et al.* (2006).

4. CONCLUSIONS

Despite their broadly uniform sedimentological characteristics, it is demonstrated in this study that the thick succession of outer shelf and upper slope marine claystones deposited in the Mandawa and Ruvuma Basins, southern Tanzania, between the Albian and Rupelian Stages are chemically and mineralogically diverse. The largely temporal variations in the abundance of the key elements Si, Al, K, Na, Mg, Th, Zr, P, Sc and the REEs are used here to define the upper and lower boundaries of the Kilwa Group and its five formations first distinguished by the Tanzania Drilling Project (TDP). The distinct chemical signatures of the various lithostratigraphic units and sub-formational chemostratigraphic units are controlled by the changes in the proportions of detrital quartz, K- and Na-feldspars, heavy minerals and REE-phosphate minerals.

The geological interpretations drawn from the geochemical and mineralogical datasets are consistent with previous interpretations that the claystones of the Kilwa Group were deposited in a low energy and distal marine environment throughout its c.83 million year duration. These claystones contain fewer silt-grade detrital minerals (mainly quartz and feldspars) and a higher proportion of clay and authigenic minerals than the more proximal marine claystones of the preceding and succeeding lithostratigraphic groups. Within this relatively uniform depositional environment, the chemistry and mineralogy of the fine-grained material entering the study area changes over time in response to climatically influenced chemical weathering of rocks in the Tanzanian hinterland and shifts in drainage patterns. In the Mandawa Basin, the influence of chemical weathering is greatest in the Paleocene, rather than at the Paleocene-Eocene Thermal Maximum or during the Early Eocene Climatic Optimum. This is because there is a provenance overprint on the geochemistry of the Eocene claystones that reflects the influx of relatively unweathered material from local greenschist and amphibolite facies metamorphic parent rocks, which were most likely sourced from the Masasi Spur.

A primary objective of this study has been to test the established lithostratigraphy of the Kilwa Group in the TDP borehole type sections drilled onshore. Integration of the chemostratigraphic framework with detailed biostratigraphic information from the study sections and comparison with the published lithostratigraphy of the Kilwa Group reveals that

all are in broad agreement. The various formations are largely equivalent to their respective chemostratigraphic package. The results presented here are consistent with previous interpretations that the Lindi Formation sediments were deposited during the Albian to the Campanian and those of the Nangurukuru Formation belong to the remainder of the Late Cretaceous. Also in agreement with TDP, it is concluded that in the Paleogene, the Kivinje Formation sediments were deposited during the Danian through to the Ypresian, those of the Masoko Formation are Ypresian and Priabonian, whilst the Pande Formation is Priabonian and Rupelian in age. In most cases, the inorganic geochemical data suggests that most of the Kilwa Group formations, as cored onshore, are thinner than formerly proposed. Only the Masoko and Lindi Formations are interpreted to be thicker than that previously defined by the TDP.

The development of a robust multidisciplinary stratigraphic framework for the sedimentary rocks deposited in the Mandawa and Ruvuma Basins between the Albian and Rupelian Stages will undoubtedly help with hydrocarbon exploration and development in both the onshore and deep offshore areas. The changes in eustacy, tectonism, global climate and regional drainage patterns that have influenced the mineralogy of the Kilwa Group claystones will allow geologists to understand better the source to sink relationships of the detrital material and improve recognition of stratigraphic horizons within the group that are more likely to produce high quality reservoir facies in the subsurface.

ACKNOWLEDGEMENTS

The authors are extremely grateful to the Tanzanian Petroleum Development Corporation (TPDC) for arranging sampling and sample exportation on several occasions. We are also grateful to Shell (Arjan Van Vliet and Jimmy Van Itterbeeck) for permitting us to include the Block 1 and 4 wells in this paper. We would also like to thank Andrea Pardon from CGG for assisting the authors with the integration and standardisation of the deep water wells and TDP biostratigraphic results. Finally, we acknowledge our partners and colleagues at the University of Greenwich, Origin Analytical Ltd, and X-Ray Minerals Ltd for their help generating the data presented in this paper.

REFERENCES

Babechuk, M. G., Widdowson, M., Kamber, B. S., 2014. Quantifying chemical weathering intensity and trace element release from two contrasting basalt profiles, Deccan Traps, India. Chemical Geology 363, 56 - 75.

Berger, A., Gnos, E., Janots, E., Fernandez, A., Giese, J. 2008. Formation and composition of rhabdophane, bastnäsite and hydrated thorium minerals during alteration: implications for geochronology and low-temperature processes. Chemical Geology 254, 238 - 248.

Berger, A., Janots, E., Gnos, E., Frei, R., Bernier, F., 2014. Rare earth element mineralogy and geochemistry in a laterite profile from Madagascar. Applied Geochemistry 41, 218 - 228.

Berggren, W. A., Kent, D. V., Swisher, C. C., Aubrey, M. P., 1995. A revised Cenozoic geochronology and chronostratigraphy. In: Berggren, W. A., Kent, D. V., Aubry, M., & Hardenbol, J. (Eds.), Geochronology, Time Scales and Global Stratigraphic Correlation. SEPM Special Publication 54, 129 - 212.

Berggren, W. A., Pearson, P. N., 2005. A revised subtropical Paleogene planktonic foraminiferal zonation. Journal of Foraminiferal Research 35, 279 - 298.

Berrocoso, A. J., Macleod, K. G., Huber, B. T., Lees, J. A., Wendler, I., Bown, P. R., Mweneinda, A. K., Londoňo, C. I., Singano, J. M., 2010. Lithostratigraphy, biostratigraphy and chemostratigraphy of Upper Cretaceous sediments from southern Tanzania: Tanzania drilling project sites 21 - 26. Journal of African Earth Sciences 57, 47 - 69.

Berrocoso, A. J., Huber, B. T., Macleod, K. G., Petrizzo, M. R., Lees, J. A., Wendler, I., Coxall, H., Mweneinda, A. K., Falzoni, F., Birch, H., Singano, J. M., Haynes, S., Cotton, L., Wendler, J., Bown, P. R., Robinson, S. A., Gould, J., 2012. Lithostratigraphy, biostratigraphy and chemostratigraphy of Upper Cretaceous and Paleogene sediments from southern Tanzania: Tanzania Drilling Project Sites 27 - 35. Journal of African Earth Sciences 70, 36 - 57.

Berrocoso, A. J., Huber, B. T., Macleod, K. G., Petrizzo, M. R., Lees, J. A., Wendler, I., Coxall, H., Mweneinda, A. K., Falzoni, F., Birch, H., Haynes, S., Bown, P. R., Robinson, S. A., Singano, J. M., 2015. The Lindi Formation (upper Albian – Coniacian) and Tanzanian Drilling Project sites 36-40 (lower Cretaceous to Paleogene): lithostratigraphy, biostratigraphy & chemostratigraphy. Journal of African Earth Sciences 101, 282 - 308.

Blow, W. H., 1979. The Cainozoic Globigerinida: a study of the morphology, taxonomy, evolutionary relationships and the stratigraphical distribution of some Globigerinida (mainly Globigerinaceae). E.J. Brill, Leiden, 1413.

Burnett, J. A., 1998. Upper Cretaceous. In: Bown (Eds.), Calcareous Nannofossil Biostratigraphy. British Micropalaeontological Society Series, Chapman & Hall: Kluwer Academic Press, 132–199.

CGG Services UK Ltd, 2017. Offshore Tanzania Blocks 1-5: Regional stratigraphic study of selected wells. Unpublished report No. 7422/Ib prepared for BG Group.

Chemostrat Ltd, 2015. Integrated chemostratigraphic & provenance study on selected wells from Blocks 1, 3 and 4. Offshore Tanzania. Unpublished report prepared for BG Group.

Chemostrat Ltd, 2016. Integrated chemostratigraphic & provenance of the sedimentary basins along coastal Tanzania: Phase 2. Unpublished report prepared for BG Group.

Condie, K. C., 1993. Chemical composition and evaluation of the upper continental crust: contrasting results from surface samples and shales. Chemical Geology 104, 1 - 37.

Craigie, N. W., 2015. Applications of chemostratigraphy in Cretaceous sediments encountered in north central Rub' al Khali Basin, Saudi Arabia. Journal of African Earth Sciences 104, 27 - 42.

Craigie, N. W., 2016. Chemostratigraphy of the Silurian Qusaiba Member, eastern Saudi Arabia. Journal of African Earth Sciences 113, 12 - 34.

Craigie, N. W., Rees, A. J., 2016. Chemostratigraphy of glaciomarine sediments in the Sarah Formation, northwest Saudi Arabia. Journal of African Earth Sciences 117, 263 - 284.

Craigie, N. W., Breuer, P., Khidir, A., 2016. Chemostratigraphy and biostratigraphy of Devonian, Carboniferous and Permian sediments encountered in eastern Saudi Arabia: an integrated approach to reservoir correlation. Marine and Petroleum Geology 72, 156 - 178.

Davison, I., Steel, I., 2017. Geology and hydrocarbon potential of the East African continental margin. Petroleum Geoscience 24, 57 - 91.

Driskill, B., Pickering, J., Rowe, H. E., 2018. Interpretation of high resolution XRF data from the Bone Spring and Upper Wolfcamp, Delaware Basin, USA. Unconventional Resources Technology Conference Paper 2901968, 1 - 25.

Fossum, K., Morton, A. C., Dypvik, H., Hudson, W. E., 2018. Integrated heavy mineral study of Jurassic to Paleogene sandstones in the Mandawa Basin, Tanzania: sediment provenance and source to sink relations. Journal of African Earth Sciences 150, 546 - 565.

Fossum, K., Dypvik, H., Haid, M. H. M., Hudson, W. E., Van Den Brink, M., 2021. Late Jurassic and Early Cretaceous sedimentation in the Mandawa Basin, coastal Tanzania. Journal of African Earth Sciences 174.

Geiger, M., Clark, D. N., Mette, W., 2004. Reappraisal of the timing of the breakup of Gondwana based on sedimentological and seismic evidence from the Morondava Basin, Madagascar. Journal of African Earth Sciences 38, 363 - 381.

Gradstein, F. M., Agterberg, F. P., Ogg, J. G., Hardenbol, J., Van Veen, P., Thierry, J., Huang, Z., 1995. A Triassic, Jurassic, and Cretaceous time scale. In: Berggren, W. A., Kent, D. V., Aubry M., & Hardenbol, J. (Eds.), Geochronology, Time Scales and Global Stratigraphic Correlation. SEPM Special Publication 54, 95 - 126.

Handley, L., O'Halloran, A., Pearson, P. N., Hawkins, E., Nicholas, C. J., Schouten, I. K., McMillan, I. K., Pancost, R. D., 2012. Changes in the hydrological cycle in tropical East Africa during the Paleocene-Eocene Thermal Maximum. Paleogeography, Paleoclimatology, Paleoecology 329-330, 10 - 21.

Hofer, G., Wagreich, M., Neuhuber, S., 2013. Geochemistry of fine-grained sediments of upper Cretaceous to Paleogene Gosau Group (Austria, Slovakia): Implications for paleoenvironmental and provenance studies. Geoscience Frontiers 4, 449 - 468.

Huber, B. T., Macleod, K. G., Tur, N. A., 2008. Chronostratigraphic framework for Upper Campanian–Maastrichtian sediments on the Blake Nose (subtropical North Atlantic). Journal of Foraminiferal Research 38, 162 - 182.

Huber B. T., Leckie, R. M., 2011. Planktic foraminiferal species turnover across deep sea Aptian/Albian boundary section. Journal of Foraminiferal Research 41, 53 - 95.

Hudson, W. E., 2010. The geological evolution of the petroleum prospective Mandawa Basin. Southern coastal Tanzania. Unpublished Ph.D. thesis. Trinity College Dublin.

Inglis, G. N., Bragg, F., Burls, N. J., Cramwinckel, M. J., Evans, D., Foster, G. L., Huber, M., Lunt, D. J., Siler, N., Steinig, S., Tierney, J. E., Wilkinson, R., Anagnostou, E., De Boer, A. M., Dunkley Jones, T., Edgar, K. M., Hollis, C. J., Hutchinson, D. K., Pancost, R., 2020. Global mean surface temperature and climate sensitivity of the early Eocene Climatic Optimum (EECO), Paleocene-Eocene Thermal Maximum (PETM), and latest Paleocene. Climate of the Past 16, 1953 – 1968.

International Subcommission on Stratigraphic Classification., 1976. In: Hedberg, H.D. (Eds), International Stratigraphic Guide. Wiley, New York, 200

Jarvis, I., Jarvis, K. E., 1992a. Inductively coupled plasma-atomic emission spectrometry in exploration geochemistry. In: Hall, G. E. M. (Eds), Geoanalysis. Journal of Geochemical Exploration 44, 139 - 200.

Jarvis, I., Jarvis, K. E., 1992b. Plasma spectrometry in the earth sciences, techniques, applications and future trends. In: Jarvis, I., & Jarvis, K. E. (Eds), Plasma Spectrometry in the Earth Sciences. Chemical Geology 95, 1 - 33.

Kent, P. E., Hunt, J. A., Johnstone, D. W., 1971. The geology and geophysics of coastal Tanzania. National Environment Research Council, Institute of Geological Sciences, London, Geophysical Paper No. 6: I-VI, 1-101.

Laveuf, C., Cornu, S., 2009. A review on the potentiality of rare earth elements to trace pedogenetic processes. Geoderma 154, 1 - 12.

Mange, M. A., Maurer, H. F. W., 1992. Heavy minerals in colour. Springer. 101 - 124.

Martini, E., 1971. Standard Tertiary and Quaternary calcareous nannoplankton zonation. In: Faranacci (Eds.), Proceedings of the Second Planktonic Conference Roma 1970, vol. 2. Edizioni Tecnoscienza, Rome, 739 - 785.

Mbede, E. I., 1991. The sedimentary basins of Tanzania - reviewed. Journal of African Earth Sciences 13 (3/4), 291 - 297.

McCabe, R., 2021. Geochemistry and stratigraphy of the Mesozoic and Cenozoic rocks encountered in the Mandawa Basin, south eastern Tanzania. Unpublished Ph.D. thesis. Trinity College Dublin.

McCabe, R., Rego, M. P., Warwick, D., Fitches, W., Lee, D. M., 2012. Chemostratigraphic characterisation of Mesozoic and Cenozoic successions: Ruvuma Basin, Tanzania. Poster presented at the East African Petroleum Conference and Exhibition, Arusha, Tanzania.

McCabe, R., Gómez-Pérez, I., Rawahi, H., Bergmann, K., Pearce, T., Dawans, J. M., 2018. Elemental Chemostratigraphy of the Late Neoproterozoic Sedimentary Successions in Oman. Oral Presentation given at the European Association of Geoscientists and Engineers 7th Arabian Plate Workshop, Muscat, Oman.

McCabe, R., Tansell, C., Roach, C., Moss, J., Gómez-Pérez, I., Baloushi, B, Thohli, B., Rawahi, H., 2019. Chemostratigraphy of Pre-Khuff sedimentary rocks encountered in the subsurface of Oman. Poster & oral presentation delivered at the American Association of Petroleum Geologists 3rd Siliciclastic Reservoirs of the Middle East Workshop, Muscat, Oman.

McLennan, S. M., 1989. Rare earth elements in sedimentary rocks: influence of provenance and sedimentary processes. In: Lipin, B. R., & McKay, G. A. (eds), Geochemistry and Mineralogy of Rare Earth Elements. Mineralogical Society of America 21, 169 - 200.

McLennan, S. M., Hemming, S., McDaniel, D. K., Hanson, G. N., 1993. Geochemical approaches to sedimentation, provenance and tectonics. Geological Society of America Special Paper 284, 21 - 40.

Miller, K. G., Kominz, M. A., Browning, J. V., Wright, J. D., Mountain, G, S., Katz, M., Sugarman. P. J., Cramer, B. S., Christie-Blick, N., Pekar, S. F., 2005. The Phanerozoic record of sea-level change. Science 310, 1293 - 1298.

Morton, A. C., Hallsworth, C. R., 1999. Processes controlling the composition of heavy mineral assemblages in sandstones. Sedimentary Geology 124, 3 - 29.

Morton, A. C., 2007. The role of heavy mineral analysis as a geosteering tool during drilling of high angle wells. In: Mange & Wright (Eds) Heavy Minerals in Use. Developments in Sedimentology 58**,** 1178.

Nederbragt, A. J., 1991. Late Cretaceous biostratigraphy and development of Heterohelicidae (planktic foraminifera). Micropaleontology 37, 329 - 372.

Nesbitt, H. W., Young, G. M., 1982. Early Proterozoic climates and plate motions inferred from major element chemistry of lutites. Nature 299, 715 – 717.

Nesbitt, H. W., Markovics, G., 1997. Weathering of granodioritic crust, long-term storage of elements in weathering profiles, and petrogenesis of silicate sediments. Geochemica et Cosmochemica Acta 61 (8), 1653 – 1670.

Nicholas, C. J., Pearson, P. N., Bown, P. R., Dunkley-Jones, T., Huber, B. T., Karega, A., Lees, J. A., McMillan, I. K., O'Halloran, A., Singano, J. M., Wade, B. S., 2006. Stratigraphy and sedimentology of the Upper Cretaceous to Paleogene Kilwa Group, southern coastal Tanzania. Journal of African Earth Sciences 45, 431 - 466.

Nicholas, C. J., Pearson, P. N., McMillan, I. K., Ditchfield, P. W., Singano, J. M., 2007. Structural evolution of southern coastal Tanzania since the Jurassic. Journal of African Earth Sciences 48, 273 - 297.

Pearce, T. J., McLean, D. J., Wray, D., Wright, D. K., Jeans, C. J., Mearns, E. W., 2005. Stratigraphy of the upper Carboniferous Schooner Formation, southern North Sea: chemostratigraphy, mineralogy, palynology and Sm-Nd isotope analysis. In: Collinson, J. D., Evans, D. J., Halliday, D. W., & Jones, N. S. (eds); Carboniferous Hydrocarbon Geology: the southern North Sea and surrounding onshore areas. Yorkshire Geological Society, Occasional Publications Series, 7,165 - 182.

Pearson, P. N., Ditchfield, P. W., Singano, J. M., Harcout-Brown, K. G., Nicholas, C. J., Olsson, R. K., Shackleton, N. J., Hall, M. A. 2001. Warm tropical sea surface temperatures in the late Cretaceous and Eocene epochs. Nature 413, 481 - 487.

Pearson, P. N., Nicholas, C. J., Singano, J. M., Bown, P. R., Coxall, H. K., Van Dongen, B. E., Huber, B. T., Karega, A., Lees, J. A., Msaky, E., Pancost, R. D., Pearson, M., Roberts, A. P., 2004. Paleogene and Cretaceous sediment cores from the Kilwa and Lindi areas of coastal Tanzania: Tanzania Drilling Project Sites 1-5. Journal of African Earth Sciences 39, 25 - 62.

Pearson, P. N., Nicholas, C. J., Singano, J. M., Bown, P. R., Coxall, H. K., Van Dongen, B. E., Huber, B. T., Karega, A., Lees, J. A., Macleod, K., McMillan, I. K., Pancost, R. D., Pearson, M., Msaky, E., 2006. Further Paleogene and Cretaceous sediment cores from the Kilwa area of coastal Tanzania: Tanzania Drilling Project Sites 6-10. Journal of African Earth Sciences 45, 279 - 317.

Pearson, P. N., Van Dongen, B. E., Nicholas, C. J., Pancost, R. D., Schouten, S., Singano, J. M., Wade, B. S., 2007. Stable warm tropical climate through the Eocene Epoch. Geological Society of America 35(3), 211 - 214.

Pearson, P. N., McMillan, I. K., Wade, B. S., Dunkley-Jones, T., Coxall, H. K., Bown, P. R., Lear, C. H., 2008. Extinction and environmental change across the Eocene-Oligocene boundary in Tanzania. Geology 36(2), 179 - 182.

Perch-Nielsen, K., 1985a. Cenozoic calcareous nannofossils. In: Bolli, H. M., Saunders, J. B., & Perch-Nielsen, K. (Eds.), Plankton stratigraphy. Cambridge University Press, 427 - 454.

Perch-Nielsen, K., 1985b. Mesozoic calcareous nannofossils. In: Bolli, H. M., Saunders, J. B., & Perch-Nielsen, K. (Eds.), Plankton stratigraphy. Cambridge University Press, 326 - 426.

Petrizzio, M. R., Falzoni, F., Premoli Silva, I., 2011. Identification of the base of the lower-to-middle Campanian Globotruncana ventricosa Zone: comments on reliability and global correlations. Cretaceous Research 32, 387 - 405.

Ratcliffe, K. T., Martin, J., Pearce, T. J., Hughes, A. D., Lawton, D. E., Wray, D. S., Bessa, F., 2006. A regional, chemostratigraphically-defined correlation framework for the late Triassic TAG-I Formation in Blocks 402 and 405a, Algeria. Petroleum Geoscience 12, 1 - 10.

Ratcliffe, K. T., Wright, A. M., Montgomery, P., Palfrey, A., Vonk, A., Vermeulen, J., Barrett, M., 2010. Application of chemostratigraphy to the Mungaroo Formation, the Gorgon Field, offshore northwest Australia. Australian Petroleum Production & Exploration Association, 371 - 388.

Ratcliffe, K. T., Wright, M., Spain, D., 2012. Unconventional methods for unconventional plays: using element data to understand shale resource plays. Petroleum Exploration Society of Australia News Resources. 89 - 93.

Robaszynski, F., Caron, M., 1979. Atlas de foraminifères planctoniques du Crétacé Moyen (mer Boréale et Téthys). Editions du Centre National de la Recherche Scientifique, Cahiers de Micropaléontologie 1, 185; 2, 181.

Robaszynski, F., Caron, M., 1995. Foraminifères planctoniques du Crétacé: commentaire de la zonation Europe-Méditerranée. Bulletin de la Société Géologique de France 166, 681 - 692.

Röhl, U., Westerhold, T., Bralower, T. J., Zachos, J. C., 2007. On the duration of the Paleocene-Eocene thermal maximum (PETM). Geochemistry, Geophysics, Geosystems 8 (12), 1 – 13.

Salman, G., Abdula, I., 1995. Development of the Mozambique and Ruvuma sedimentary basins, offshore Mozambique. Sedimentary Geology 96, 7 - 41.

Salminen, R., Batista, M. J., Bidovec, M., Demetriades, A., De Vivo, B., De Vos, W., Duris, M., Gilucis, A., Gregorauskiene, V., Halamic, J., Heitzmann, P., Lima, A., Jordan, G., Klaver, G., Klein, P., Lis, J., Locutra, J., Marsina, K., Mazreku, A., O'Connor, P. J., Olsson, S. Å., Ottesen, R. T., Petersell, V., Plant, J. A., Reeder, S., Salpeteur, I., Sandström, H., Siewers, U., Steenfelt, A., Tarvainen, T., 2005. Geochemical Atlas of Europe. Part 1: Background Information, Methodology and Maps. Espoo, Geological Survey of Finland.

Sano, J., Ratcliffe, K. T., Spain, D. R., 2013. Chemostratigraphy of the Haynesville Shale. In: Hammes, U. & Gale, J. (eds); Geology of the Haynesville Gas Shale in East Texas and West Louisianna, U.S.A. American Association of Petroleum Geologists Memoir 105, 137 – 154.

Šimiček, D., Bábek, O., Leichmann, J., 2012. Outcrop gamma-ray logging of siliciclastic turbidites: separating the detrital provenance signal from facies in the foreland-basin turbidites of the Moravo-Silesian Basin, Czech Republic. Sedimentary Geology 261 - 262, 50 - 64.

Sissingh, W., 1977. Biostratigraphy of Cretaceous calcareous nannoplankton. Geologie en Mijnbouw 56, 37 - 65.

Sissingh, W., 1978. Microfossils, biostratigraphy and stage - stratotypes of the Cretaceous. Geologie en Mijnbouw 57 (3), 433 - 440.

Sliter, W. V., 1989. Biostratigraphic zonation for Cretaceous planktonic foraminifers examined in thin section. Journal of Foraminiferal Research 19, 1 - 19.

Sluijs, A., Schouten, S., Donders, T. H., Schoon, P. L., Röhl, U., Reichart, G-J., Sangiorgi, F., Kim, J-H., Sinninghe Damasté, J. S., Brinkhuis, H., 2009. Warm and wet conditions in the Arctic region during the Eocene Thermal Maximum 2. Nature Geoscience 2, 770 – 780.

Stap, L., Lourens, L., Van Dijk, A., Schouten, S., Thomas, E., 2010. Coherent pattern and timing of the carbon isotope excursion and warming during Eocene Thermal Maximum 2 as recorded in planktic and benthic foraminifera. Geochemistry, Geophysics, Geosystems 11(11), 1 – 10.

Svensden, J., Friis, H., Stollofen, H., Hartley, N., 2007. Facies discrimination in a mixed fluvio-eolian setting using elemental whole-rock geochemistry – applications for reservoir characterisation. Journal of Sedimentary Research 77, 23 – 33.

Tansell, C., Moss, J., Gómez-Pérez, I., Thohli, B., McCabe, R., Fairey, B, 2021. Chemostratigraphy and provenance of the Amdeh Formation (Members I to III), northern Oman. Oral Presentation given at the European Association of Geoscientists and Engineers 4th Siliciclastic Reservoirs of the Middle East Workshop.

Taylor, S. R., McLennan, S. M., 1985. The continental crust: its composition and evolution. Blackwell Scientific Publication.

Van Der Weijden, C. H., 2002. Pitfalls of normalisation of marine geochemical data using a

common divisor. Marine Geology 184, 167 - 187.

Wilson, M. J., 2004. Weathering of the primary rock-forming minerals: processes, products and rates. Clay Minerals 39, 233 - 266.

Zachos, J. C., Dickens, G. R., Zeebe, R. E., 2008. An early Cenozoic perspective on greenhouse warming and carbon-cycle dynamics. Nature 451 (17), 279 - 283.

FIGURES

Figure 1: Location of the TDP sites in the Mandawa Basin and offshore exploration wells examined in this paper (Geological map modified from McCabe, 2021, Fig. 4.1)**.**

Figure 2: Chronostratigraphy of logged TDP boreholes (modified from Berrocoso *et al.,* 2015, Fig 3. and Nicholas *et al.,* 2006, Fig. 5).

Figure 3: The Kilwa Group Composite section and deepwater study wells examined in this paper.

Figure 4: Comparison of major element and mineral data for selected TDP core samples.

Figure 5: EV1 and EV2 calculated from PCA of the claystone dataset.

Figure 6: Sequence-level chemostratigraphic correlation of the study sections.

Figure 7: Package and unit-level chemostratigraphic correlation of the study sections.

Figure 8: Mineralogy of the Kilwa Group rocks, including mineral ratios & indices supporting the geological interpretations.

Figure 9: Chondrite-normalised REE plots for each of the chemostratigraphic zones recognised in this study.

Figure 10: Comparison of the Si/Al ratio with the global sea level curve (modified from Miller *et al.,* 2005, Fig. 3).

Figure 11: Geochemical evidence for climatic and hydrological variations in Tanzania during the Late Paleocene and Early Eocene.

Figure 12: Comparison of the elemental ratios with the δ18O curve in TDP-12 and TDP-17.

Figure 13: Lithostratigraphic correlation of the study sections.

Figure 14: Comparison of the chemostratigraphic and lithostratigraphic schemes of the Kilwa Group, plus proposed revisions to the onshore stratigraphy.

Figure 15: Comparison of the $CaCO_3$ curve with the geochemical parameters employed to define the Lindi and Nangurukuru Formations in this study.

APPENDIX 1: SAMPLE PREPARATION & ANALYTICAL PROTOCOLS FOR ICP-OES & -MS

All samples have been analysed by inductively-coupled plasma - optical emission spectroscopy (ICP-OES) and inductively-coupled plasma - mass spectrometry (ICP-MS) at the laboratories of Origin Analytical (UK). Approximately 5g of material per core sample was ground in an agate mortar, with the resultant homogenised powder being used for both ICP-OES and -MS analysis. The powders were dried in an oven at 60ºC for 5 minutes to drive off any internal moisture. For the cutting samples, approximately 1-2g of a single lithology, interpreted from supplied lithological information as representing the *in situ* subsurface rock, was isolated under a binocular microscope and powdered by pestle and mortar.

The powdered samples were prepared by applying an alkali fusion procedure similar to that described by Jarvis & Jarvis (1992a & b). The procedure involves fusing 0.25g of sample with 1.25g of $LiBO_2$ flux in a carbon crucible at 1050ºC for 15 minutes. The mixture was then immediately transferred into beakers containing 120ml of 3.5%v/v of HNO_3. The solution was converted to an aerosol and introduced to the ICP instruments for analysis. For ICP-OES analysis, the samples were run on a Thermo ICAP 6500 instrument. For ICP-MS analysis, samples were run on a Thermo XSeries 2 instrument. Both instruments are calibrated using internal rock standards and certified reference materials (CRMS: samples of a known chemical composition) are run in line with the geological material at 20 sample intervals, allowing for instrumental anomalies and analytical drift to be corrected.

APPENDIX 2: SAMPLE PREPARATION & ANALYTICAL PROTOCOLS FOR WR- & CF-XRD

Sample preparation and XRD analysis were conducted by X-Ray Minerals Ltd in the UK. The preparation procedure for WR analysis involved micronising 2g of powdered rock in ethanol using a McCrone Micronising Mill to obtain a powder with a mean particle diameter of between 5µm and 10µm. The slurry was dried overnight at 80°C, re-crushed to a fine powder and back-packed into a steel sample holder, producing a randomly orientated sample for presentation to the X-ray beam. Whole-rock samples were scanned on a PANalytical X'Pert 3 diffractometer using a CuKα radiation source at 40 kV and 40 mA. Whole-rock

samples were scanned from 4.5 to 75° (2θ) at a step size of 0.013 and nominal time per step of 0.2 s (continuous scanning mode).

The preparation procedure for CF analysis involved taking a 5g split of the sample that was disaggregated at the WR stage of preparation and separating the <2 μm fraction by centrifuge. The CF XRD mount is obtained by filtering the clay suspension through a Millipore glass micro-fibre filter and drying the filtrate on the filter paper. The samples were analysed as an untreated clay, after saturation with ethylene glycol vapour overnight and following heating at 380°C for 2 hours, with a further heating to 550°C for one hour. Clay filters were scanned on a Philips PW1730 Generator using a using X-ray radiation from a copper anode at 40kV, 40mA. Clay filters were scanned from 3 to 35° (2θ) at a step size of 0.05° and 2 s step time.

Identification of unknown minerals was achieved by using Traces (v.6) by GBC Scientific Equipment and HighScore Plus (v.4) by PANalytical software. Quantitative phase analysis on whole rock samples used the Rietveld method with BGMN AutoQuan software.

APPENDIX 3: SAMPLE PREPARATION & ANALYTICAL PROTOCOLS FOR CLAYSTONE HMA USING RAMAN SPECTROSCOPY

The heavy minerals were separated from the core samples at Origin Analytical UK and analysed at the University of Greenwich, UK. The rock was carefully disaggregated and the heavy minerals were separated from the light minerals in a lithium heteropolytungstate solution (LST Fastfloat, 2.89 g/cm3) using the funnel separation technique (e.g., Mange and Maurer, 1992). A wide grain size window (10μm to 250μm) was employed to acquire the entire heavy mineral assemblage from each sample. The heavy mineral grains were loosely scattered on a petrographic slide and analysed using a Horiba LabRam Raman microscope equipped with a 532nm green laser.

Between 133 and 1103 transparent heavy mineral grains were analysed per sample. The Raman spectra acquired were compared to a reference database of heavy mineral spectra to identify their mineralogy.

Chemostratigraphic and Mineralogical Examination of the Kilwa Group Claystones, Coastal Tanzania: An Alternative Approach to Refine the Lithostratigraphy

Ross McCabe [a, b*], Christopher J. Nicholas [b], Bill Fitches [c], David Wray [d], Tim Pearce [a]

[a] Chemostrat Ltd, Unit 2 Ravenscroft Court, Buttington Cross Enterprise Park, Welshpool, Powys, UK.

[b] Department of Geology, Trinity College, University of Dublin, Dublin 2, Ireland.

[c] Leeds, W. Yorkshire, UK.

[d] School of Science, University of Greenwich, Chatham Maritime, Kent, UK.

[*]Corresponding author. Tel: +44 (0) 1938 555 330. Email: McCaber2@tcd.ie.

Abstract

The Cretaceous and Paleogene marine sedimentary rocks that crop out along southern coastal Tanzania have been the focus of the Tanzanian Drilling Project (TDP) since 2001. The comprehensive lithological and chronostratigraphic examination of over forty shallow cores by the TDP culminated in the formal definition of the Kilwa Group: a claystone-dominated succession comprising five formations deposited in middle to outer shelf and upper slope marine environments along a passive continental margin. Onshore, the TDP has cored important palaeoclimatic events within the Kilwa Group. Offshore, the group forms the reservoir and seal of several gas fields discovered in southern Tanzania.

The formations of the Kilwa Group cored onshore, have been differentiated from each other largely by variations in subsidiary lithologies (sandstones and limestones), rather than by diagnostic characteristics of their dominant lithology (olive grey claystone). To test and refine the lithostratigraphy of the Kilwa Group, a forensic examination of the claystones using whole-rock inorganic geochemistry, mineralogical analysis and detailed biostratigraphy, is employed in this study.

1210 core samples collected from 20 onshore TDP boreholes and 185 cutting samples acquired from three wells located in offshore in Blocks 1 and 4 are examined by inductively-coupled plasma optical emission spectroscopy and mass spectrometry, whole-rock and clay fraction X-ray diffraction analysis and heavy mineral analysis using Raman spectroscopy. The different methodologies are used to produce a claystone-based chemostratigraphic framework for the Kilwa Group that comprises three sequences, five packages and six units, and links the shallow subsurface rocks onshore to the deep subsurface stratigraphy offshore.

The multidisciplinary geochemical and mineralogical approach reveals that variations in detrital quartz, feldspars (K and Na), heavy minerals, phosphatic minerals and clay minerals (particularly illite, smectite and kaolinite) are key for defining the claystone-based stratigraphy of the Kilwa Group. The variation in the abundance of these mineral through time highlight mostly temporal changes in depositional environment, chemical weathering and sediment provenance that occurred in Tanzania during the Cretaceous and Paleogene.

Integration of the chemostratigraphic framework with detailed biostratigraphic information from the study sections and comparison with the published lithostratigraphy of the Kilwa Group onshore reveals that all three stratigraphic schemes are in broad agreement. Nevertheless, refinements are proposed based on the new chemostratigraphic results. It is suggested here that the top and base of the Kilwa Group is older than previously reported (base–Albian and intra-Rupelian, respectively, rather than the end of both stages) and in most cases, the geochemical data suggests that most of the Kilwa Group formations, as cored onshore, are thinner than formerly proposed. Only the Masoko and Lindi Formations are interpreted to be thicker than previously defined by the TDP.

Key words:

Chemostratigraphy; Lithostratigraphy; Kilwa Group; Provenance; Environment; Climate.

1. INTRODUCTION

Cretaceous and Paleogene (Albian to Oligocene) rocks that were deposited in middle to outer shelf and upper slope marine environments, crop out along stretches of coastal Tanzania, south of Dar es Salaam (**Figures 1** and **2**). The Mandawa and northern Ruvuma coastal basins in which these rocks were deposited, began to form during breakup of Gondwana in the late Triassic and Jurassic Periods (e.g., Kent *et al.,* 1971; Mbede, 1991; Salman & Abdula, 1995; Geiger *et al.,* 2004; Nicholas *et al.,* 2007; Davison & Steel, 2017). The marine rocks examined in this study were deposited during a period of tectonic stability, when a widespread marine transgression advanced across the East African passive continental margin and brought about the deposition of a thick succession of claystones (Pearson *et al.,* 2004 & 2006; Nicholas *et al.,* 2006 & 2007; Berrocoso *et al.,* 2010, 2012 & 2015).

Since 2001, these rocks have attracted the attention of geoscientists interested in understanding climate change over the past 120 million years because of the discovery of exceptionally well-preserved planktonic foraminifer shells in the claystones (Pearson *et al.*, 2001, 2004, 2007, 2008; Nicholas *et al.,* 2006; Berrocoso *et al.,* 2010, 2012, 2015). According to Pearson *et al.* (2004), the shells appear glassy under the reflected light microscope and, under scanning electron microscope, have retained their microgranular textures. Pearson *et al.* (2004) attributed the excellent preservation of the shells to their encasement within claystones whose impermeability inhibited movement of diagenetic fluids. With little or no diagenetic alteration, these shells are considered to have retained their original seawater-derived C and O isotopic composition so are excellent candidates for the accurate determination of palaeoclimate during the Late Cretaceous and Paleogene (Pearson *et al.,* 2001).

Whilst the quality of the foraminifer shells is excellent, the present-day outcrop exposures along the coastal margin are poor and restricted to the shoreline and roadsides (Pearson *et al.*, 2004, 2008). Consequently, the Tanzanian Drilling Project (TDP), an international collective of geoscientists, was assembled in 2001. One of the main objectives of the TDP was to conduct shallow coring of these Cretaceous and Paleogene marine sediments, on which more detailed palaeoclimatic, stratigraphic and palaeoceanographic studies could be based (Pearson *et al.,* 2004).

In total, 40 shallow boreholes have been drilled by the TDP in three main areas between the administrative centres of Kilwa and Lindi (**Figures 1** and **2**). The first 20 boreholes, drilled between 2002 and 2005, retrieved core from Late Cretaceous and Paleogene rocks (see Nicholas *et al.*, 2006, for a comprehensive review). The succeeding twenty TDP boreholes, drilled between 2007 and 2009, retrieved core from progressively older sections (Berrocoso *et al.*, 2010, 2012, 2015; Mweneinda, 2014), though most were drilled to core the Cenomanian-Turonian boundary. The boreholes have penetrated sediments as old as the Barremian-Aptian and possibly older in the basal sandstones of TDP-40A (**Figure 2**).

Among its many achievements, the TDP has cored rare onshore sedimentary successions that span the Paleocene-Eocene Thermal Maximum (PETM) event at the Paleocene-Eocene boundary (c.55.8 Ma - Nicholas *et al.*, 2006; **Figure 2**). The PETM lasted approximately 170 Ka (Röhl *et al.*, 2007), during which time sea temperatures increased abruptly by 5ºC globally and 8ºC locally (Handley *et al.*, 2012). Compared to the other successive hyperthermal events during the Eocene, such as the Eocene Thermal Maximum 2 (ETM2) that occurred around 53.7 Ma and lasted approximately 100 Ka (Stap *et al.*, 2010; **Figure 2**), the PETM experienced the greatest warming sustained over the longest time and, as such, has been extensively studied to understand better the impact of `greenhouse' gas-induced global climate change. Additionally, the Kilwa Group contains the Eocene-Oligocene boundary, which according to Pearson *et al.* (2008), records an episode of global cooling, marking the end of the extended period of predominantly 'greenhouse' conditions on Earth that extended back into the Mesozoic.

The bulk of the sedimentary succession cored onshore corresponds with what was formally defined by the TDP as the Kilwa Group (Nicholas *et al.*, 2006). The group consisted of four formations: Nangurukuru (Santonian to upper Maastrichtian), Kivinje (upper Paleocene to lower Eocene), Masoko (middle Eocene) and Pande (upper Eocene to lower Oligocene). Based on evidence from the more recent cores, Berrocoso *et al.* (2015) considered the group to be as old as Albian and defined a fifth formation at the base called the Lindi Formation (Albian to Coniacian - see **Table 1**).

Claystones are the dominant lithology of all five formations and all were deposited in middle to outer shelf and upper slope marine environments. Nicholas *et al.* (2006) separated the upper four formations by variations in their subordinate and sporadic intercalations of sandstones and carbonates, both of which are rarely more than a metre thick. In contrast, Berrocoso *et al.* (2015) considered that the Lindi Formation is distinguishable from the Nangurukuru Formation by subtle differences in the sedimentary features and colour of the predominant claystones (**Table 1**).

As reflected in **Table 1**, the lithological differences between the formations of the Kilwa Group are subtle and the claystones themselves (with the probable exception of the Lindi Formation claystones) are all broadly similar. This study seeks to test, improve and refine the division of the Kilwa Group claystones using bulk rock elemental chemostratigraphy.

Table 1. Lithological characteristics of the stratigraphic units of the Kilwa Group (after Nicholas *et al.*, 2006 and Berrocoso *et al.*, 2015)

Formations of the Kilwa Group	Main Lithology	Secondary Lithologies	Minimum Thickness (m)
Pande Fm. (upper Eocene to lower Oligocene: Nicholas *et al.*, 2006)	Soft, light olive grey or blue-grey clays, mottled with yellowish orange sandy clays[a]	White, massive, micritic limestones and/or calcarenites, with benthic foraminifera and clay rip-up clasts	202
Masoko Fm. (middle Eocene: Nicholas *et al.*, 2006)	Soft, light olive grey clays, mottled with yellowish orange sandy clays[a]	Orange-brown limestones cemented by sparry calcite, with large *Nummulites*, well-rounded coarse quartz grains, normal grading and cross lamination	173
Kivinje Fm. (upper Paleocene to lower Eocene: Nicholas *et al.*, 2006)	Hard/blocky, olive grey claystones, mottled with yellowish orange, sandy clay[a]	Common sandy partings throughout, occasionally developing into thin, partly cemented calcarenites with small bioclasts	401
Nangurukuru Fm. (Santonian to upper Maastrichtian: Nicholas *et al.*, 2006)	Hard/blocky, olive grey claystones, mottled with yellowish orange, sandy clay[a]	Sporadic, massive, carbonate-cemented, turbiditic sandstones, centimetric to metric in thickness	385
Lindi Fm. (upper Albian to Coniacian: Berrocoso *et al.*, 2015)	Interbeds of dark grey to black claystones and siltstones, with common finely-laminated, possibly organic-rich intervals[b]	Minor occurrences of cm-thick brownish grey, fine to coarse sandstone, generally massive and occasionally top-laminated	194

[a] Colour of weathered sediments

[b] Colour of fresh sediments

Minimum formation thickness calculated from TDP cores

Chemostratigraphy is an interpretative methodology that employs whole-rock inorganic geochemical data to characterise rock units. Chemostratigraphy has long been utilised in the oil and gas industry to address regional and reservoir-level stratigraphic issues (e.g., Pearce *et al.*, 2005; Ratcliffe *et al.*, 2006, 2010, 2012; McCabe *et al.*, 2012, 2018, 2019; Craigie, 2015, 2016; Craigie & Rees, 2016; Craigie *et al.*, 2016; McCabe, 2021; Tansell *et al.*, 2021). The temporal and spatial changes in the geochemical characteristics of clastic sedimentary rocks detected within the framework reflect changes in mineralogy that, themselves, are governed by changes in provenance, climate, depositional environment and diagenetic history. One of the principal advantages in using chemostratigraphy is that variations in chemistry can be detected in successions of otherwise apparently uniform sedimentary rocks, thus making it ideal for studies of the Kilwa Group claystones.

Most TDP boreholes pass through short lengths of the stratigraphy that have, in general, only been correlated locally. As well as being hampered by outcrop quality, demonstration by the TDP of the extent to which the Kilwa Group could be correlated was hindered by the fact that, at the time, there were few hydrocarbon wells drilled in the area that intersected the group. Moreover, it was not the objective of the TDP to tie the onshore stratigraphy to continuous and potentially more complete sedimentary successions encountered in the subsurface. Nicholas *et al.* (2006) noted that the Kilwa Group forms part of the seal rock in the Songo Songo gas field and it is now understood that the group constitutes reservoir and seal rocks in the deep water exploration wells drilled outboard of the TDP study area (Sansom, 2018). Thus, a better understanding of the development and interrelationships of the group between the onshore and offshore areas will contribute to the understanding of the hydrocarbon geology in the region.

To demonstrate these interrelationships, the chemostratigraphic results of three deep water exploration wells, Pweza-1, Taachui-1 and Taachui-1ST, are included in this study (**Figure 3**). These wells, and several others, were analysed by Chemostrat Ltd (2015, 2016 unpublished reports) for BG Group in Blocks 1, 3 and 4 (**Figure 1**) and permission has been granted by Shell, the present operator, to show the results here. Pweza-1 is located within Block 4, approximately 90km NW of Kilwa town and is selected because it intersects a succession of clastic rocks deposited throughout the Paleogene and Cretaceous (Rupelian to Albian). Taachui-1 and -1ST are located within Block 1, approximately 20km from the mainland between the Pande and Lindi areas (**Figure 1**). These wells are included because

they intersect a thick Cretaceous succession (Berriasian to Campanian). For Taachui-1 and -1ST, different parts of the Cretaceous stratigraphy were sampled in each well. Late Cretaceous samples were only available from the Taachui-1 pilot borehole, whereas older rocks were intersected (and sampled) by the side-track. In this study, Taachui-1 and -1ST are spliced together at the Cenomanian-Turonian boundary and treated as one well (see **Figure 3**). A comprehensive biostratigraphic (combined palynology, nannopalaeontology and micropalaeontology) examination of the study wells was conducted by CGG Services UK Ltd (CGG, 2017) and some of the results are incorporated here. Prior to this study, and as far as is known, these wells had not been placed within a formal lithostratigraphic framework. The completeness of the Palaeogene and Cretaceous sedimentary succession encountered in these wells ensures that a comprehensive chemostratigraphic framework for the Kilwa Group can be established between the onshore and offshore areas.

2. METHODS

2.1 SAMPLE COLLECTION

For this study, 1210 samples were collected for geochemical analysis. Samples have been taken from 15 of the first 20 boreholes cored by the TDP (**Figure 2**; **Table 2**). These cores penetrate much of the Paleogene succession, as well as the Campanian and Maastrichtian sedimentary rocks. The successions of Paleogene age are generally well represented in the cores, although there are two c.5 Ma uncored time gaps, one in the Late Eocene (Upper Bartonian and Lower Priabonian Stages) and the other in the Early Paleocene (Lower Selandian and Danian Stages) (**Figure 2**). Sediments deposited during the Late Eocene gap were recorded by Nicholas *et al.* (2006) at outcrop along Kitunda Shore, although the samples from this area were not collected and analysed as part of this study. Despite many attempts at coring them, Early Paleocene rocks have yet to be identified at outcrop or in the shallow subsurface of the Mandawa Basin (Nicholas *et al.*, 2006). A third c.5 Ma uncored time gap is also present in the sediments of lower Campanian age (**Figure 2**).

Samples have also been taken from 6 of the second set of 20 boreholes cored by Berrocoso *et al.* (2010, 2012, 2015; **Figure 2**). These cores are also from successions of Middle – Upper Cretaceous age (Barremian / Aptian to Campanian Stages). Few of the cores sample the Lower Cretaceous, and the Early-Middle Albian (c.7 Ma) is very poorly represented. Only a short (c.8m) interval of Middle Albian (*Ticinella primula* planktonic foraminifera zone) has been intersected, which is in TDP-40 (A&B; **Figure 2**).

The core samples have been collected approximately every metre but due to time constraints, samples from TDP-37 and TDP-39 were collected at approximately ten metre intervals. All the lithologies present in the core intervals were sampled. However, in this study, only the claystones are examined because: 1, claystones are the dominant lithology in the Kilwa Group; 2, unique physical / chemical characteristics of the Kilwa Group claystones have yet to be identified that would support the formation-level lithostratigraphic framework proposed by Nicholas *et al.,* (2006) and Berrocoso *et al.,* (2015); and 3, the subsidiary lithologies are few and unevenly distributed throughout the Kilwa Group sedimentary succession so are of little use for defining lithostratigraphic units and boundaries.

Table 2. Summary of TDP cores sampled for this study.

TDP Core	Sandstone	Claystone	Carbonate	Total
TDP-01	4	44	3	51
TDP-02	1	67	5	73
TDP-03	0	35	0	35
TDP-04	0	6	2	8
TDP-07B	0	99	8	107
TDP-08	1	19	0	20
TDP-09	1	73	0	74
TDP-10	1	90	6	97
TDP-12	2	100	9	111
TDP-13	0	81	4	85
TDP-14	0	20	0	20
TDP-17	8	60	7	75
TDP-18	0	23	1	24
TDP-19	0	38	5	43
TDP-23	1	79	0	80
TDP-24A	5	52	0	57
TDP-31	2	81	2	85
TDP-37	0	51	1	52
TDP-39	0	36	0	36
TDP-40A	16	61	0	77
GRAND TOTAL	42	1115	53	1210

185 ditch cutting samples have been collected and analysed from wells Pweza-1, Taachui-1 and Taachui-1ST (**Table 3**). In contrast to the high-resolution sampling of the cores, the cutting samples were taken approximately every 25 metres in each well (**Figure 3**).

Table 3. Summary of the wells sampled for this study.

Well	Sandstone	Claystone	Carbonate	Total
Pweza-1	17	53	1	71
Taachui-1	19	27	1	47
Taachui-1ST	9	58	0	67
GRAND TOTAL	45	138	2	185

Detailed biostratigraphic analysis of the TDP boreholes cores and study wells has been conducted by the TDP (Pearson *et al.*, 2004, 2006; Nicholas *et al.*, 2006; Mweneinda, 2014; Berrocoso *et al.*, 2015) and CGG (2017) and the zonations are plotted on **Figure 3**. The literature sources for the various planktonic foraminifera and calcareous nannofossil zones employed by the TDP and CGG are presented in **Table 4**. For ease of presentation, CGG converted the Cretaceous calcareous nannofossil zonation scheme of Sissingh (1977), used by them on Pweza-1, Taachui-1 and Taachui-1ST, to that of Burnett (1998), which was used by the TDP (A. Pardon, 2021, *pers. comm.*).

Table 4: Sources of Cretaceous and Paleogene planktonic foraminifera and calcareous nannofossil zonation schemes employed in Tanzania by the TDP (Nicholas *et al.*, 2006; Berrocoso *et al.*, 2015) and CGG (2017).

Period	TDP			CGG	
	Planktonic Foraminifera Zones	Calcareous Nannofossil Zones		Planktonic Foraminifera Zones	Calcareous Nannofossil Zones
Paleogene	Sliter (1989)	Martini (1971)		Blow (1979)	Martini (1971)
	Nederbragt (1991)				
	Gradstein *et al.* (1995)				
	Robaszynski & Caron (1995)				
	Huber *et al.* (2008)				
	Huber & Leckie (2011)				
	Petrizzio *et al.* (2011)				
Cretaceous	Berggren *et al.* (1995)	Burnett (1998)		Robaszynski *et al.* (1979 & 1984)	Sissingh (1977 & 1978)
	Berggren & Pearson (2005)				Perch-Nielsen (1985a&b)

2.2 SAMPLE ANALYSIS

All samples were analysed by inductively-coupled plasma - optical emission spectroscopy (ICP-OES) and inductively-coupled plasma - mass spectrometry (ICP-MS) at the laboratories of Origin Analytical, UK. The sample preparation and analytical protocols employed by Origin Analytical are given in **Appendix 1**. The ICP-OES and ICP-MS analyses yielded quantitative data for ten major elements (Al_2O_3, SiO_2, TiO_2, Fe_2O_3, MnO, MgO, CaO, Na_2O, K_2O, P_2O_5) and thirty-six trace elements (Ba, Be, Cs, Co, Cr, Cu, Ga, Hf, Mo, Nb, Ni, Rb, S, Sc, Sr, Ta, Th, U, V, Y, Zn, Zr) including fourteen rare earth elements (La, Ce, Pr, Nd, Sm, Eu, Gd, Tb, Dy, Ho, Er, Tm, Yb, Lu). For brevity, all the elements are referred to in the text by their appropriate chemical symbol, with the symbols for the major elements being taken to imply oxides, for example, K = K_2O, Al = Al_2O_3 and Mg = MgO.

To support the mineralogical and geological interpretations drawn from the elemental data, 12 claystone core samples were subjected to whole-rock (WR-) and clay fraction (CF-) X-ray diffraction (XRD) analysis and 11 samples have been subjected to heavy mineral analysis (HMA) by Raman spectroscopy (sample positions for each analytical method are presented on **Figure 3**). In both instances, sample selection was guided by the geochemical data and most chemostratigraphic zones are represented in the XRD and HMA datasets. For HMA, multiple claystone core samples had to be combined to obtain a volume of material (c.50g to 100g of rock) that would yield enough heavy minerals for analysis. Heavy mineral (HM) recovery was sufficient in all but two samples: the uppermost Maastrichtian of TDP-37 and the Priabonian of TDP-12 (see **Figure 3**).

XRD analysis and related sample preparations were conducted by X-Ray Minerals Ltd, UK following the procedures described in **Appendix 2**. XRD analysis yielded quantitative data for 14 minerals in the TDP core samples. The most common mineral species included: quartz, calcite, aragonite, orthoclase, plagioclase, muscovite, illite, mixed layer illite+smectite and kaolinite. Accessory minerals included: dolomite, siderite, pyrite, anatase, gypsum and chlorite.

The heavy minerals were separated from the claystone core samples at Origin Analytical, UK and analysed by Raman spectroscopy at the University of Greenwich, UK, following preparation and analytical procedures described in **Appendix 3**. Between 133 and 1103 transparent heavy mineral grains were analysed per sample. In the TDP claystones, recorded heavy mineral species include allanite, anatase, apatite, baryte, brookite, chloritoid, epidote, garnet, kyanite, monazite, pyroxene, rutile, spinel, staurolite, titanite, tourmaline, xenotime, and zircon.

2.3 KILWA GROUP COMPOSITE SECTION

Details of the lithostratigraphy, biostratigraphy and, in many instances, stable isotope chemistry for each of the forty cores taken by the TDP in the coastal Mandawa and Ruvuma Basins were described by Pearson *et al.* (2004, 2006), Nicholas *et al.* (2006), Berrocoso *et al.* (2010, 2012, 2015) and Mweneinda (2014). Nicholas *et al.* (2006) noted that there is no single stratotype section for any of the formations of the Kilwa Group (see also Berrocoso *et al.*, 2015). Consequently, the various formations have been defined by composite stratotype sections following guidelines of the International Subcommission on Stratigraphic Classification (1976). The composite stratotype for the entire Kilwa Group, developed by Nicholas *et al.* (2006) and Berrocoso *et al.* (2015), is illustrated in **Figure 2**.

Using the concept of the composite stratotype, a Kilwa Group composite section (KGCS) is created in this study to illustrate the inorganic geochemical evolution of the Kilwa Group through the Cretaceous and Paleogene Epochs (**Figure 3**). The KGCS consists of multiple TDP cores stacked on each other in chronostratigraphic order with no stratigraphic overlap (interpreted from the detailed biostratigraphic results of each TDP core). All the lithostratigraphic, chronostratigraphic and biostratigraphic information included on the KGCS is taken from Pearson *et al.* (2004, 2006), Nicholas *et al.* (2006) and Berrocoso *et al.* (2010, 2012, 2015). The benefit of this approach is that an appreciable weight of information is displayed simply and effectively. It allows for geochemical trends to be observed in the dataset that are broader than that of individual TDP cores and therefore enables testing of the validity of lithostratigraphic boundaries that are currently in place. The KGCS does not record subsurface depths, rather the cumulative thickness of the Kilwa Group, as currently cored.

A degree of caution is exercised when employing composite sections. Firstly, when stacking separate cores on each other, time breaks are inevitable, as it is unlikely that each successive TDP core in the composite will follow on from the previous one continuously and without any loss of time. Whilst chemostratigraphic boundaries may inadvertently coincide at the boundary between two cores (indicating that the chemostratigraphic boundary has not been cored by the TDP), real unconformities are picked only where they occur within a core.

Secondly, coring bias may have the undesired effect of over-, or under- emphasising the thickness and indeed the lithological composition of key (chemo-) stratigraphic zones. This issue is impossible to mitigate with the available core material collected by the TDP and improvements can only be made through additional shallow coring of key time intervals, particularly in the Paleocene and Early Cretaceous. The detailed biostratigraphic analysis conducted on the TDP cores (**Figures 2** and **3**) shows that most internationally recognised planktonic foraminifera and calcareous nannofossil zones are recorded. Thus, the chemostratigraphic characterisation presented on the composite section in this study is considered as a reasonably comprehensive representation of the Kilwa Group. Further mitigation of coring bias is achieved in this paper by comparison of the KGCS to wells Taachui-1ST and Pweza-1, which have intersected Paleocene and Cretaceous sedimentary successions that have not yet been cored onshore (**Figure 3**).

Finally, lateral variations in geochemical composition of the rocks caused by changes in depositional environment or sediment provenance may occur between cores situated in different localities. These variations may be strong enough to affect the geochemical composition of the sediments, obscuring subtle temporal geochemical trends in cores collected from the same locality. Lateral variations in the geochemical composition of the TDP claystones is not regarded as a strong control on the specific key elements and element ratios utilised to define the chemostratigraphic framework. Most of the cores were cut along the strike of the palaeo-shelf on a passive margin and encountered rocks deposited in closely similar environments (see **Figure 2**). Down - dip variations in the geochemical composition of the TDP claystones is not regarded as a strong control on the key element ratios employed in this study. As will be demonstrated through the integration of the chemostratigraphic framework with the detailed biostratigraphic zonations of the study sections, particularly the wells drilled outboard of the TDP cores (see **Section 4**), all but one of the chemostratigraphic boundaries represent synchronous events. These events, including those that define the top

and base of the Kilwa Group and its formations, are interpreted to reflect temporal variations in climate, depositional environment and / or provenance, rather than lateral changes.

2.4 SYNTHETIC GAMMA (CHEMGR)

In chemostratigraphic studies, a ChemGR trace is often calculated from the K, Th and U chemical data acquired from cuttings samples as a means of cross-checking the validity of material analysed (see Ratcliffe *et al.*, 2010 and Šimíček *et al.*, 2012). The operation involves superimposing the ChemGR on the wireline GR and determining how closely the two log traces match. The closer the match, the more likely it is that the data represents the *in situ* rocks in the subsurface and not contaminants (e.g., caved rock, drilling additive). The operation is demonstrated using the geochemical data acquired from the cuttings from wells Taachui-1, Taachui-1ST and Pweza-1 in **Figure 3**: the close match between the GR and ChemGR traces indicates that the data acquired is representative of the *in situ* rocks in the subsurface. In the Kilwa Group sedimentary rocks analysed (core and cutting samples), claystones have an average ChemGR API value of 102, whereas sandstones and carbonates have average API values of 61 and 35, respectively.

As all the TDP data were acquired from core samples, uncertainties regarding data validity with respect to caving or other contamination are not an issue. Nevertheless, the ChemGR is calculated for all samples to provide a visual representation of lithological variations throughout the KGCS. The ChemGR profile for the KGCS is displayed on **Figure 3**. The high API-equivalent values recorded throughout confirm that claystone is the dominant lithology, although layers with lower API-equivalent values do exist and correspond to limestone and sandstone interbeds. Whilst the equivalent aged sections in the two exploration wells are also generally clay-prone, thicker sand bodies have been intersected throughout the Cretaceous and Paleogene (**Figure 3**).

3. RESULTS & DISCUSSION

3.1 GEOCHEMISTRY & MINERALOGY

A comprehensive examination of all elements acquired by ICP analysis has been conducted and 23 index elements have been identified as key for defining the chemostratigraphic framework of the Kilwa Group. The index elements are Si, Al, Mg, K, Na, P, Zr, Th, Sc, the light rare earth elements (LREEs: La, Ce, Pr, Nd) and the heavy rare earth elements (HREEs: Ho, Er, Tm, Yb, Lu). To understand the geological controls acting on the key elements, their mineralogical affinities must be established (Ratcliffe *et al.* 2012, Craigie, 2015, Craigie & Rees, 2016). In this study, this objective is achieved through direct element-mineral comparisons and statistical modelling of the elemental dataset.

Direct comparison of key major elements to their likely dominant mineral hosts in the TDP claystones is presented as a series of binary diagrams on **Figure 4**. In general, a positive linear relationship is observed between Si and quartz, Ca and Ca-carbonates+gypsum, K and K-feldspar, Na and plagioclase, Al and kaolinite and Fe+Mg and illite+smectite. Craigie (2015) reports that direct comparison or major elements to framework and matrix minerals is usually possible only when the minerals occur in abundances >1% of the bulk rock (i.e., above the limits of analytical detection by XRD analysis). Moreover, comparison of major and trace elements to dominant HMs is less straightforward for several reasons, including differences in preparation and analytical procedures, different HMs having similar trace element chemistries, or chemistries that can be eclipsed by major minerals (e.g., Ca-silicates vs. Ca-carbonates and Al-HMs such as andalusite, sillimanite and kyanite vs. kaolinite, etc.) and the breakdown of chemically unstable heavy minerals to clay. Consequently, whilst HM data is utilised in this study, comparison of major and trace elements to dominant HMs is not attempted.

Sano *et al.* (2007) suggest that whilst direct comparison of elemental and mineralogical data can provide a basic understanding of which minerals are controlling some elements and element ratios, understanding can be enhanced by examining element-element relationships by using principal components analysis (PCA). PCA has been used widely in chemostratigraphic studies to improve understanding of element-element and element-

mineral relationships (Svensden *et al.*, 2007; Ratcliffe *et al.*, 2012; Sano *et al.*, 2013; Craigie, 2015 and references cited therein). PCA reduces the total variability in a dataset to a smaller number of variables known as principal components. Principal component scores, determined from the eigen vectors (EV), are assigned to each sample and can be plotted on a binary diagram. The closer the variables (i.e., elements) plot to one another on the diagram, the more closely they are related in the dataset. By identifying groups of clustered elements, it is possible to infer the minerals or mineral groups that may be controlling them.

The EV1 and EV2 scores for the claystones examined in this study, which account for 37.5% and 13%, respectively, of the total variance in the dataset, are plotted on **Figure 5**. Five broad element groups are observed and are discussed below. The interpretation of the likely mineralogical controls on the various element groups are based on the element-mineral relationships summarised by Salminen *et al.* (2005) and supported by the whole-rock, clay fraction and heavy mineral data acquired on the claystones in this study (see **Figures 4** and **8**).

Group 1: Includes Ca, Sr and Mn. The XRD data presented in **Figure 4** indicates that Ca is associated with Ca-carbonates and gypsum. The close association of Sr and Mn, suggests that these elements are controlled by similar mineral phases.

Group 2: Includes Zr and Hf. This cluster of elements is interpreted to be controlled almost exclusively by zircon, which commonly occurs in all the samples subjected to HM analysis (**Figure 8**).

Group 3: Includes Si only. As demonstrated in **Figure 4**, quartz is the likely dominant host of Si in the claystone dataset.

Group 4: Includes K, Na, Ti, Nb, Ta, Y, P, U, the HREEs and the middle rare earth elements (MREEs: Sm, Eu, Gd, Tb, Dy). This cluster of elements is interpreted to be controlled by a variety of minerals including K- and Na-feldspar, mica, garnet (Y, MREEs and HREEs), apatite (P and U) and rutile (Ti, Nb and Ta). All these minerals are commonly reported in the HM and XRD datasets (see **Figure 8**).

Group 5: Includes Al, Ga, Rb, Cs, Sc, Cu, Co, Be, Th, LREEs, Mg, Fe, Ni and Cr. This cluster of elements is likely controlled by the clay minerals (smectite, illite and kaolinite are common in the claystone XRD dataset) and fine grained REE-phosphate minerals (monazite, florencite, rhabdophane - Laveuf & Cornu, 2009; Berger *et al.*, 2008, 2014).

Based on the element-element relationships considered above and the mineralogical data presented in this study, the dominant key minerals controlling the index elements are presented on **Table 5**.

Table 5: Dominant mineral controls of the key index elements employed in this study.

Element	Dominant Minerals
Si	Quartz
Al	Clay minerals
Mg & Sc	Smectite
K	K-feldspar, mica, illite
Na	Na-plagioclase
Zr	Zircon
Ti	Rutile
P, Th & LREEs	LREE-phosphate minerals (apatite, monazite, rhabdophane)
HREEs	Zircon & garnet

The key elements have been combined to produce the following geochemical ratios: Si/Al, Zr/Th, Th/Sc, P/Al, LREE/HREE and Mg/Al. Element ratios are employed instead of the individual elements to demonstrate stratigraphic changes between minerals and to negate the effects of dilution by carbonates or quartz (Van der Weijden, 2002). The mineralogical significance of these ratios is considered in the following paragraphs and summarised on **Table 6**.

The chemical index of alteration (CIA) developed by Nesbitt & Young (1982) and McLennan *et al.* (1993) is also employed in the Kilwa Group chemostratigraphic framework. The CIA quantifies the degree of weathering of K, Na and Ca silicate minerals and concentration of residual Al in the form of alteration clays in sedimentary rocks relative to the unweathered upper continental crust. The CIA calculation is as follows:

$$CIA= Al_2O_3/(Al_2O_3+K_2O+Na_2O+CaO)x100$$

As presented in **Figure 4**, Ca abundance in the Kilwa Group claystones is overwhelmingly influenced by carbonate and sulphate minerals and not by Ca-silicates. Thus, for this paper, CaO is removed from the CIA calculation and the index reflects the weathering of only the Na and K minerals in the Kilwa Group claystones relative to the upper continental crust. On the relevant figures and in the text, the profile is referred to as CIA (-CaO).

Table 6: Key element ratios and indices employed in this study and their mineralogical interpretation.

Geochemical Ratio / Index	Mineralogical Interpretation: Abundance and Relative Abundance of Minerals
Si/Al	Quartz relative to clay
P/Al	All P-bearing minerals (detrital and/or authigenic) relative to clay
Zr/Th	Zircon relative to Th-bearing minerals (e.g., monazite, apatite, rhabdophane)
Th/Sc	Minerals derived from a felsic source relative to those derived from a ferromagnesian source (see McLennan, 1989; McLennan *et al.*, 1993; Nesbitt & Markovics, 1997)
LREE/HREE	LREE-phosphate minerals (e.g., apatite, monazite, rhabdophane) relative to HREE-rich varieties (e.g., garnet and zircon).
Mg/Al	All Mg-bearing minerals (e.g., smectite & ferromagnesian heavy minerals) relative to kaolinite

As discussed in **Section 3.3**, the chemostratigraphic framework proposed for the Kilwa Group claystones is interpreted to be controlled by a variety of geological factors acting on the sediments prior to, or during deposition. These include the mineralogy of the parent rocks, changes in sediment provenance, chemical weathering and depositional environment. Post-depositional diagenetic processes acting on the claystones is considered minimal in the study area, particularly in the successions cored onshore. These rocks have never been deeply buried and, as interpreted by Pearson *et al.* (2001), the claystones likely inhibited movement of diagenetic fluids, resulting in the excellent preservation of the foraminifer shells throughout the group.

3.2 CHEMOSTRATIGRAPHIC FRAMEWORK OF THE KILWA GROUP

The work presented in this paper builds upon that of McCabe (2021), who demonstrated the chemostratigraphic characteristics of the Kilwa Group, as cored by the TDP, but did not correlate the KGCS to broadly contemporary rocks encountered in the subsurface. McCabe developed a chemostratigraphic framework for the subsurface of the Mandawa Basin that comprised ten chemostratigraphic sequences: four of which are discussed in this paper (see

Table 7). The Kilwa Group itself is largely equivalent to the Middle-Late Cretaceous Sequence (MLC) and Paleogene Sequence (Pg; **Figure 6**).

Table 7: Chemostratigraphic sequences defined in the Mandawa Basin.
(Sequences in bold text are those examined in this paper).

Chemostratigraphic Sequence Name	Abbreviation
Late Paleogene to Neogene Sequence	**LPg-Ng**
Paleogene Sequence	**Pg**
Middle-Late Cretaceous Sequence	**MLC**
Early Cretaceous Sequence	**EC**
Late Jurassic to Early Cretaceous Sequence	LJEC
Middle Jurassic Sequence (a & b)	MJ (a&b)
Early-Middle Jurassic Sequence	EMJ
Early Jurassic Sequence	EJ
Late Triassic to Early Jurassic Sequence	LTEJ

Chemostratigraphic Sequences MLC and Pg are divided into higher resolution chemostratigraphic packages and some of the packages are divided into even higher resolution chemostratigraphic units. The various chemostratigraphic divisions recognised in the Kilwa Group claystones, as well as the key element ratios used to define them and observed minerals / mineral changes supporting the geological interpretations, are described in **Table 8**, and presented on **Figures 6, 7** and **8**.

Table 8: Geochemical and mineralogical characteristics of the claystone-based chemostratigraphic divisions examined in this study.

Sequence	Claystone Characteristics	Package	Claystone Characteristics	Unit	Claystone Characteristics
LPg-Ng	Low Th/Sc values and high CIA (-CaO) values				
	Highest epidote and lowest garnet percentages				
Pg	Highest Th/Sc values, high CIA (-CaO) values. Lowest Si/Al and Zr/Th values.	Pg3	Lower and upwardly decreasing LREE/HREE & Mg/Al values		
			Slight increase in quartz and decrease in kaolinite		
	Low apatite, plus low and upwardly decreasing garnet percentages. Elevated titanite. Presence of epidote	Pg2	High P/Al, Mg/Al and LREE/HREE values. Lower CIA (-CaO) values		
		Pg1	Low P/Al & Mg/Al values. High LREE/HREE values, highest CIA (-CaO) values	Pg1c	low and upwardly increasing P/Al & Mg/Al values
				Pg1b	Lowest P/Al and Mg/Al values
	Elevated kaolinite (kaolinite/K+Na minerals) values than MLC Sequence			Pg1a	low and upwardly decreasing P/Al & Mg/Al values
			Lowest apatite percentages		lowest apatite percentages
			Highest kaolinite values		
MLC	Low Th/Sc values, intermediate CIA (-CaO) values	MLC2	Intermediate LREE/HREE & CIA values		
			Lowest ZTi index		
			Highest calcite values		
	Garnet-dominated heavy mineral assemblage. Apatite percentages higher than Pg Sequence. Epidote is absent	MLC1	Low HREE/LREE & High P/Al values	MLC1c	High Mg/Al values & Low CIA (-CaO) values
	Lower kaolinite (kaolinite/K+Na minerals) values than Pg Sequence			MLC1b	Intermediate Mg/Al and CIA (-CaO) values
					Subtle increase in kaolinite values
				MLC1a	High Mg/Al values & lowest CIA (-CaO) values
EC	Highest Si/Al & Zr/Th values. Lowest CIA (-CaO) & LREE/HREE values				
	Highest apatite percentages. Low garnet percentages				
	Quartz and plagioclase-rich				

3.3 PALAEOGEOGRAPHIC, PALAEOCLIMATIC AND PROVENANCE CONTROLS ON THE CHEMOSTRATIGRAPHIC ZONES

The geochemical and mineralogical evolution of the Kilwa Group is discussed below using the various chemostratigraphic sequences, packages and units as the framework. The palaeogeographic, environmental and palaeoclimatic significance of the key element ratios employed to define the chemostratigraphic framework are also considered here.

3.3.1 EC Sequence

The EC Sequence is the oldest chemostratigraphic sequence discussed in this paper. It is present in TDP-40 and Taachui-1ST but has not been penetrated by Pweza-1 (**Figure 6**). When compared to the succeeding chemostratigraphic sequences, the high Si/Al and Zr/Th values and low LREE/HREE values that characterise the EC Sequence claystones are attributed to an overall abundance of detrital quartz; zircon and other HREE-bearing heavy minerals relative to LREE and Th-bearing minerals and clay minerals. The XRD data confirms that, when compared to all succeeding analysed samples, the claystone analysed from the EC Sequence is the most quartz-rich and clay mineral-depleted (**Figure 8**).

The geochemical and mineralogical composition of the EC Sequence claystones is interpreted to be indicative of a depositional environment of sufficiently high energy to deposit a higher proportion of silt-grade quartz and zircon than the claystones of the succeeding chemostratigraphic sequences and retain a higher proportion of the finer-grained mineral phases in suspension. Based on their geochemical and sedimentological examination of mudrock and siltstone cores from the Wolfcamp and Bone Springs Formations, USA, Driskill *et al.* (2018) offered a similar geological interpretation for the same elemental relationships. Driskill *et al.* demonstrated that siltstones generally had higher Si/Al and Zr values than the mudrocks and that, because of its strong relationship with Al, Th was likely associated with heavy minerals present in the clay size fraction. It is likely, therefore, that the EC Sequence rocks are siltstones that have a higher proportion of coarser grained terrigenous material, whereas the MLC rocks represent mudstones that have a higher proportion of clay minerals and clay-sized heavy minerals. The upward decrease in silt-grade terrigenous minerals observed between the EC and MLC Sequences probably indicates a change in depositional environment.

In the Mandawa Basin, a similar conclusion was reached by Berrocoso *et al.* (2015), who reported that the sediments encountered in TDPs 40A&B were deposited in a proximal marine setting with a relatively high terrigenous input. Indeed, Berrocoso *et al.* suggested that the sandstones encountered in the lower portion of TDP-40A may be indicative of a terrestrial setting, rather than the shallow-marine environments encountered in the middle and upper reaches of the borehole. Berrocoso *et al.* (2010) reported that the energy of deposition throughout most of the cored interval of TDP-24A (downwards from 11m; their 'lithofacies 2') is lower than that of the underlying sediments but still higher than that of younger sediments. Their interpretation is corroborated by the results acquired in this paper, because from the Albian to the end of the Cenomanian in both TDP-24 and the deep water wells, there is an upward decrease in Si/Al and Zr/Th values recorded in the claystones of the KGCS, which is indicative of a gradual decrease in energy leading to a reduction in the proportion of coarse grained detrital minerals (quartz and zircon) within the marine environment (**Figure 6**).

3.3.2 MLC Sequence

The MLC Sequence is the oldest complete chemostratigraphic sequence cored by the TDP boreholes and intersected by wells Taachui-1 & -1ST and Pweza-1. The MLC Sequence equates to the sedimentary rocks deposited during the Albian Stage and the Late Cretaceous. In contrast to the preceding chemostratigraphic sequence, detrital quartz and zircon are lower in abundance in the claystones of the MLC Sequence. This interpretation is supported by the geochemical data (lower Si/Al, and Zr/Th values - **Figure 6**) and XRD data (lower quartz and higher proportion of clay minerals and / or carbonate minerals - **Figure 8**). The geochemical and mineralogical composition of the MLC Sequence claystones is indicative of a depositional environment of sufficiently low energy to impede the transportation and deposition of silt-grade detrital minerals (quartz and zircon) to the outer shelf and upper slope environments and favour the deposition of finer-grained minerals out of suspension.

This environmental interpretation corroborates conclusions reached by Berrocoso *et al.* (2015) and Sansom (2018). Based on sedimentological analysis of the TDP cores, Berrocoso *et al.* reported that the depositional setting of the Lindi Formation claystones was low energy most of the time. Using 3D seismic and well data from the offshore areas covered by Blocks 1, 3 and 4, Sansom considered that a rapid increase in water depths and westward retreat of

continental clastic supply systems occurred during the widespread end-Aptian marine transgression. Thus, the study area rapidly transitioned from a proximal to a distal outer shelf marine environment between Sequences EC and MLC.

3.3.2.1 MLC Packages

Two chemostratigraphic packages are recognised in the MLC Sequence of the KGCS and the deep water wells. The Package MLC1 claystones were deposited during the Albian to early Campanian (calcareous nannofossil zone UC14; **Figure 14**), whereas the Package MLC2 claystones were deposited throughout the remainder of the Cretaceous. The claystones of Package MLC2 have LREE/HREE, CIA (-CaO) values and Mg/Al values between those in the claystones of the preceding package and the succeeding sequence (**Figure 7**). The difference in claystone chemistry is related to a change in the proportion of LREE-bearing minerals relative to HREE varieties and a decrease in felsic minerals and illite+smectite. The decrease in these minerals marks the start of an uninterrupted upward increase in the amount of chemically weathered material being deposited in the marine environment between the Campanian and Thanetian Stages. This weathering interpretation is supported by the XRD results presented in **Figure 8**. Sample TDP-37 (43.81m core depth, 801.87m composite depth) analysed from the Maastrichtian of Package MLC2 contains more kaolinite relative to feldspar (high kaolinite/K+Na mineral values) and illite+smectite than the analysed claystones in the preceding package.

Unlike the more substantial LREE enrichment relative to HREE that occurs in the claystones of Packages Pg1 and Pg2 (see below, this section) which is related to LREE enrichment, a comparison of the chondrite-normalised REE patterns of the TDP claystones with the chondrite-normalised REE patterns of the Post Archaean Australian Shale (PAAS) (Condie, 1993; **Figure 9**) reveals that the fractionation in the Package MLC2 claystones is mainly related to depletion of HREEs and, to a lesser extent, MREEs. The MREEs and HREEs are often enriched in chemically resistant heavy minerals, such as garnet and zircon (Salminen *et. al.*, 2006; Laveuf & Cornu, 2009). Consequently, the depletion in MREEs and HREEs relative to average shale may indicate that these heavy minerals are in low abundance in the Campanian and Maastrichtian rocks because of changes in hydrodynamic sorting, energy and / or sediment provenance.

Using 3D seismic data, Sansom (2018) reported that the high-energy north-flowing contour currents that influenced the depositional architecture of the Albian to Early Campanian sediments between the study area and the Seagap Fault shifted outboard of that structure during the Middle Campanian to Maastrichtian (i.e., during the deposition of the MLC2 claystones). This shift led to an overall decrease in energy in the study area that is likely to account for the change in REE composition of the Kilwa Group claystones during this time.

Based on the heavy mineral data acquired from the MLC Sequence claystones, there is little variation in the percentages of garnet and zircon relative to other recorded heavy minerals in the assemblage that could be used to support the interpretation of the LREE/HREE ratio variation in Package MLC2 (**Figure 8**). However, the zircon-tourmaline (ZTi) index (Morton, 2007) of the heavy minerals acquired from the Kilwa Group claystones, shows that the combined sample from the Maastrichtian interval of TDP-37 has the lowest recorded values in the study interval. According to Morton (2007), the ZTi index reflects differences in hydrodynamic sorting rather than provenance because zircon and tourmaline have different densities (4.7 vs. 3-3.25g/cm^3, respectively: Mange & Maurer, 1992). Thus, the higher proportion of less dense heavy minerals relative to denser species indicates that the energy of environment was probably lower during the deposition of the Package MLC2 claystones than that of the preceding chemostratigraphic package.

MLC1 Units

Package MLC1 is divided into three chemostratigraphic units (MLC1a-c), all of which are recognised in the Kilwa Group composite and the deep water exploration wells (**Figure 7**). The threefold division is based on up-section fluctuations in the Mg/Al and CIA (-CaO) values of the MLC1 claystones, with the lowest and highest values, respectively, encountered in Unit MLC1b. As with the more substantial change in values of these geochemical parameters that defines the package-level division of the MLC Sequence, the fluctuations in Mg/Al and CIA (-CaO) values recorded in the Package MLC1 claystones reflect more subtle changes in chemical weathering episodes during the earlier stages of the Late Cretaceous. The weathering interpretation is supported by the XRD data (**Figure 8**), which shows that kaolinite values are highest in the TDP-31 claystone analysed within Unit MLC1b.

From the chronostratigraphic information of the study intervals, the onset of this earlier (and shorter lived) episode of chemical weathering occurred around the end of the Cenomanian (top *Rotalipora cushmani* planktonic foraminifera zone; **Figure 14**). The decrease in chemical weathering that marks the top of Unit MLC1b is diachronous (the only diachronous chemical boundary observed in this study). In the KGCS and in well Pweza-1, the top of MLC1b is picked in the Santonian / Late Coniacian (base of the *Dicarinella asymmetrica* zone), whereas in well Taachui-1ST, the base of the unit is older and picked within the *Dicarinella concavata* zone (Late Turonian). The diachronous change in chemical weathering observed in the study area during the Late Cretaceous could be related to the location of Taachui-1ST away from the influence of the large Rufiji and Ruvuma river catchments (**Figure 1**). Accordingly, the smaller river systems that drained the Mandawa Basin directly may have transported and deposited less weathered material to the outboard area earlier than in the north and south of the study area. Regardless of the diachronous onset of recovery from chemical weathering, the highest Mg/Al values and lowest CIA (-CaO) values encountered in the claystones on Unit MLC1c occur within the Santonian / Late Coniacian (coincident with the *D. asymmetrica* zone).

3.3.3 Pg Sequence

The Pg Sequence equates to the sediments deposited during the Paleogene up to and including the early Oligocene (Rupelian). Compared to the previous chemostratigraphic sequences, the high(est) CIA (-CaO) values encountered in the claystones of the Pg Sequence (**Figure 6**) reflect a period of intense chemical weathering of rocks in the Tanzanian hinterland that resulted in the deposition of K- and Na-depleted minerals in the marine environment. The chemistry is supported by the XRD data, which shows that all analysed samples from the Pg Sequence have the highest kaolinite and kaolinite/K+Na mineral values (**Figure 8**). The increase in weathering during the greater part of the Paleogene occurs during a time when global marine temperatures were between 10^{o}C and 14^{o}C warmer than the present day (Zachos *et al.*, 2008; Pearson *et al.*, 2001; Handley *et al.*, 2012).

The high Th/Sc and LREE/HREE values of the Pg Sequence claystones correspond to an increase in the abundance of detrital Th-bearing minerals relative to Sc-rich minerals (e.g., pyroxene and smectite - Wilson, 2004; Salminen *et al.*, 2005). Th and Sc are useful for

determining variations in sediment provenance in sedimentary rocks due to their insolubility and immobile character during transport, diagenesis, weathering and metamorphism (e.g., Taylor & McLennan, 1985; McLennan, 1989; Condie, 1993; McLennan *et al.,* 1993; Hofer *et al.,* 2013). The Th/Sc ratio is particularly useful for distinguishing derivation from mafic and felsic source areas because Th is more abundant in felsic crustal rocks and Sc is generally more abundant in mafic rocks (McLennan, 1989). Most Pg Sequence claystones have Th/Sc values above 0.95 (baseline of the blue colour fill – **Figure 6**), maximum values of 1.5 and average values of 1.05, which are interpreted to mark an increase in the contribution of detrital material derived from a predominantly felsic crustal source area.

A change in sediment provenance across the Cretaceous – Palaeogene boundary is, in part, supported by the HM data acquired from the Kilwa Group claystones (**Figure 8**). Whilst garnet dominates the HM assemblage in the Cretaceous claystones of the MLC Sequence, it is generally lower in abundance in the Paleogene claystones of the Pg Sequence. Apatite is also less abundant in the claystones of the Pg Sequence. Conversely, titanite is generally more abundant in the Pg Sequence claystones and minerals such as epidote and kyanite are also present, although the latter two become more prominent in the assemblage during the Eocene.

Similar trends were observed in the HM assemblages of the TDP sandstones examined optically by Fossum *et al.* (2018; **Figure 8**). Based on their work, sandstones with a garnet-dominated heavy mineral assemblage were identified as the most common in the Mesozoic and Cenozoic successions of the Mandawa Basin. Using electron probe micro analysis (EPMA) they also suggested that the garnets indicate derivation from a wide range of sources, including amphibolite and granulite facies metamorphic rocks. Those authors proposed that the garnet-rich sands were likely eroded from parent rocks located in the interior of Tanzania and transported to the study area from the palaeo-Rufiji River to the north.

Fossum *et al.* (2018) also recognised an influx of garnet-depleted and epidote-dominated sandstones during the Eocene and Oligocene (**Figure 8**). As well as lower percentages of garnet in the overall HM assemblage, a reduction in chemical diversity of garnet species (as determined by EPMA) in these sandstones indicates derivation from fewer metamorphic localities. Fossum *et al.* suggested that the epidote-dominated sandstones were likely sourced

from the Masasi Spur and transported to the study area by the Matandu and Mbemkuru Rivers to the west.

The results of the heavy mineral analysis conducted on the Kilwa Group claystones in this study are broadly supportive of the results and conclusions of Fossum *et al.* (2018). However, it is suggested here that the change in provenance from garnet-dominated to epidote- (and titanite-) dominated rocks occurred during the Paleocene (Selandian Stage at least), rather than the Middle Eocene (**Figure 8**).

The chondrite-normalised REE data presented in **Figure 9**, demonstrate that the LREE/HREE fractionation in the Pg Sequence claystones is controlled as much by LREE enrichment as it is by HREE depletion. LREEs are often present in primary minerals that are susceptible to chemical weathering so the LREE-HREE fractionation may also be related to a change in climatic and environmental conditions that increased chemical weathering and erosion of LREE-rich sediments in the hinterland. In this instance, LREE enrichment as a function of weathering is favoured as a stronger control on the LREE/HREE ratio than HREE depletion triggered by changes in environment and provenance. According to Laveuf & Cornu (2009) and Babechuk *et al.* (2014), LREEs are retained (or more retained than MREEs and HREEs) in laterites during *in situ* chemical weathering and the MREEs and HREEs tend to be leached to deeper parts of the profile (Berger *et al.*, 2014). If a change in climatic and environmental conditions in the hinterland caused laterites to be partially eroded, then the resultant material deposited in the offshore area is likely to be LREE rich.

3.3.3.1. Package Pg1

The Pg Sequence is divided into three chemostratigraphic packages. The claystones of Package Pg1 have the lowest P/Al values encountered in the Kilwa Group study interval, indicating that they contain the fewest phosphatic minerals (**Figure 7**). The heavy mineral data acquired on the Kilwa Group claystones support the geochemical results, as they show that apatite values are lowest in Package Pg1 (**Figure 8**). The decrease in detrital apatite may be related to a change in sediment provenance during the Paleocene and Eocene. However, apatite is chemically unstable under some climactic and environmental conditions (Morton & Hallsworth, 1999) and it also possible that the decrease in this mineral is related to a change

in either sediment provenance or climate / environment during the Paleogene.

On balance, it is likely that the decrease in P/Al values observed in the Package Pg1 claystones is controlled by a change in climate and / or environment during the Early Paleogene. The decrease in P/Al values coincides with an increase in global sea level during the Paleocene, reaching a maximum during the early Eocene (**Figure 10**). Indeed, the global sea level curve presented by Miller *et al.* (2005) is largely the inverse of the Si/Al curve. The combination of the geochemical data and sea-level information strongly suggests that the Package Pg1 claystones were deposited in the most distal and / or deeper water environments than those of the preceding sequence and succeeding packages.

Pg1 Units

Package Pg1 is divided into three chemostratigraphic units (Pg1a-c). All three are recognised in Pweza-1, whereas only parts of Units Pg1a and Pg1c have been cored by the TDP (**Figure 7**). The threefold division is based on up-section fluctuations in the Mg/Al and CIA (-CaO) values of the Pg1 claystones. The lowest Mg/Al values and highest CIA (-CaO) values (and lowest and highest values in the entire study interval), are encountered in Unit Pg1b. As with the units of the MLC1 Package, the unit-level change in chemistry of the Kilwa Group claystones is interpreted to reflect a decrease in detrital K-, Na- and Mg-bearing minerals (feldspars and illite+smectite) in response to an increase in chemical weathering of the detrital clastic material prior to deposition in the marine environment.

The claystones from most weathered sources encountered in the Kilwa Group study interval do not coincide with the PETM at 55.5 Ma or the Early Eocene Climatic Optimum (EECO; 53.3 - 49.1 Ma; Inglis *et al.,* 2020; **Figure 2**) but occur during late Selandian (58 - 59 Ma) (**Figure 7**). Indeed, from the upwardly increasing Mg/Al values and upwardly decreasing CIA (-CaO) values throughout Unit P1b, it is argued that during the late Thanetian and early Ypresian (and including the PETM), the claystones of the Kivinje Formation were derived from progressively less weathered sources. Based on the heavy mineral data acquired in this study and by Fossum *et al.* (2018; **Figure 8**), it is likely that the observed upward decrease in chemically weathered material of the Package Pg1c claystones is related to a gradual change in drainage onshore.

These arguments do not imply that the influence of the PETM, EECO and other Eocene thermal maxima (ETM) cannot be observed in the geochemical data. Based on their work on TDP-14, Handley *et al.* (2012), noted an increase in Ti/Al and Si/Al values in the claystones at the PETM and interpreted the data to reflect a period of enhanced terrestrial input related to changes in the hydrological cycle. The same geochemical trends are recognised in the geochemical data acquired for this study (**Figure 11**) and thus support the interpretation of Handley *et al*. Additionally, from the heavy mineral data acquired from the TDP-14 claystones, there is an increase in the Ti-bearing minerals rutile and titanite within the PETM interval (**Figure 8**).

When the CIA (-CaO) and Mg/Al ratios are included and the TDP-14 interval studied by Handley *et al.* (2012) is expanded to include TDPs 7B and 8, several features are observed (**Figure 11**). Firstly, the Ti/Al and Si/Al excursions at the PETM are preceded by an increase in CIA (-CaO) values and a decrease in Mg/Al values, indicating that a weathering episode builds up to, and then terminates at the period of enhanced terrestrial input. Secondly, this trend is not unique and a similarly large increase in chemical weathering that terminates at a period of enhanced terrestrial input occurs within TDP-8 and may relate to the 'Eocene thermal maximum 2', which is the second major, but shorter-lived (<50,000 years), hyperthermal event that occurred around 53.5 million years ago (Sluijs *et al.*, 2009). Thirdly, a series of similar, but even shorter lived and less pronounced events occur throughout TDP-7B and may reflect cyclical oscillations in the hydrological cycle associated with the EECO. These short-lived geochemical features in the CIA (-CaO) and Mg/Al curves that may be influenced by Eocene climatic events are excursions that stand out against decreasing and increasing trends, respectively, which may be related to changes in drainage onshore (**Figure 11**). Indeed, the decrease in CIA (-CaO) values, increase in Mg/Al values, as well as highest proportions of titanite and epidote encountered in the Pg2 claystones that are diagnostic of the package (**Figures 7** and **8**), may represent the period of maximum contribution of detritus from greenschist and amphibolite facies metamorphic rocks during the Paleogene portion of the Kilwa Group.

3.3.3.2. Package Pg2

In the study area, the Package Pg2 claystones were deposited between the Ypresian and Priabonian Stages (**Figure 7**). As discussed in the **Pg1 Units** section above, the subtle decrease in CIA (-CaO) values and increase in Mg/Al and P/Al values of the Package Pg2 claystones, corresponds to an influx of minerals (feldspars, phosphates, illite+smectite) that were probably derived from a local metamorphic source area in the Tanzanian hinterland that is also rich in titanite and epidote but depleted in garnet (**Figure 8**).

3.3.3.3. Package Pg3

The decrease in LREE/HREE values in the Package Pg3 claystones is indicative of a change in climatic and / or environmental conditions that contributed to an overall reduction in chemical weathering, transportation and deposition of (L)REE-rich material from the hinterland to the study area. The decrease in LREE/HREE values coincides with the decrease in sea surface temperatures inferred by Pearson *et al.* (2007) in the late Eocene and early Oligocene, which further supports the argument that the REE fractionation in the Kilwa Group claystones is, at least in part, climate controlled. Additionally, Jacobs (2004) noted that, across many parts of Africa, palaeobotanical data suggests a re-establishment of forested areas during the late Eocene. That reforestation may have led to greater stabilisation of soil in the hinterland, leading to decreased soil erosion.

Throughout Package Pg3 in TDP-12, there is a general upward increase in Si/Al and Zr/Th values that, as mentioned above in this section, is likely to reflect an increase in energy of the marine environment favouring the deposition of silt-grade detrital minerals over finer-grained Al-silicate and clay minerals (**Figure 6**). The increase is probably related to a change to more shallow / proximal marine conditions triggered by eustatic sea level drop (Miller *et al.* 2005 - **Figure 10**). Indeed, Nicholas *et al.* (2006) attributed the Pande Formation claystones to a shallower marine environment than that of the claystones of the preceding formations.

A rapid but short-lived increase in Si/Al and Zr/Th values are recorded in the claystones of the upper 25m of TDP-12, throughout much of TDP-17 and may be represented by the only Package Pg3 claystone analysed in Pweza-1 (**Figures 6** and **12**). The change in chemistry is, again, related to an increase in silt-grade detrital quartz and zircon relative to finer-grained

Al-silicate and clay minerals and likely controlled by an increase in hydrodynamic energy of the marine environment. The change in energy occurs during the Rupelian and coincides with the early Oligocene glacial maximum that marks the transition from the Eocene into the Oligocene (Pearson *et al.*, 2008). Despite a sample gap in TDP-17 (**Figure 12**), the increase in Si/Al and Zr/Th values coincides with the second step in δ18O stable isotope values recorded by Pearson *et al.* (2008) and Lear *et al.* (2008), which they attribute to ice-sheet advance over the poles. Claystones with similarly high Si/Al and Zr/Th values are not present in TDP-1 (see the LPg-Ng Sequence of the KGCS on **Figure 6**), which suggests that the period of high energy was short-lived and did not continue later into the Rupelian Stage.

3.3.4. LPg-Ng Sequence.

The claystones of the LPg-Ng Sequence record low Th/Sc and LREE/HREE values that are interpreted to record a decrease in the abundance of detrital Th-bearing minerals during the late Paleogene and Neogene. This chemical signature highlights a change in sediment provenance, perhaps returning to something similar to that during the deposition of the MLC Sequence sediments. Although the LPg-Ng Sequence is poorly defined in the TDP cores, upper Oligocene and Miocene claystones with a similar chemical composition have been analysed by McCabe *et al.* (2012) in the Ruvuma Basin, which demonstrates that the LPg-Ng Sequence is both temporally and laterally extensive along the Tanzanian coastal margin. It is hypothesised here that the trigger for the change in provenance is the onset of tectonic activity associated with the East African Rift System (possibly the onset of the EARS 1 rifts described by Macgregor, 2014).

3.4 CHEMOSTRATIGRAPHY, LITHOSTRATIGRAPHY & BIOSTRATIGRAPHY

The chemostratigraphic framework has been integrated with the detailed biostratigraphic zonation schemes assigned to the TDP boreholes and deep water wells (**Figure 13**). The stratigraphic frameworks derived from these two approaches match at a biozone level and demonstrate that all but one of chemostratigraphic boundaries represent synchronous events in Tanzania during the deposition of the Kilwa Group sediments. The integration of the chemostratigraphic, biostratigraphic and lithostratigraphic schemes for the Kilwa Group are presented in **Table 9**.

Table 9: Comparison of the chemostratigraphic and lithostratigraphic framework for the Kilwa Group presented in this paper with the planktonic foraminifera and calcareous nannofossil zones identified in the study interval.

Lithostratigraphy		Chemostratigraphy			Top / Base	Planktonic Foraminifera Zone		Calcareous Nannofossil Zone	
Group	**Formation**	**Sequence**	**Package**	**Unit**					
Kilwa	Pande	Pg	3		T.	**T.** P18		**T.** NP21	
					B.	**T.** P15		NP18 (?)	
	Masoko		2		T.				
					B.	**T.** P6b		**T.** NP11	
	Kivinje		1	c	T.				
					B.	**T.** P4b (?)		**I.** NP9a	
				b	T.				
					B.	**T.** P4a(?)		**I.** NP6	
				a	T.				
					B.	**T.** *A mayaroensis*		**T.** UC20	
	Nangurukuru	MLC	2		T.				
					B.	**T.** *D. asymmetrica*		**B.** UC14	
	Lindi		1	c	T.				
					B.	**B.** *D. asymmetrica*	**B.** *D. concavata:* (Taachui)	**I.** UC10	**I.** UC9 (Taachui)
				b	T.				
					B.	**B.** *W. archaeocreta*		**I.** UC4	
				a	T.				
					B.	**B.** *M. Rischi*		**B.** BC22	

T. = Top, **B.** = Base, **I.** – Inter.

One of the objectives of this study is to compare the chemostratigraphic framework established here with the lithostratigraphy of the Kilwa Group and its associated formations proposed by Nicholas *et al.* (2006) and Berrocoso *et al.* (2015) on the TDP boreholes. **Figure 14** presents the comparison and reveals that overall, there is a good match between the chemostratigraphic and lithostratigraphic schemes. Even so, refinements to the lithostratigraphic scheme are proposed based on the chemostratigraphy and biostratigraphy.

Nicholas *et al.* (2006) proposed that the Kilwa Group spanned a c.55 Ma interval of time, covering the Santonian to Rupelian and Berrocoso *et al.* (2015) extended the base of the group to the Upper Albian. However, it is suggested that the Kilwa Group spans the whole of the Albian to middle Rupelian Stages (c.83 Ma.). Accordingly, the Kilwa Group is equivalent to chemostratigraphic Sequences MLC and Pg, the claystones of which are interpreted to have been deposited during the period of maximum transgression in the passive margin tectonic phase.

The base of the Kilwa Group is picked at c.8m in TDP-40, which corresponds to the Aptian – Middle Albian unconformity identified biostratigraphically by Mweneinda (2014) and Berrocoso *et al.* (2015). The revised interpretation, based on the inorganic geochemical data, suggests that the MC Sequence rocks encountered in TDP-40, Taachui-1 and -1ST correspond to the underlying Mavuji Group (Hudson, 2010; Fossum *et al.,* 2021; McCabe, 2021).

The suggested revision of the top of the Kilwa Group corresponding with the top of the Pg Sequence is closely comparable to that originally interpreted by Nicholas *et al.* (2006). Both the lithostratigraphic and chemostratigraphic results place the termination within the lower Oligocene. However, it is suggested here that the top is placed at the top of the NP21 calcareous nannofossil zone rather that the top of the NP23 zone. The revised interpretation, based on the inorganic geochemical data, would suggest that TDP-1 represents the earliest sediments of a new group of formations (the 'Songo Songo Group' of Hudson, 2010 and Fossum *et al.,* 2021) that continue through the remainder of the Oligocene Epoch and probably into the Neogene Period.

In this study, the Lindi Formation equates to Package MLC1. Based on the inorganic geochemical data, the top of the formation extends into the Campanian Stage (base of nannofossil zone UC15b – although in the deep water wells, the base occurs in the UC14 zone, which has not been cored by the TDP). The result of the proposed revision of the Lindi Formation is that the Nangurukuru Formation would equate to Package MLC2 and is restricted to most of the Campanian and Maastrichtian Stages only (**Figure 14**).

The placement of the top of the Lindi Formation into the Campanian conflicts with the interpretation of Berrocoso *et al.* (2015), who picked the boundary within the Coniacian-Santonian interval of TDP-39 (between core parts 28-30 and around the top of the *D. concavata* zone). Using carbonate data acquired from stable isotope analysis, Berrocoso *et al.* placed the formation top at the base of a sharp $CaCO_3$ increase in the TDP-39 claystones and argued that the Nangurukuru Formation is generally more calcareous than the Lindi Formation. Whilst the $CaCO_3$ data acquired for this study is broadly supportive of the interpretations made by Berrocoso *et al.,* the $CaCO_3$ trend is not consistent between the two formations in the TDP cores and in the deep water wells. The Campanian sediments encountered in TDP-23 (assigned to the Nangurukuru Formation by Berrocoso *et al.,* 2015) also have low $CaCO_3$ values (**Figure 15**). Additionally, McCabe (2021) reported that age-equivalent outcrops to the Lindi Formation in the Mandawa Basin are not consistently calcareous either but do have similar REE signatures that are consistently definitive of Package MLC1. Thus, it is argued here that the REEs provide a more consistent means of differentiating the Lindi and Nangurukuru claystones and not $CaCO_3$, which appears more variable.

Nicholas *et al.* (2006) placed the top of the Kivinje Formation within a 10m interval (between 53-62m) in TDP-2. The interval marks the first appearance of large benthic foraminiferal coquinas, which are characteristic of the Masoko Formation, and a change in hardness of the clay. In this study, the Kivinje Formation equates to Package Pg1 and is slightly thinner than that proposed by Nicholas *et al.* (2006). The geochemical data picks a strong boundary between TDPs 2 and 3 and suggests that the true chemostratigraphic boundary lies somewhere between nannofossil zones NP11 and NP14 (**Figure 14**). The integration of the chemostratigraphic and biostratigraphic results from well Pweza-1 support this lithostratigraphic assignment. In both the well and TDP boreholes, calcareous nannofossil zones NP12 and NP13 are absent. In addition, the boundary marks the change in depositional environment associated with the Kivinje (most distal marine) and Masoko (more proximal marine) Formations. Acceptance of Package Pg1 as representing the Kivinje Formation would make the formation slightly thinner than originally defined.

Finally, Package Pg2 is interpreted to correspond to the Masoko Formation, whereas Package Pg3 is interpreted to equate to the Pande Formation (**Figure 14**). The revised boundary between the two formations is picked within TDP-12, rather than the top of TDP-4 (i.e., within the Priabonian Stage, rather than at the Bartonian / Priabonian boundary). The proposed revision makes the Pande Formation half as thick as that proposed by Nicholas *et al.* (2006) (100m vs. 210m), whereas the Masoko Formation is approximately a third thicker (248m vs. 170m) than that inferred by Nicholas *et al.* (2006).

4. CONCLUSIONS

Despite their broadly uniform sedimentological characteristics, it is demonstrated in this study that the thick succession of outer shelf and upper slope marine claystones deposited in the Mandawa and Ruvuma Basins, southern Tanzania, between the Albian and Rupelian Stages are chemically and mineralogically diverse. The largely temporal variations in the abundance of the key elements Si, Al, K, Na, Mg, Th, Zr, P, Sc and the REEs are used here to define the upper and lower boundaries of the Kilwa Group and its five formations first distinguished by the Tanzania Drilling Project (TDP). The distinct chemical signatures of the various lithostratigraphic units and sub-formational chemostratigraphic units are controlled by the changes in the proportions of detrital quartz, K- and Na-feldspars, heavy minerals and REE-phosphate minerals.

The geological interpretations drawn from the geochemical and mineralogical datasets are consistent with previous interpretations that the claystones of the Kilwa Group were deposited in a low energy and distal marine environment throughout its c.83 million year duration. These claystones contain fewer silt-grade detrital minerals (mainly quartz and feldspars) and a higher proportion of clay and authigenic minerals than the more proximal marine claystones of the preceding and succeeding lithostratigraphic groups. Within this relatively uniform depositional environment, the chemistry and mineralogy of the fine-grained material entering the study area changes over time in response to climatically influenced chemical weathering of rocks in the Tanzanian hinterland and shifts in drainage patterns. In the Mandawa Basin, the influence of chemical weathering is greatest in the Paleocene, rather than at the Paleocene-Eocene Thermal Maximum or during the Early Eocene Climatic Optimum. This is because there is a provenance overprint on the geochemistry of the Eocene claystones that reflects the influx of relatively unweathered material from local greenschist and amphibolite facies metamorphic parent rocks, which were most likely sourced from the Masasi Spur.

A primary objective of this study has been to test the established lithostratigraphy of the Kilwa Group in the TDP borehole type sections drilled onshore. Integration of the chemostratigraphic framework with detailed biostratigraphic information from the study sections and comparison with the published lithostratigraphy of the Kilwa Group reveals that

all are in broad agreement. The various formations are largely equivalent to their respective chemostratigraphic package. The results presented here are consistent with previous interpretations that the Lindi Formation sediments were deposited during the Albian to the Campanian and those of the Nangurukuru Formation belong to the remainder of the Late Cretaceous. Also in agreement with TDP, it is concluded that in the Paleogene, the Kivinje Formation sediments were deposited during the Danian through to the Ypresian, those of the Masoko Formation are Ypresian and Priabonian, whilst the Pande Formation is Priabonian and Rupelian in age. In most cases, the inorganic geochemical data suggests that most of the Kilwa Group formations, as cored onshore, are thinner than formerly proposed. Only the Masoko and Lindi Formations are interpreted to be thicker than that previously defined by the TDP.

The development of a robust multidisciplinary stratigraphic framework for the sedimentary rocks deposited in the Mandawa and Ruvuma Basins between the Albian and Rupelian Stages will undoubtedly help with hydrocarbon exploration and development in both the onshore and deep offshore areas. The changes in eustacy, tectonism, global climate and regional drainage patterns that have influenced the mineralogy of the Kilwa Group claystones will allow geologists to understand better the source to sink relationships of the detrital material and improve recognition of stratigraphic horizons within the group that are more likely to produce high quality reservoir facies in the subsurface.

ACKNOWLEDGEMENTS

The authors are extremely grateful to the Tanzanian Petroleum Development Corporation (TPDC) for arranging sampling and sample exportation on several occasions. We are also grateful to Shell (Arjan Van Vliet and Jimmy Van Itterbeeck) for permitting us to include the Block 1 and 4 wells in this paper. We would also like to thank Andrea Pardon from CGG for assisting the authors with the integration and standardisation of the deep water wells and TDP biostratigraphic results. Finally, we acknowledge our partners and colleagues at the University of Greenwich, Origin Analytical Ltd, and X-Ray Minerals Ltd for their help generating the data presented in this paper.

REFERENCES

Babechuk, M. G., Widdowson, M., Kamber, B. S., 2014. Quantifying chemical weathering intensity and trace element release from two contrasting basalt profiles, Deccan Traps, India. Chemical Geology 363, 56 - 75.

Berger, A., Gnos, E., Janots, E., Fernandez, A., Giese, J. 2008. Formation and composition of rhabdophane, bastnäsite and hydrated thorium minerals during alteration: implications for geochronology and low-temperature processes. Chemical Geology 254, 238 - 248.

Berger, A., Janots, E., Gnos, E., Frei, R., Bernier, F., 2014. Rare earth element mineralogy and geochemistry in a laterite profile from Madagascar. Applied Geochemistry 41, 218 - 228.

Berggren, W. A., Kent, D. V., Swisher, C. C., Aubrey, M. P., 1995. A revised Cenozoic geochronology and chronostratigraphy. In: Berggren, W. A., Kent, D. V., Aubry, M., & Hardenbol, J. (Eds.), Geochronology, Time Scales and Global Stratigraphic Correlation. SEPM Special Publication 54, 129 - 212.

Berggren, W. A., Pearson, P. N., 2005. A revised subtropical Paleogene planktonic foraminiferal zonation. Journal of Foraminiferal Research 35, 279 - 298.

Berrocoso, A. J., Macleod, K. G., Huber, B. T., Lees, J. A., Wendler, I., Bown, P. R., Mweneinda, A. K., Londoňo, C. I., Singano, J. M., 2010. Lithostratigraphy, biostratigraphy and chemostratigraphy of Upper Cretaceous sediments from southern Tanzania: Tanzania drilling project sites 21 - 26. Journal of African Earth Sciences 57, 47 - 69.

Berrocoso, A. J., Huber, B. T., Macleod, K. G., Petrizzo, M. R., Lees, J. A., Wendler, I., Coxall, H., Mweneinda, A. K., Falzoni, F., Birch, H., Singano, J. M., Haynes, S., Cotton, L., Wendler, J., Bown, P. R., Robinson, S. A., Gould, J., 2012. Lithostratigraphy, biostratigraphy and chemostratigraphy of Upper Cretaceous and Paleogene sediments from southern Tanzania: Tanzania Drilling Project Sites 27 - 35. Journal of African Earth Sciences 70, 36 - 57.

Berrocoso, A. J., Huber, B. T., Macleod, K. G., Petrizzo, M. R., Lees, J. A., Wendler, I., Coxall, H., Mweneinda, A. K., Falzoni, F., Birch, H., Haynes, S., Bown, P. R., Robinson, S. A., Singano, J. M., 2015. The Lindi Formation (upper Albian – Coniacian) and Tanzanian Drilling Project sites 36-40 (lower Cretaceous to Paleogene): lithostratigraphy, biostratigraphy & chemostratigraphy. Journal of African Earth Sciences 101, 282 - 308.

Blow, W. H., 1979. The Cainozoic Globigerinida: a study of the morphology, taxonomy, evolutionary relationships and the stratigraphical distribution of some Globigerinida (mainly Globigerinaceae). E.J. Brill, Leiden, 1413.

Burnett, J. A., 1998. Upper Cretaceous. In: Bown (Eds.), Calcareous Nannofossil Biostratigraphy. British Micropalaeontological Society Series, Chapman & Hall: Kluwer Academic Press, 132–199.

CGG Services UK Ltd, 2017. Offshore Tanzania Blocks 1-5: Regional stratigraphic study of selected wells. Unpublished report No. 7422/Ib prepared for BG Group.

Chemostrat Ltd, 2015. Integrated chemostratigraphic & provenance study on selected wells from Blocks 1, 3 and 4. Offshore Tanzania. Unpublished report prepared for BG Group.

Chemostrat Ltd, 2016. Integrated chemostratigraphic & provenance of the sedimentary basins along coastal Tanzania: Phase 2. Unpublished report prepared for BG Group.

Condie, K. C., 1993. Chemical composition and evaluation of the upper continental crust: contrasting results from surface samples and shales. Chemical Geology 104, 1 - 37.

Craigie, N. W., 2015. Applications of chemostratigraphy in Cretaceous sediments encountered in north central Rub' al Khali Basin, Saudi Arabia. Journal of African Earth Sciences 104, 27 - 42.

Craigie, N. W., 2016. Chemostratigraphy of the Silurian Qusaiba Member, eastern Saudi Arabia. Journal of African Earth Sciences 113, 12 - 34.

Craigie, N. W., Rees, A. J., 2016. Chemostratigraphy of glaciomarine sediments in the Sarah Formation, northwest Saudi Arabia. Journal of African Earth Sciences 117, 263 - 284.

Craigie, N. W., Breuer, P., Khidir, A., 2016. Chemostratigraphy and biostratigraphy of Devonian, Carboniferous and Permian sediments encountered in eastern Saudi Arabia: an integrated approach to reservoir correlation. Marine and Petroleum Geology 72, 156 - 178.

Davison, I., Steel, I., 2017. Geology and hydrocarbon potential of the East African continental margin. Petroleum Geoscience 24, 57 - 91.

Driskill, B., Pickering, J., Rowe, H. E., 2018. Interpretation of high resolution XRF data from the Bone Spring and Upper Wolfcamp, Delaware Basin, USA. Unconventional Resources Technology Conference Paper 2901968, 1 - 25.

Fossum, K., Morton, A. C., Dypvik, H., Hudson, W. E., 2018. Integrated heavy mineral study of Jurassic to Paleogene sandstones in the Mandawa Basin, Tanzania: sediment provenance and source to sink relations. Journal of African Earth Sciences 150, 546 - 565.

Fossum, K., Dypvik, H., Haid, M. H. M., Hudson, W. E., Van Den Brink, M., 2021. Late Jurassic and Early Cretaceous sedimentation in the Mandawa Basin, coastal Tanzania. Journal of African Earth Sciences 174.

Geiger, M., Clark, D. N., Mette, W., 2004. Reappraisal of the timing of the breakup of Gondwana based on sedimentological and seismic evidence from the Morondava Basin, Madagascar. Journal of African Earth Sciences 38, 363 - 381.

Gradstein, F. M., Agterberg, F. P., Ogg, J. G., Hardenbol, J., Van Veen, P., Thierry, J., Huang, Z., 1995. A Triassic, Jurassic, and Cretaceous time scale. In: Berggren, W. A., Kent, D. V., Aubry M., & Hardenbol, J. (Eds.), Geochronology, Time Scales and Global Stratigraphic Correlation. SEPM Special Publication 54, 95 - 126.

Handley, L., O'Halloran, A., Pearson, P. N., Hawkins, E., Nicholas, C. J., Schouten, I. K., McMillan, I. K., Pancost, R. D., 2012. Changes in the hydrological cycle in tropical East Africa during the Paleocene-Eocene Thermal Maximum. Paleogeography, Paleoclimatology, Paleoecology 329-330, 10 - 21.

Hofer, G., Wagreich, M., Neuhuber, S., 2013. Geochemistry of fine-grained sediments of upper Cretaceous to Paleogene Gosau Group (Austria, Slovakia): Implications for paleoenvironmental and provenance studies. Geoscience Frontiers 4, 449 - 468.

Huber, B. T., Macleod, K. G., Tur, N. A., 2008. Chronostratigraphic framework for Upper Campanian–Maastrichtian sediments on the Blake Nose (subtropical North Atlantic). Journal of Foraminiferal Research 38, 162 - 182.

Huber B. T., Leckie, R. M., 2011. Planktic foraminiferal species turnover across deep sea Aptian/Albian boundary section. Journal of Foraminiferal Research 41, 53 - 95.

Hudson, W. E., 2010. The geological evolution of the petroleum prospective Mandawa Basin. Southern coastal Tanzania. Unpublished Ph.D. thesis. Trinity College Dublin.

Inglis, G. N., Bragg, F., Burls, N. J., Cramwinckel, M. J., Evans, D., Foster, G. L., Huber, M., Lunt, D. J., Siler, N., Steinig, S., Tierney, J. E., Wilkinson, R., Anagnostou, E., De Boer, A. M., Dunkley Jones, T., Edgar, K. M., Hollis, C. J., Hutchinson, D. K., Pancost, R., 2020. Global mean surface temperature and climate sensitivity of the early Eocene Climatic Optimum (EECO), Paleocene-Eocene Thermal Maximum (PETM), and latest Paleocene. Climate of the Past 16, 1953 – 1968.

International Subcommission on Stratigraphic Classification., 1976. In: Hedberg, H.D. (Eds), International Stratigraphic Guide. Wiley, New York, 200

Jarvis, I., Jarvis, K. E., 1992a. Inductively coupled plasma-atomic emission spectrometry in exploration geochemistry. In: Hall, G. E. M. (Eds), Geoanalysis. Journal of Geochemical Exploration 44, 139 - 200.

Jarvis, I., Jarvis, K. E., 1992b. Plasma spectrometry in the earth sciences, techniques, applications and future trends. In: Jarvis, I., & Jarvis, K. E. (Eds), Plasma Spectrometry in the Earth Sciences. Chemical Geology 95, 1 - 33.

Kent, P. E., Hunt, J. A., Johnstone, D. W., 1971. The geology and geophysics of coastal Tanzania. National Environment Research Council, Institute of Geological Sciences, London, Geophysical Paper No. 6: I-VI, 1-101.

Laveuf, C., Cornu, S., 2009. A review on the potentiality of rare earth elements to trace pedogenetic processes. Geoderma 154, 1 - 12.

Mange, M. A., Maurer, H. F. W., 1992. Heavy minerals in colour. Springer. 101 - 124.

Martini, E., 1971. Standard Tertiary and Quaternary calcareous nannoplankton zonation. In: Faranacci (Eds.), Proceedings of the Second Planktonic Conference Roma 1970, vol. 2. Edizioni Tecnoscienza, Rome, 739 - 785.

Mbede, E. I., 1991. The sedimentary basins of Tanzania - reviewed. Journal of African Earth Sciences 13 (3/4), 291 - 297.

McCabe, R., 2021. Geochemistry and stratigraphy of the Mesozoic and Cenozoic rocks encountered in the Mandawa Basin, south eastern Tanzania. Unpublished Ph.D. thesis. Trinity College Dublin.

McCabe, R., Rego, M. P., Warwick, D., Fitches, W., Lee, D. M., 2012. Chemostratigraphic characterisation of Mesozoic and Cenozoic successions: Ruvuma Basin, Tanzania. Poster presented at the East African Petroleum Conference and Exhibition, Arusha, Tanzania.

McCabe, R., Gómez-Pérez, I., Rawahi, H., Bergmann, K., Pearce, T., Dawans, J. M., 2018. Elemental Chemostratigraphy of the Late Neoproterozoic Sedimentary Successions in Oman. Oral Presentation given at the European Association of Geoscientists and Engineers 7th Arabian Plate Workshop, Muscat, Oman.

McCabe, R., Tansell, C., Roach, C., Moss, J., Gómez-Pérez, I., Baloushi, B, Thohli, B., Rawahi, H., 2019. Chemostratigraphy of Pre-Khuff sedimentary rocks encountered in the subsurface of Oman. Poster & oral presentation delivered at the American Association of Petroleum Geologists 3rd Siliciclastic Reservoirs of the Middle East Workshop, Muscat, Oman.

McLennan, S. M., 1989. Rare earth elements in sedimentary rocks: influence of provenance and sedimentary processes. In: Lipin, B. R., & McKay, G. A. (eds), Geochemistry and Mineralogy of Rare Earth Elements. Mineralogical Society of America 21, 169 - 200.

McLennan, S. M., Hemming, S., McDaniel, D. K., Hanson, G. N., 1993. Geochemical approaches to sedimentation, provenance and tectonics. Geological Society of America Special Paper 284, 21 - 40.

Miller, K. G., Kominz, M. A., Browning, J. V., Wright, J. D., Mountain, G, S., Katz, M., Sugarman. P. J., Cramer, B. S., Christie-Blick, N., Pekar, S. F., 2005. The Phanerozoic record of sea-level change. Science 310, 1293 - 1298.

Morton, A. C., Hallsworth, C. R., 1999. Processes controlling the composition of heavy mineral assemblages in sandstones. Sedimentary Geology 124, 3 - 29.

Morton, A. C., 2007. The role of heavy mineral analysis as a geosteering tool during drilling of high angle wells. In: Mange & Wright (Eds) Heavy Minerals in Use. Developments in Sedimentology 58**,** 1178.

Nederbragt, A. J., 1991. Late Cretaceous biostratigraphy and development of Heterohelicidae (planktic foraminifera). Micropaleontology 37, 329 - 372.

Nesbitt, H. W., Young, G. M., 1982. Early Proterozoic climates and plate motions inferred from major element chemistry of lutites. Nature 299, 715 – 717.

Nesbitt, H. W., Markovics, G., 1997. Weathering of granodioritic crust, long-term storage of elements in weathering profiles, and petrogenesis of silicate sediments. Geochemica et Cosmochemica Acta 61 (8), 1653 – 1670.

Nicholas, C. J., Pearson, P. N., Bown, P. R., Dunkley-Jones, T., Huber, B. T., Karega, A., Lees, J. A., McMillan, I. K., O'Halloran, A., Singano, J. M., Wade, B. S., 2006. Stratigraphy and sedimentology of the Upper Cretaceous to Paleogene Kilwa Group, southern coastal Tanzania. Journal of African Earth Sciences 45, 431 - 466.

Nicholas, C. J., Pearson, P. N., McMillan, I. K., Ditchfield, P. W., Singano, J. M., 2007. Structural evolution of southern coastal Tanzania since the Jurassic. Journal of African Earth Sciences 48, 273 - 297.

Pearce, T. J., McLean, D. J., Wray, D., Wright, D. K., Jeans, C. J., Mearns, E. W., 2005. Stratigraphy of the upper Carboniferous Schooner Formation, southern North Sea: chemostratigraphy, mineralogy, palynology and Sm-Nd isotope analysis. In: Collinson, J. D., Evans, D. J., Halliday, D. W., & Jones, N. S. (eds); Carboniferous Hydrocarbon Geology: the southern North Sea and surrounding onshore areas. Yorkshire Geological Society, Occasional Publications Series, 7,165 - 182.

Pearson, P. N., Ditchfield, P. W., Singano, J. M., Harcout-Brown, K. G., Nicholas, C. J., Olsson, R. K., Shackleton, N. J., Hall, M. A. 2001. Warm tropical sea surface temperatures in the late Cretaceous and Eocene epochs. Nature 413, 481 - 487.

Pearson, P. N., Nicholas, C. J., Singano, J. M., Bown, P. R., Coxall, H. K., Van Dongen, B. E., Huber, B. T., Karega, A., Lees, J. A., Msaky, E., Pancost, R. D., Pearson, M., Roberts, A. P., 2004. Paleogene and Cretaceous sediment cores from the Kilwa and Lindi areas of coastal Tanzania: Tanzania Drilling Project Sites 1-5. Journal of African Earth Sciences 39, 25 - 62.

Pearson, P. N., Nicholas, C. J., Singano, J. M., Bown, P. R., Coxall, H. K., Van Dongen, B. E., Huber, B. T., Karega, A., Lees, J. A., Macleod, K., McMillan, I. K., Pancost, R. D., Pearson, M., Msaky, E., 2006. Further Paleogene and Cretaceous sediment cores from the Kilwa area of coastal Tanzania: Tanzania Drilling Project Sites 6-10. Journal of African Earth Sciences 45, 279 - 317.

Pearson, P. N., Van Dongen, B. E., Nicholas, C. J., Pancost, R. D., Schouten, S., Singano, J. M., Wade, B. S., 2007. Stable warm tropical climate through the Eocene Epoch. Geological Society of America 35(3), 211 - 214.

Pearson, P. N., McMillan, I. K., Wade, B. S., Dunkley-Jones, T., Coxall, H. K., Bown, P. R., Lear, C. H., 2008. Extinction and environmental change across the Eocene-Oligocene boundary in Tanzania. Geology 36(2), 179 - 182.

Perch-Nielsen, K., 1985a. Cenozoic calcareous nannofossils. In: Bolli, H. M., Saunders, J. B., & Perch-Nielsen, K. (Eds.), Plankton stratigraphy. Cambridge University Press, 427 - 454.

Perch-Nielsen, K., 1985b. Mesozoic calcareous nannofossils. In: Bolli, H. M., Saunders, J. B., & Perch-Nielsen, K. (Eds.), Plankton stratigraphy. Cambridge University Press, 326 - 426.

Petrizzio, M. R., Falzoni, F., Premoli Silva, I., 2011. Identification of the base of the lower-to-middle Campanian Globotruncana ventricosa Zone: comments on reliability and global correlations. Cretaceous Research 32, 387 - 405.

Ratcliffe, K. T., Martin, J., Pearce, T. J., Hughes, A. D., Lawton, D. E., Wray, D. S., Bessa, F., 2006. A regional, chemostratigraphically-defined correlation framework for the late Triassic TAG-I Formation in Blocks 402 and 405a, Algeria. Petroleum Geoscience 12, 1 - 10.

Ratcliffe, K. T., Wright, A. M., Montgomery, P., Palfrey, A., Vonk, A., Vermeulen, J., Barrett, M., 2010. Application of chemostratigraphy to the Mungaroo Formation, the Gorgon Field, offshore northwest Australia. Australian Petroleum Production & Exploration Association, 371 - 388.

Ratcliffe, K. T., Wright, M., Spain, D., 2012. Unconventional methods for unconventional plays: using element data to understand shale resource plays. Petroleum Exploration Society of Australia News Resources. 89 - 93.

Robaszynski, F., Caron, M., 1979. Atlas de foraminifères planctoniques du Crétacé Moyen (mer Boréale et Téthys). Editions du Centre National de la Recherche Scientifique, Cahiers de Micropaléontologie 1, 185; 2, 181.

Robaszynski, F., Caron, M., 1995. Foraminifères planctoniques du Crétacé: commentaire de la zonation Europe-Méditerranée. Bulletin de la Société Géologique de France 166, 681 - 692.

Röhl, U., Westerhold, T., Bralower, T. J., Zachos, J. C., 2007. On the duration of the Paleocene-Eocene thermal maximum (PETM). Geochemistry, Geophysics, Geosystems 8 (12), 1 – 13.

Salman, G., Abdula, I., 1995. Development of the Mozambique and Ruvuma sedimentary basins, offshore Mozambique. Sedimentary Geology 96, 7 - 41.

Salminen, R., Batista, M. J., Bidovec, M., Demetriades, A., De Vivo, B., De Vos, W., Duris, M., Gilucis, A., Gregorauskiene, V., Halamic, J., Heitzmann, P., Lima, A., Jordan, G., Klaver, G., Klein, P., Lis, J., Locutra, J., Marsina, K., Mazreku, A., O'Connor, P. J., Olsson, S. Å., Ottesen, R. T., Petersell, V., Plant, J. A., Reeder, S., Salpeteur, I., Sandström, H., Siewers, U., Steenfelt, A., Tarvainen, T., 2005. Geochemical Atlas of Europe. Part 1: Background Information, Methodology and Maps. Espoo, Geological Survey of Finland.

Sano, J., Ratcliffe, K. T., Spain, D. R., 2013. Chemostratigraphy of the Haynesville Shale. In: Hammes, U. & Gale, J. (eds); Geology of the Haynesville Gas Shale in East Texas and West Louisianna, U.S.A. American Association of Petroleum Geologists Memoir 105, 137 – 154.

Šimiček, D., Bábek, O., Leichmann, J., 2012. Outcrop gamma-ray logging of siliciclastic turbidites: separating the detrital provenance signal from facies in the foreland-basin turbidites of the Moravo-Silesian Basin, Czech Republic. Sedimentary Geology 261 - 262, 50 - 64.

Sissingh, W., 1977. Biostratigraphy of Cretaceous calcareous nannoplankton. Geologie en Mijnbouw 56, 37 - 65.

Sissingh, W., 1978. Microfossils, biostratigraphy and stage - stratotypes of the Cretaceous. Geologie en Mijnbouw 57 (3), 433 - 440.

Sliter, W. V., 1989. Biostratigraphic zonation for Cretaceous planktonic foraminifers examined in thin section. Journal of Foraminiferal Research 19, 1 - 19.

Sluijs, A., Schouten, S., Donders, T. H., Schoon, P. L., Röhl, U., Reichart, G-J., Sangiorgi, F., Kim, J-H., Sinninghe Damasté, J. S., Brinkhuis, H., 2009. Warm and wet conditions in the Arctic region during the Eocene Thermal Maximum 2. Nature Geoscience 2, 770 – 780.

Stap, L., Lourens, L., Van Dijk, A., Schouten, S., Thomas, E., 2010. Coherent pattern and timing of the carbon isotope excursion and warming during Eocene Thermal Maximum 2 as recorded in planktic and benthic foraminifera. Geochemistry, Geophysics, Geosystems 11(11), 1 – 10.

Svensden, J., Friis, H., Stollofen, H., Hartley, N., 2007. Facies discrimination in a mixed fluvio-eolian setting using elemental whole-rock geochemistry – applications for reservoir characterisation. Journal of Sedimentary Research 77, 23 – 33.

Tansell, C., Moss, J., Gómez-Pérez, I., Thohli, B., McCabe, R., Fairey, B, 2021. Chemostratigraphy and provenance of the Amdeh Formation (Members I to III), northern Oman. Oral Presentation given at the European Association of Geoscientists and Engineers 4th Siliciclastic Reservoirs of the Middle East Workshop.

Taylor, S. R., McLennan, S. M., 1985. The continental crust: its composition and evolution. Blackwell Scientific Publication.

Van Der Weijden, C. H., 2002. Pitfalls of normalisation of marine geochemical data using a

common divisor. Marine Geology 184, 167 - 187.

Wilson, M. J., 2004. Weathering of the primary rock-forming minerals: processes, products and rates. Clay Minerals 39, 233 - 266.

Zachos, J. C., Dickens, G. R., Zeebe, R. E., 2008. An early Cenozoic perspective on greenhouse warming and carbon-cycle dynamics. Nature 451 (17), 279 - 283.

FIGURES

Figure 1: Location of the TDP sites in the Mandawa Basin and offshore exploration wells examined in this paper (Geological map modified from McCabe, 2021, Fig. 4.1)**.**

Figure 2: Chronostratigraphy of logged TDP boreholes (modified from Berrocoso *et al.,* 2015, Fig 3. and Nicholas *et al.,* 2006, Fig. 5).

Figure 3: The Kilwa Group Composite section and deepwater study wells examined in this paper.

Figure 4: Comparison of major element and mineral data for selected TDP core samples.

Figure 5: EV1 and EV2 calculated from PCA of the claystone dataset.

Figure 6: Sequence-level chemostratigraphic correlation of the study sections.

Figure 7: Package and unit-level chemostratigraphic correlation of the study sections.

Figure 8: Mineralogy of the Kilwa Group rocks, including mineral ratios & indices supporting the geological interpretations.

Figure 9: Chondrite-normalised REE plots for each of the chemostratigraphic zones recognised in this study.

Figure 10: Comparison of the Si/Al ratio with the global sea level curve (modified from Miller *et al.,* 2005, Fig. 3).

Figure 11: Geochemical evidence for climatic and hydrological variations in Tanzania during the Late Paleocene and Early Eocene.

Figure 12: Comparison of the elemental ratios with the δ18O curve in TDP-12 and TDP-17.

Figure 13: Lithostratigraphic correlation of the study sections.

Figure 14: Comparison of the chemostratigraphic and lithostratigraphic schemes of the Kilwa Group, plus proposed revisions to the onshore stratigraphy.

Figure 15: Comparison of the $CaCO_3$ curve with the geochemical parameters employed to define the Lindi and Nangurukuru Formations in this study.

APPENDIX 1: SAMPLE PREPARATION & ANALYTICAL PROTOCOLS FOR ICP-OES & -MS

All samples have been analysed by inductively-coupled plasma - optical emission spectroscopy (ICP-OES) and inductively-coupled plasma - mass spectrometry (ICP-MS) at the laboratories of Origin Analytical (UK). Approximately 5g of material per core sample was ground in an agate mortar, with the resultant homogenised powder being used for both ICP-OES and -MS analysis. The powders were dried in an oven at 60ºC for 5 minutes to drive off any internal moisture. For the cutting samples, approximately 1-2g of a single lithology, interpreted from supplied lithological information as representing the *in situ* subsurface rock, was isolated under a binocular microscope and powdered by pestle and mortar.

The powdered samples were prepared by applying an alkali fusion procedure similar to that described by Jarvis & Jarvis (1992a & b). The procedure involves fusing 0.25g of sample with 1.25g of $LiBO_2$ flux in a carbon crucible at 1050ºC for 15 minutes. The mixture was then immediately transferred into beakers containing 120ml of 3.5%v/v of HNO_3. The solution was converted to an aerosol and introduced to the ICP instruments for analysis. For ICP-OES analysis, the samples were run on a Thermo ICAP 6500 instrument. For ICP-MS analysis, samples were run on a Thermo XSeries 2 instrument. Both instruments are calibrated using internal rock standards and certified reference materials (CRMS: samples of a known chemical composition) are run in line with the geological material at 20 sample intervals, allowing for instrumental anomalies and analytical drift to be corrected.

APPENDIX 2: SAMPLE PREPARATION & ANALYTICAL PROTOCOLS FOR WR- & CF-XRD

Sample preparation and XRD analysis were conducted by X-Ray Minerals Ltd in the UK. The preparation procedure for WR analysis involved micronising 2g of powdered rock in ethanol using a McCrone Micronising Mill to obtain a powder with a mean particle diameter of between 5µm and 10µm. The slurry was dried overnight at 80°C, re-crushed to a fine powder and back-packed into a steel sample holder, producing a randomly orientated sample for presentation to the X-ray beam. Whole-rock samples were scanned on a PANalytical X'Pert 3 diffractometer using a CuKα radiation source at 40 kV and 40 mA. Whole-rock

samples were scanned from 4.5 to 75° (2θ) at a step size of 0.013 and nominal time per step of 0.2 s (continuous scanning mode).

The preparation procedure for CF analysis involved taking a 5g split of the sample that was disaggregated at the WR stage of preparation and separating the <2 μm fraction by centrifuge. The CF XRD mount is obtained by filtering the clay suspension through a Millipore glass micro-fibre filter and drying the filtrate on the filter paper. The samples were analysed as an untreated clay, after saturation with ethylene glycol vapour overnight and following heating at 380°C for 2 hours, with a further heating to 550°C for one hour. Clay filters were scanned on a Philips PW1730 Generator using a using X-ray radiation from a copper anode at 40kV, 40mA. Clay filters were scanned from 3 to 35° (2θ) at a step size of 0.05° and 2 s step time.

Identification of unknown minerals was achieved by using Traces (v.6) by GBC Scientific Equipment and HighScore Plus (v.4) by PANalytical software. Quantitative phase analysis on whole rock samples used the Rietveld method with BGMN AutoQuan software.

APPENDIX 3: SAMPLE PREPARATION & ANALYTICAL PROTOCOLS FOR CLAYSTONE HMA USING RAMAN SPECTROSCOPY

The heavy minerals were separated from the core samples at Origin Analytical UK and analysed at the University of Greenwich, UK. The rock was carefully disaggregated and the heavy minerals were separated from the light minerals in a lithium heteropolytungstate solution (LST Fastfloat, 2.89 g/cm3) using the funnel separation technique (e.g., Mange and Maurer, 1992). A wide grain size window (10μm to 250μm) was employed to acquire the entire heavy mineral assemblage from each sample. The heavy mineral grains were loosely scattered on a petrographic slide and analysed using a Horiba LabRam Raman microscope equipped with a 532nm green laser.

Between 133 and 1103 transparent heavy mineral grains were analysed per sample. The Raman spectra acquired were compared to a reference database of heavy mineral spectra to identify their mineralogy.

Figure 1

Click here to access/download;Figure;Figure 1 - 2 Column Image.pdf

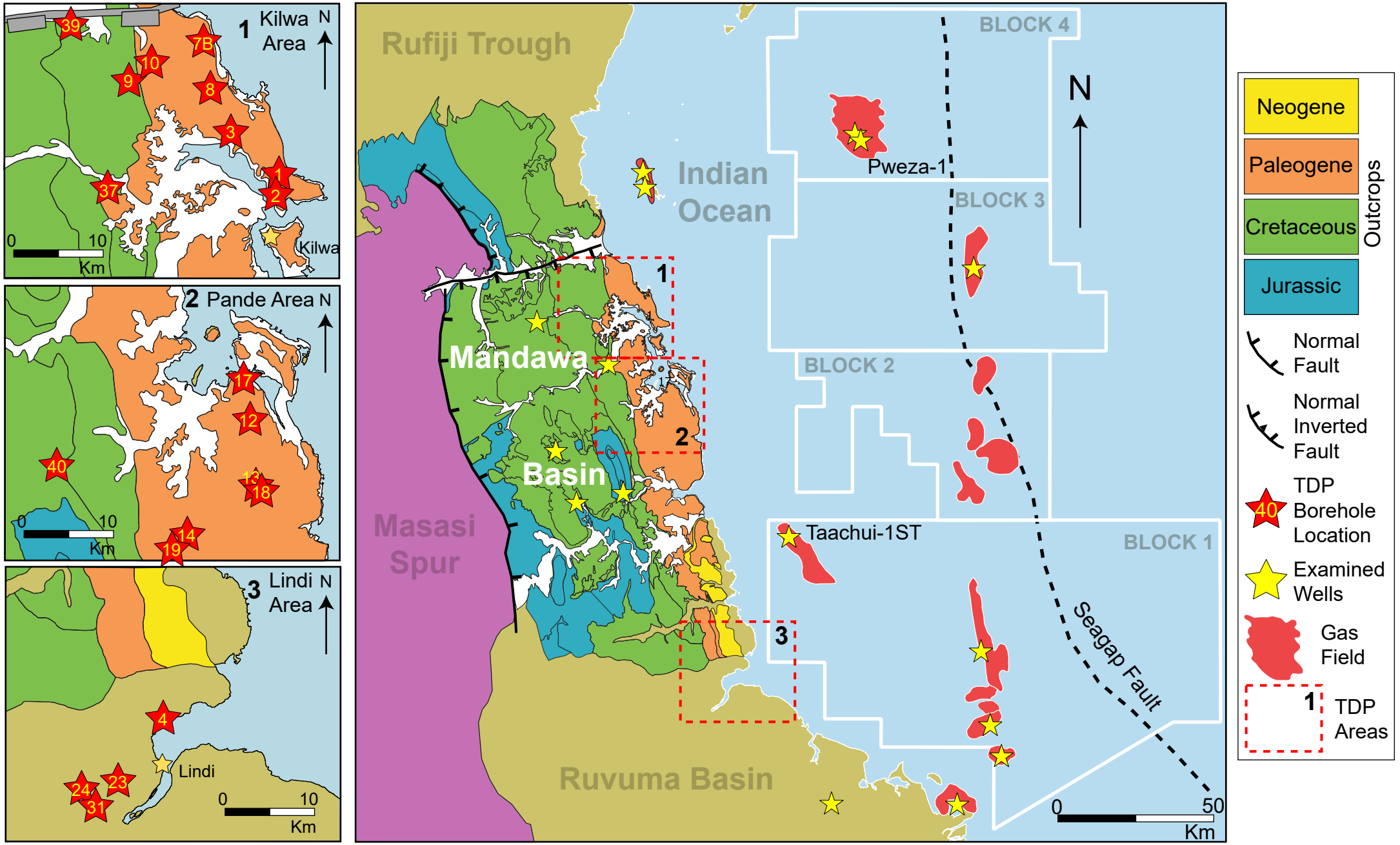

Figure 2

Click here to access/download;Figure;Figure 2 - 2 Column Image.pdf

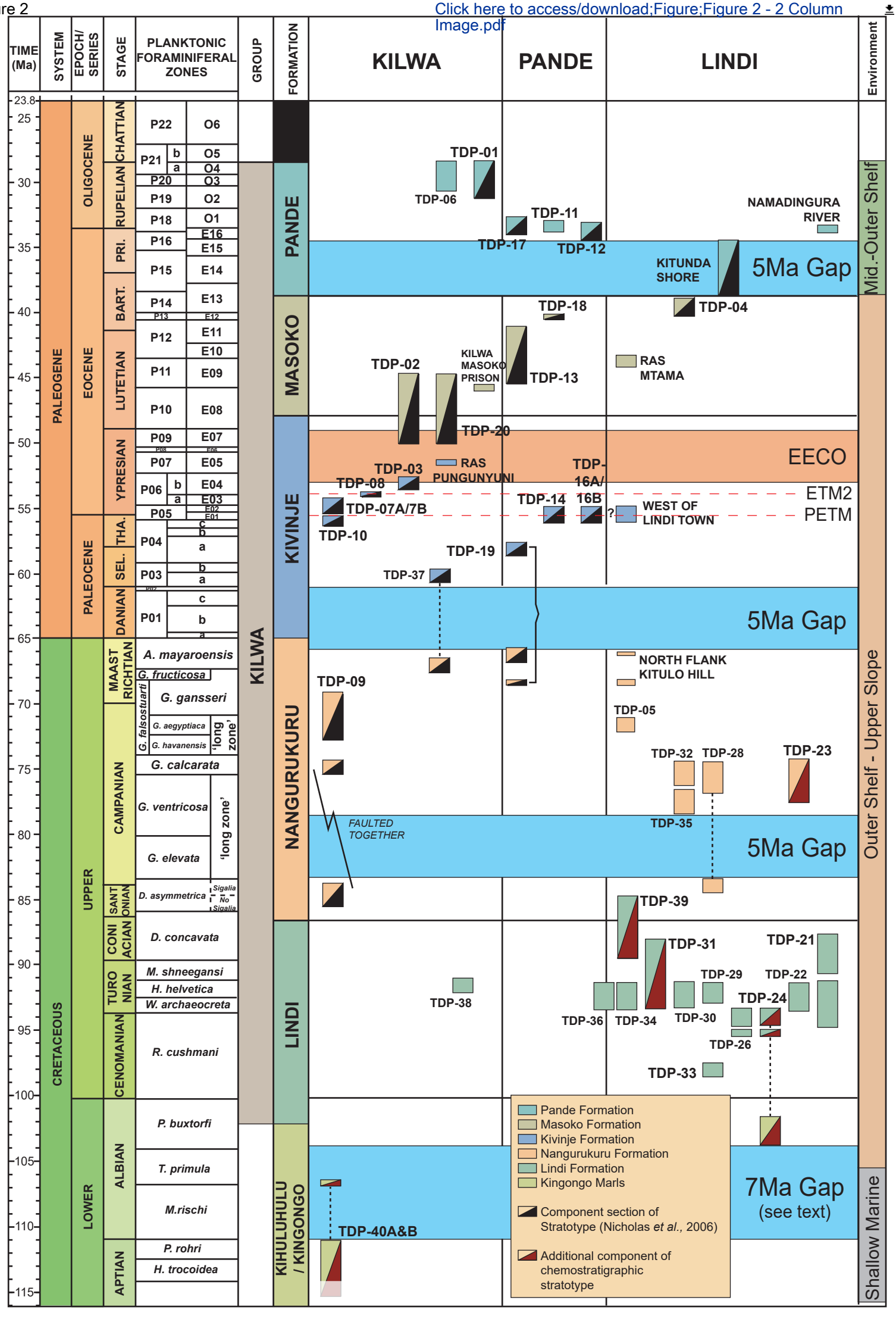

Figure 3

Click here to access/download;Figure;Figure 3 - 2 Column Image.pdf

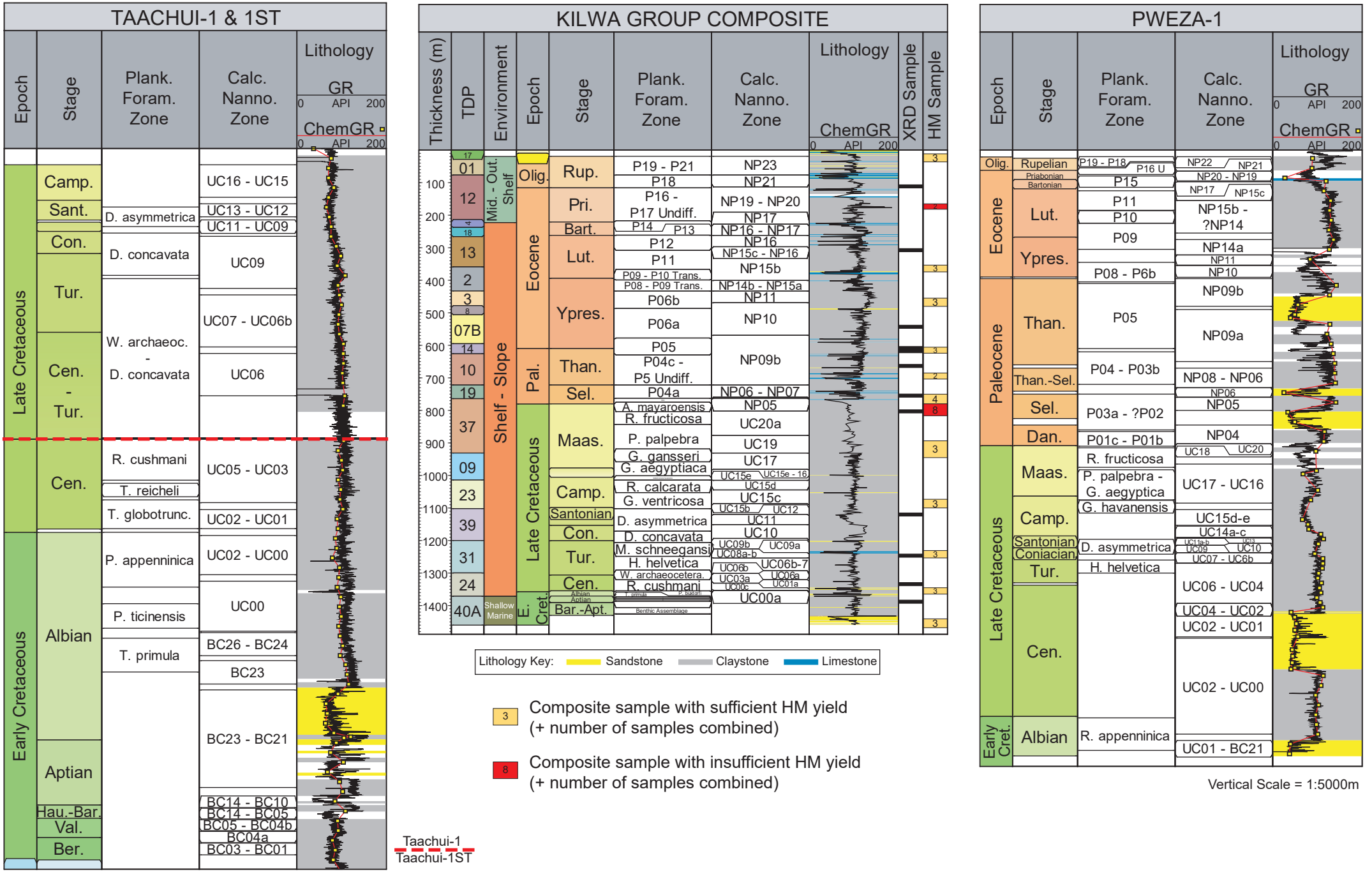

Figure 4

Click here to access/download;Figure;Figure 4 - 2 Column Image.pdf

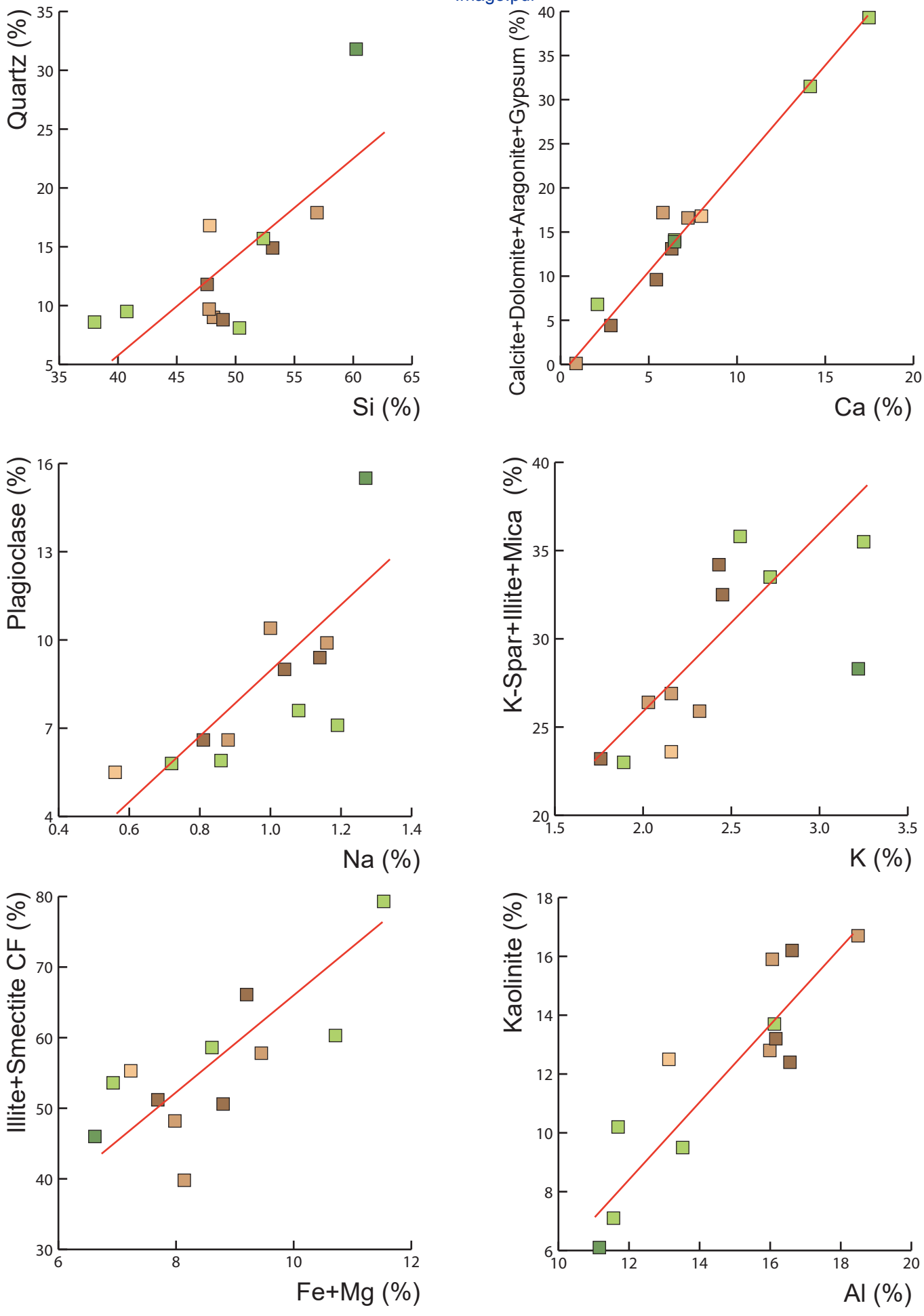

Figure 5

Click here to access/download;Figure;Figure 5 - 1 Column Image.pdf

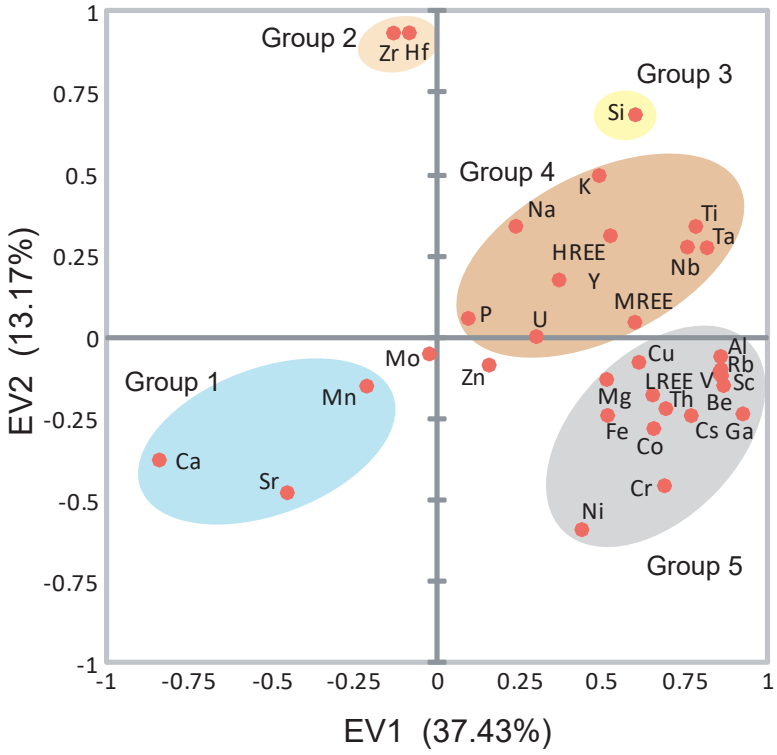

Figure 6

Click here to access/download;Figure;Figure 6 - 2 Column Image.pdf

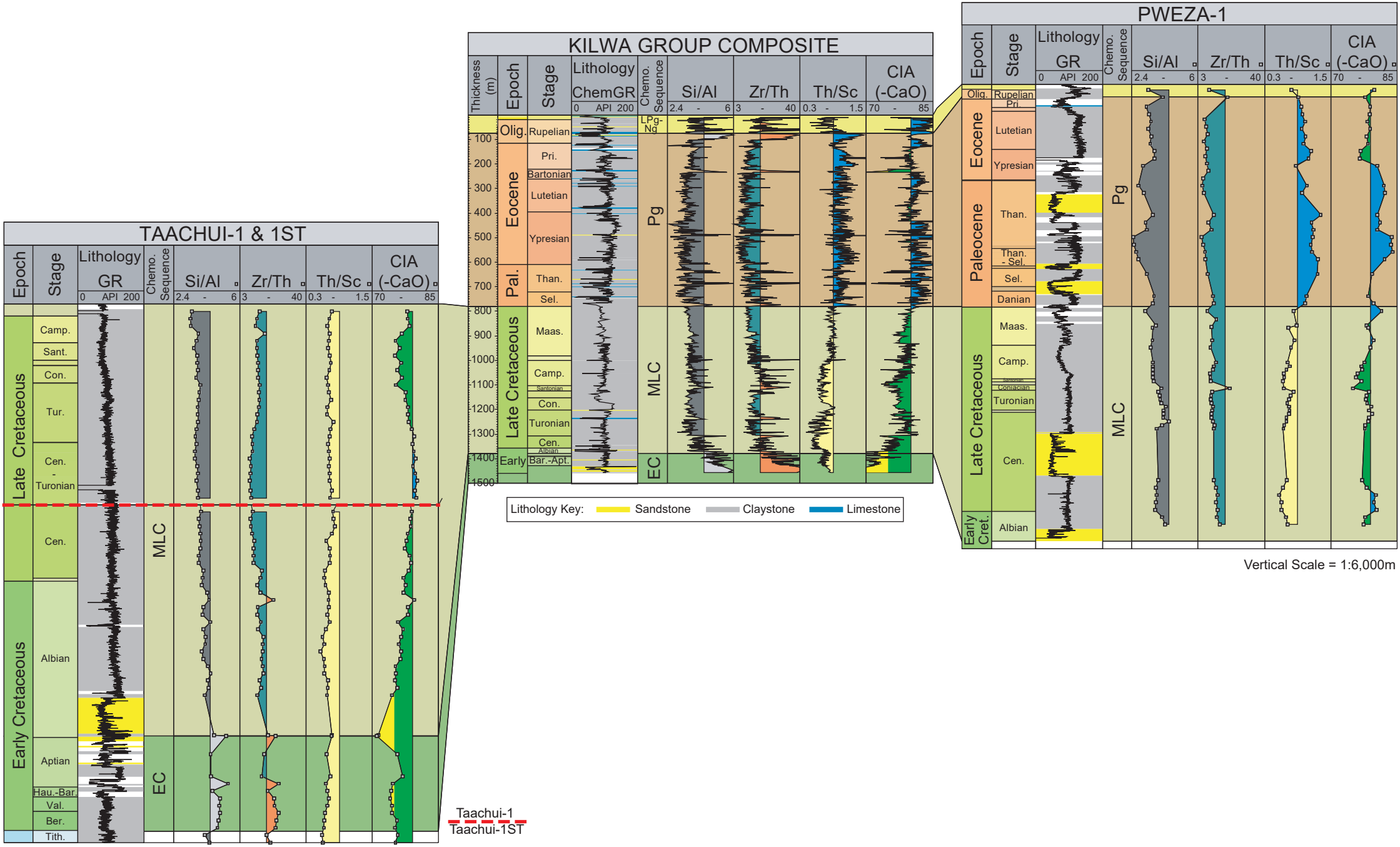

Figure 7

Click here to access/download;Figure;Figure 7 - 2 Column Image.pdf

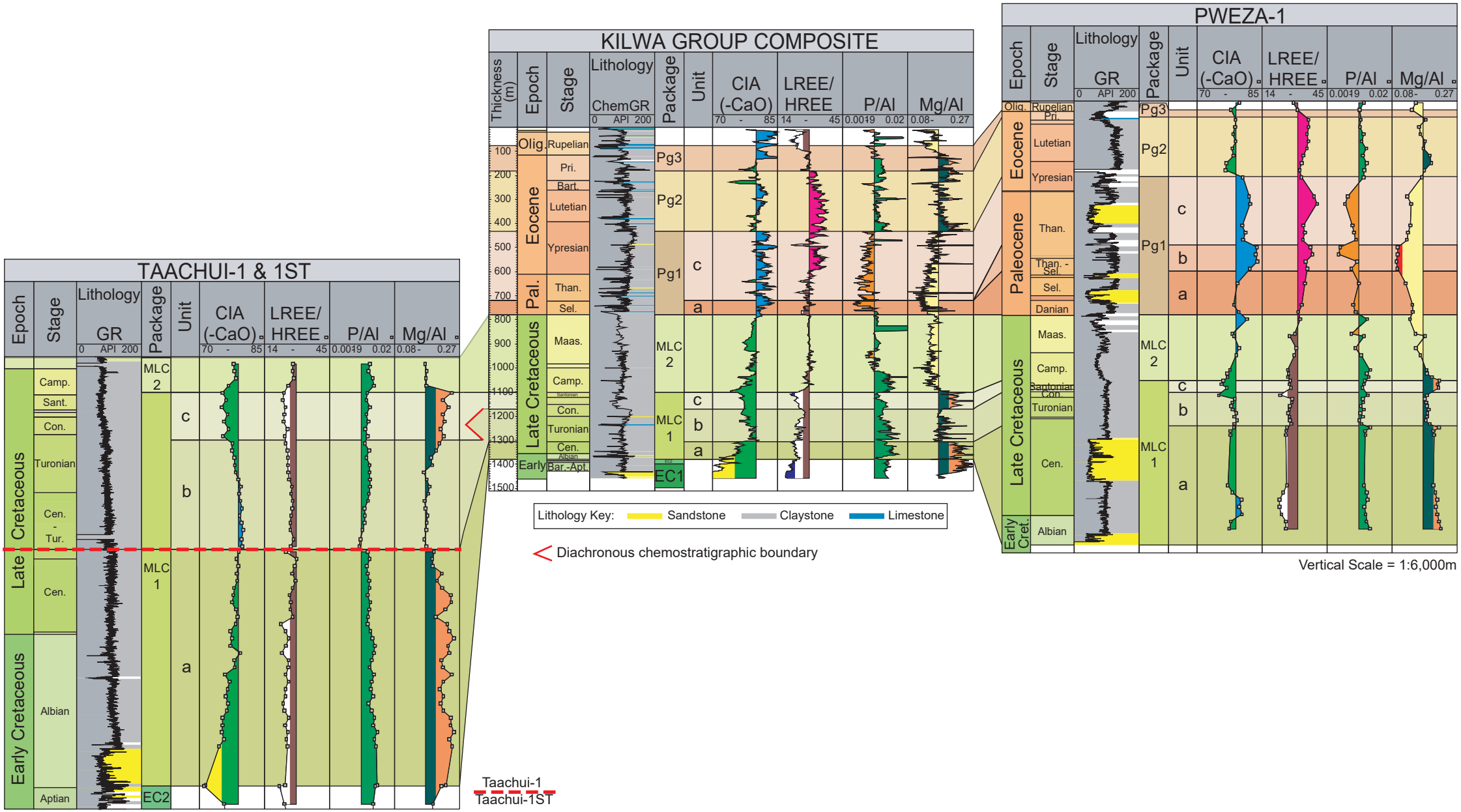

Figure 8

Click here to access/download;Figure;Figure 8 - 2 Column Image.pdf

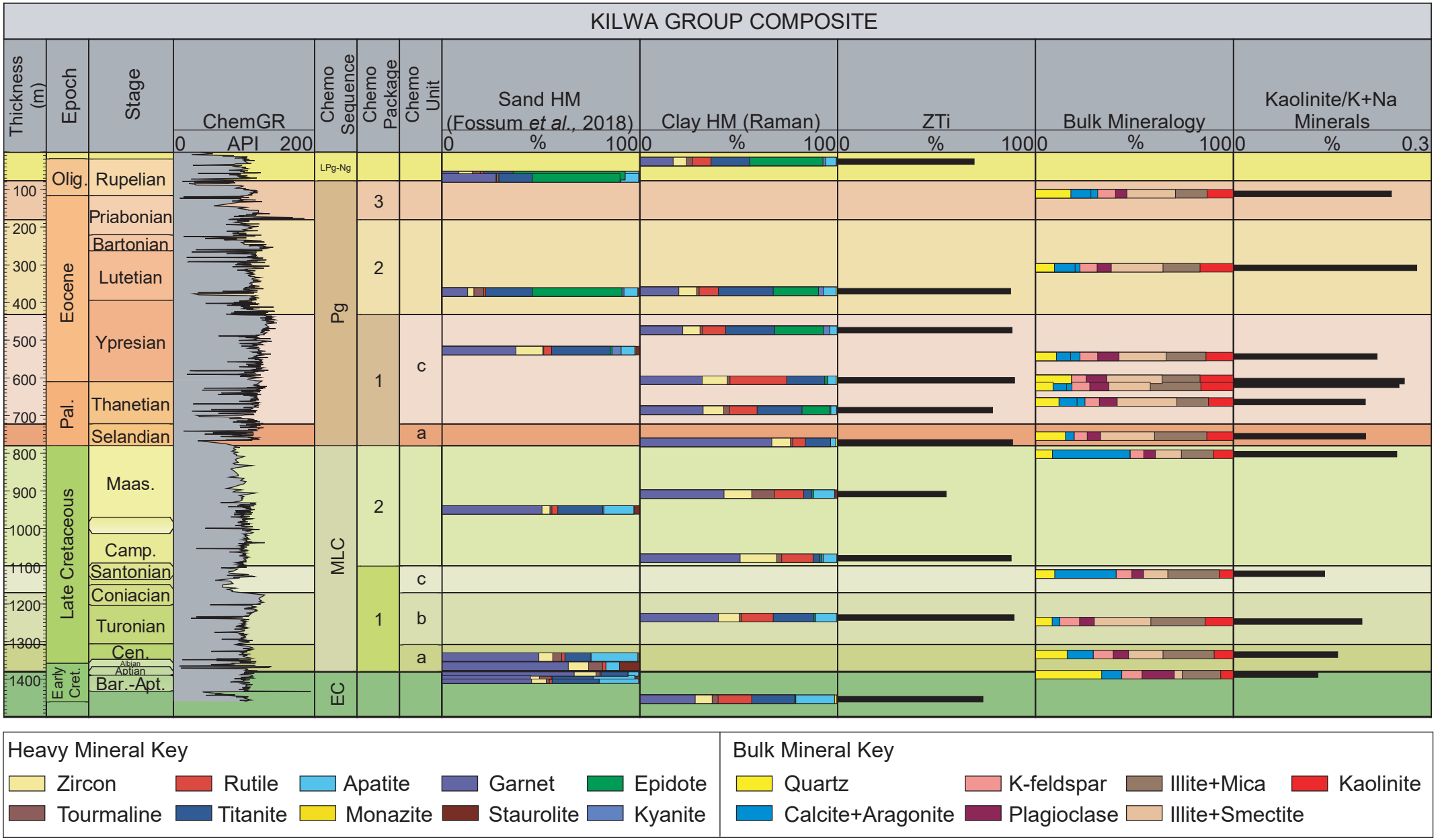

Figure 9

Click here to access/download;Figure;Figure 9 - 2 Column Image.pdf

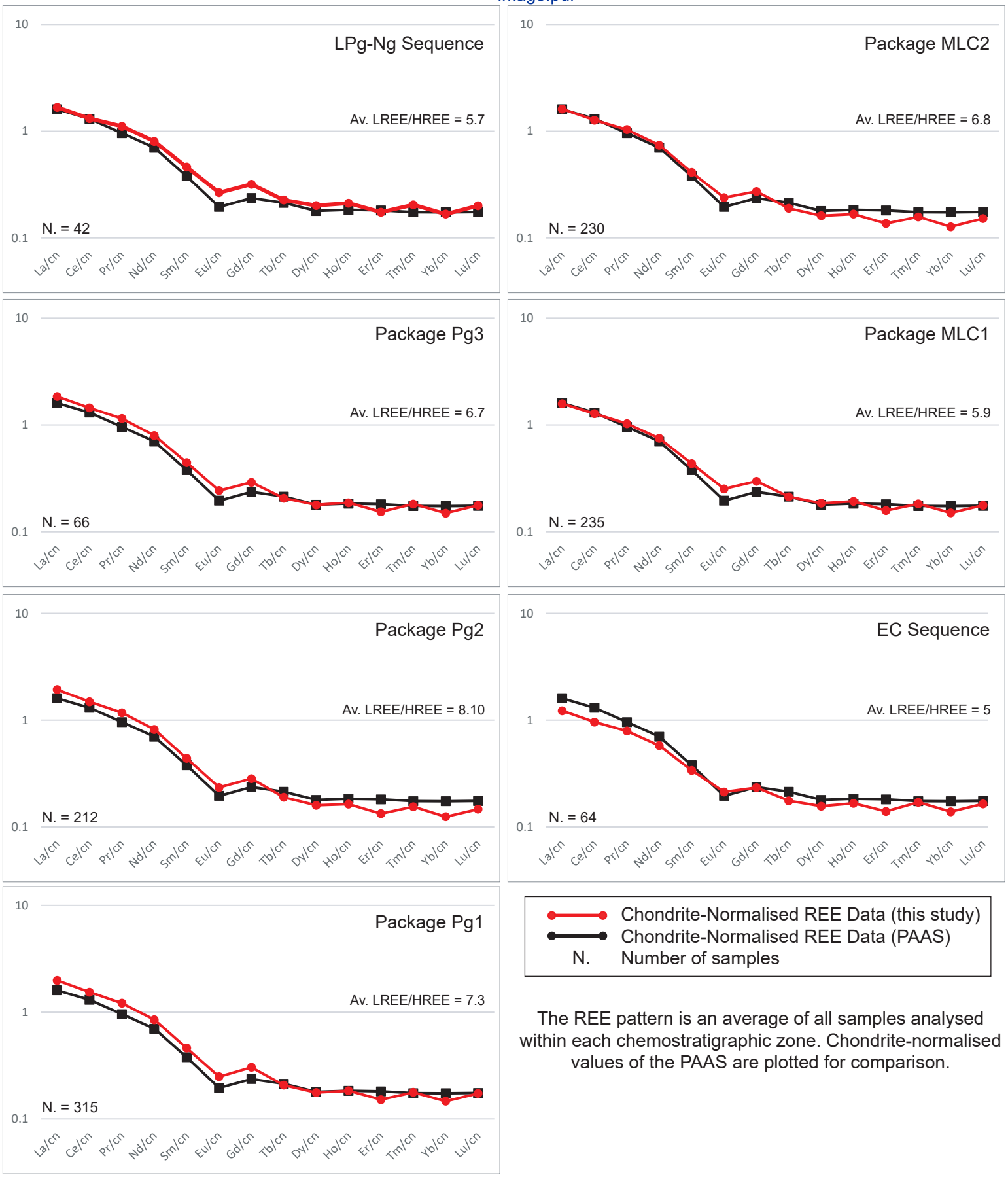

The REE pattern is an average of all samples analysed within each chemostratigraphic zone. Chondrite-normalised values of the PAAS are plotted for comparison.

Figure 10

Click here to access/download;Figure;Figure 10 - 2 Column Image.pdf

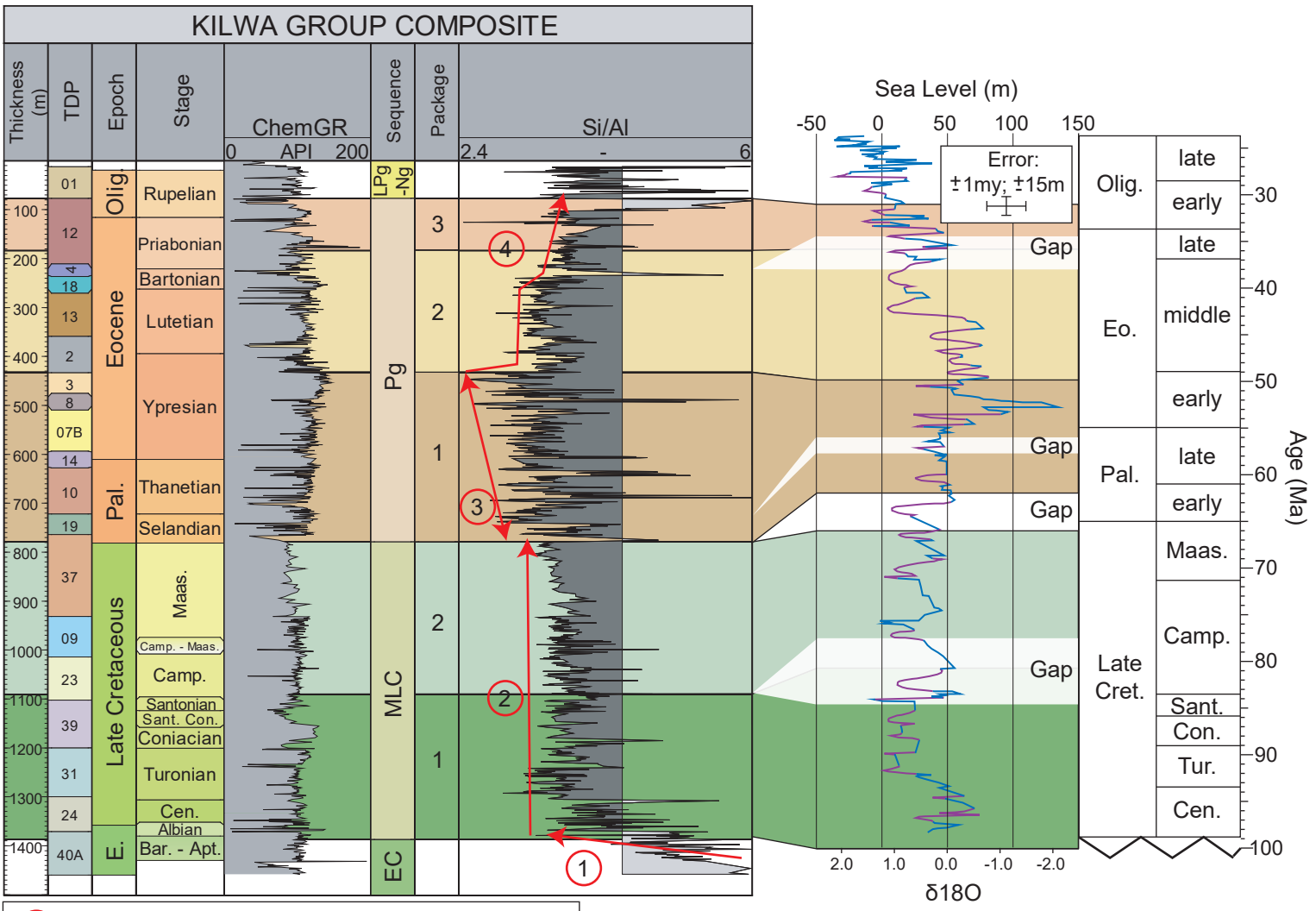

1 High-energy shallow marine claystones

2 Marine transgression

3 Lowest energy distal marine claystones

4 Stepped regression (gradual increase in energy)

Global sea-level derived from backstripped data

Global sea-level derived from δ18O data

Global sea level curve modified from Miller et al. (2005)

Gap = uncored stratigraphy

Figure 11

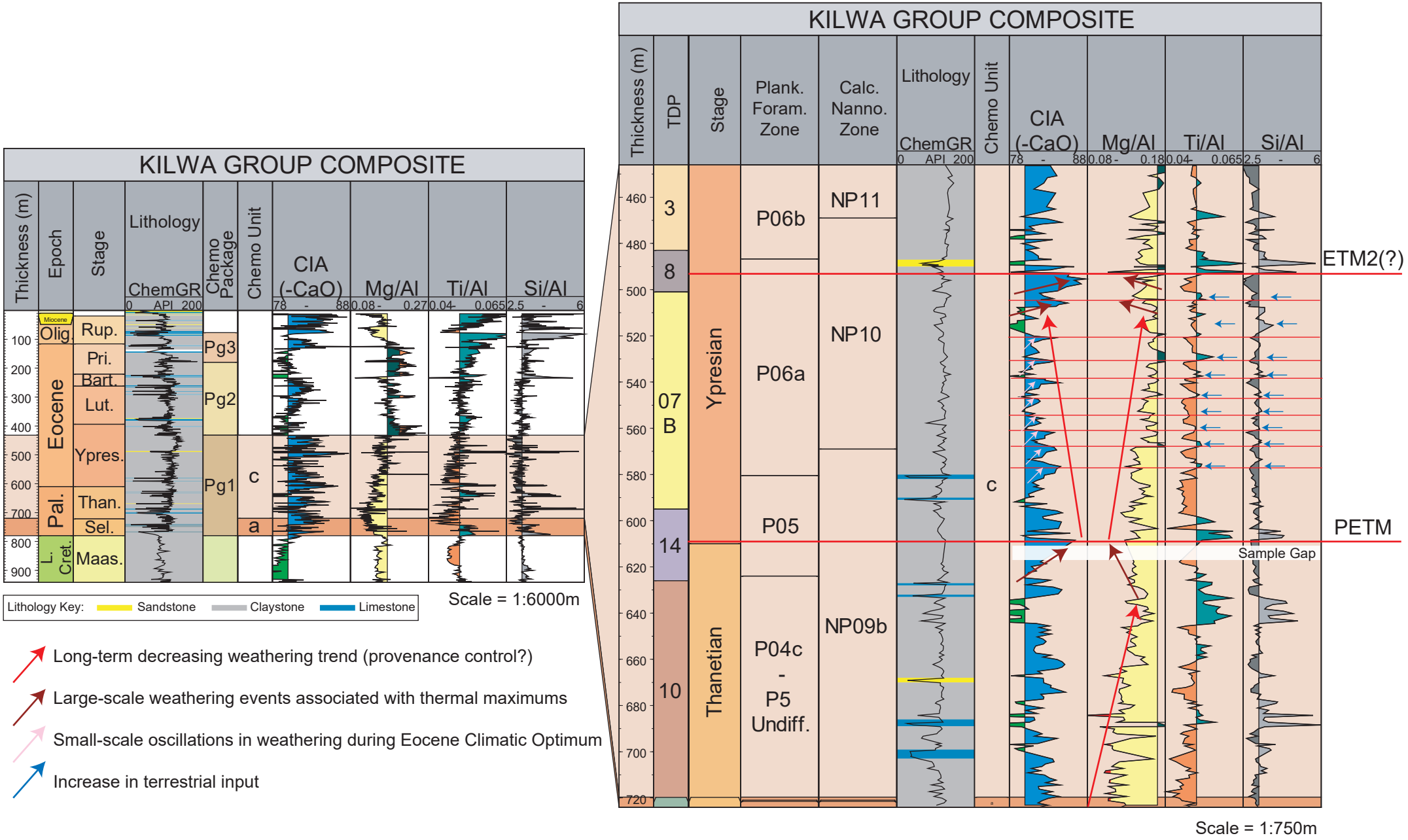

Figure 12

Click here to access/download;Figure;Figure 12 - 2 Column Image.pdf

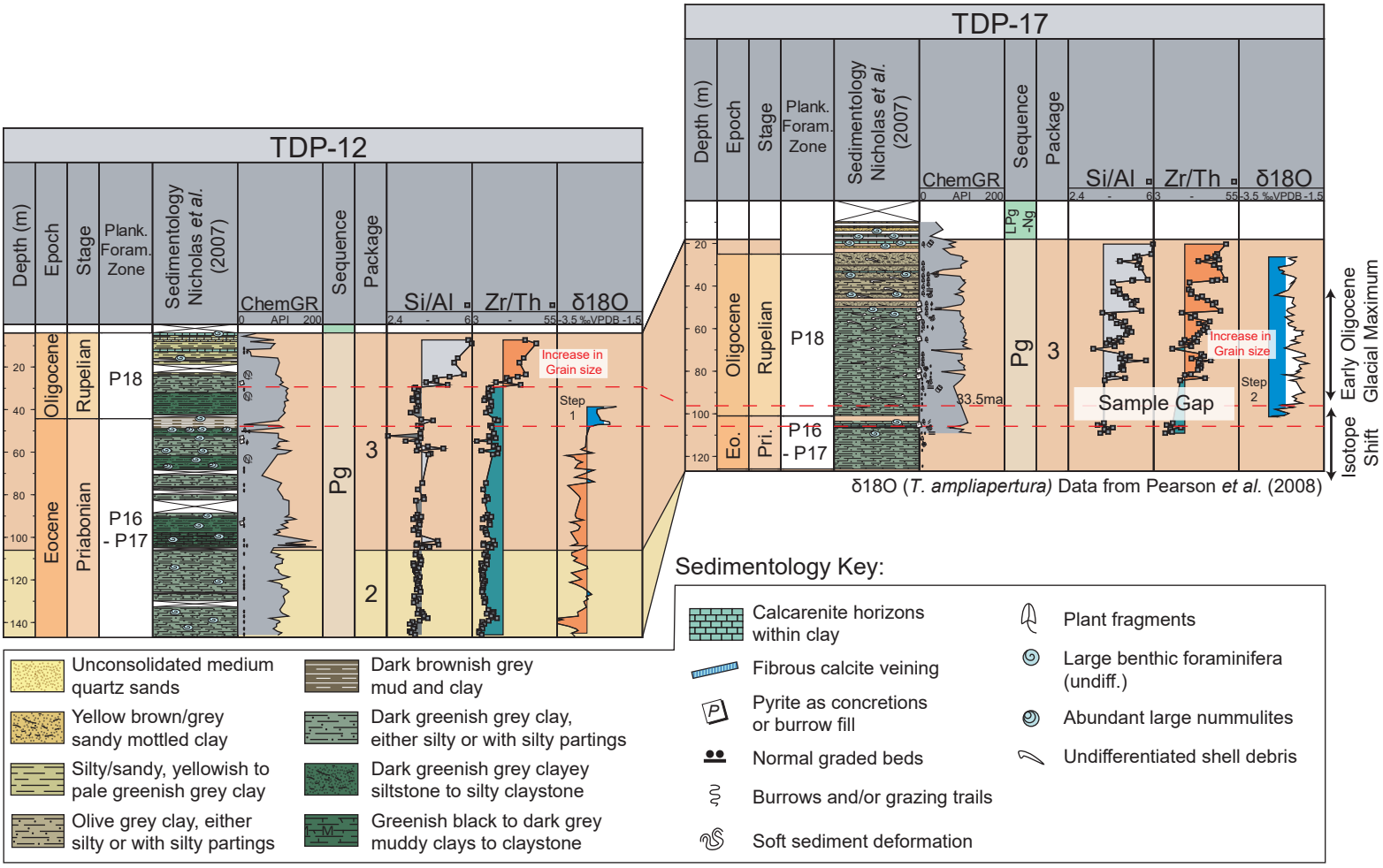

Figure 13

Click here to access/download;Figure;Figure 13 - 2 Column Image.pdf

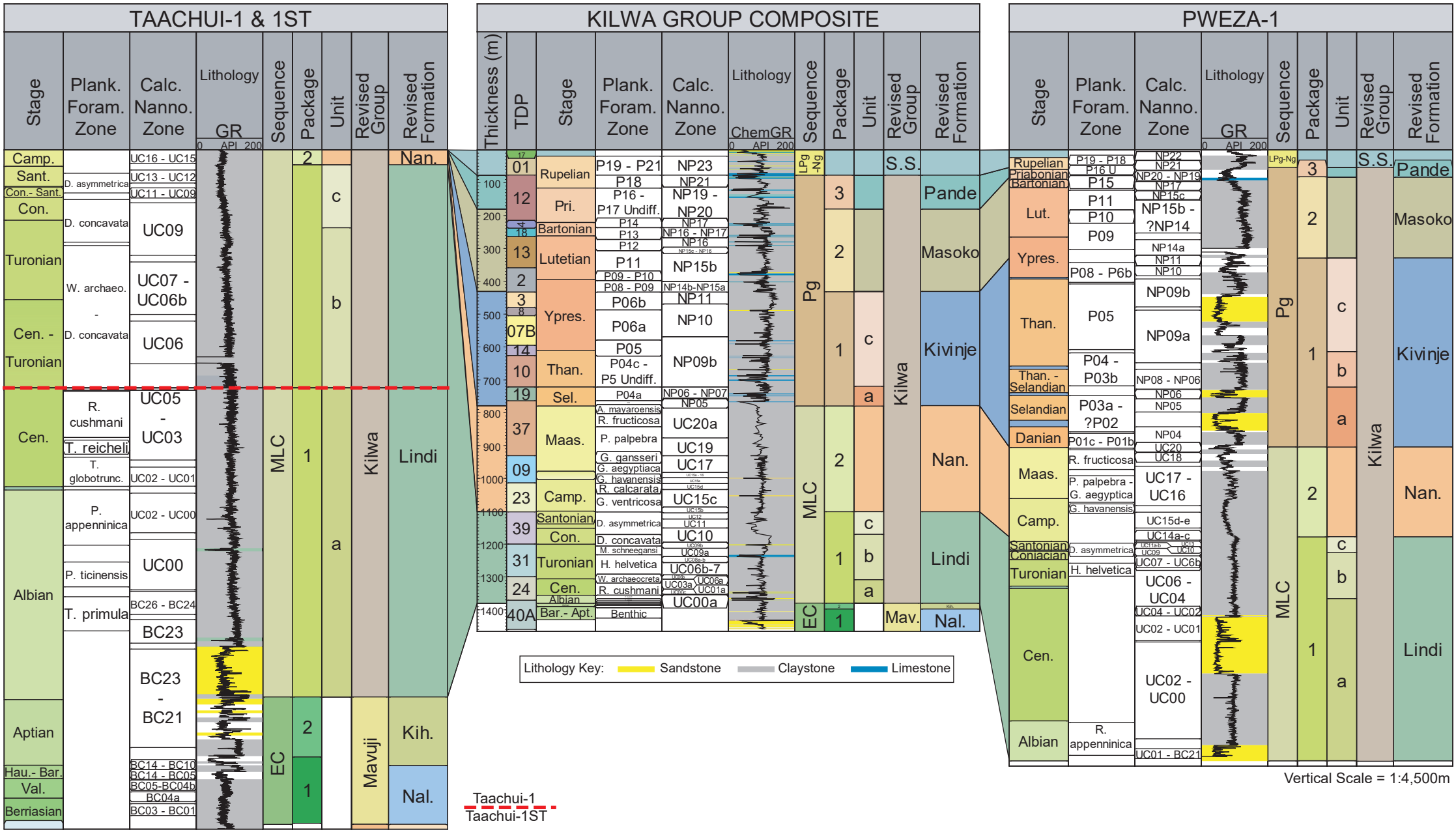

Figure 14

Click here to access/download;Figure;Figure 14 - 2 Column Image.pdf

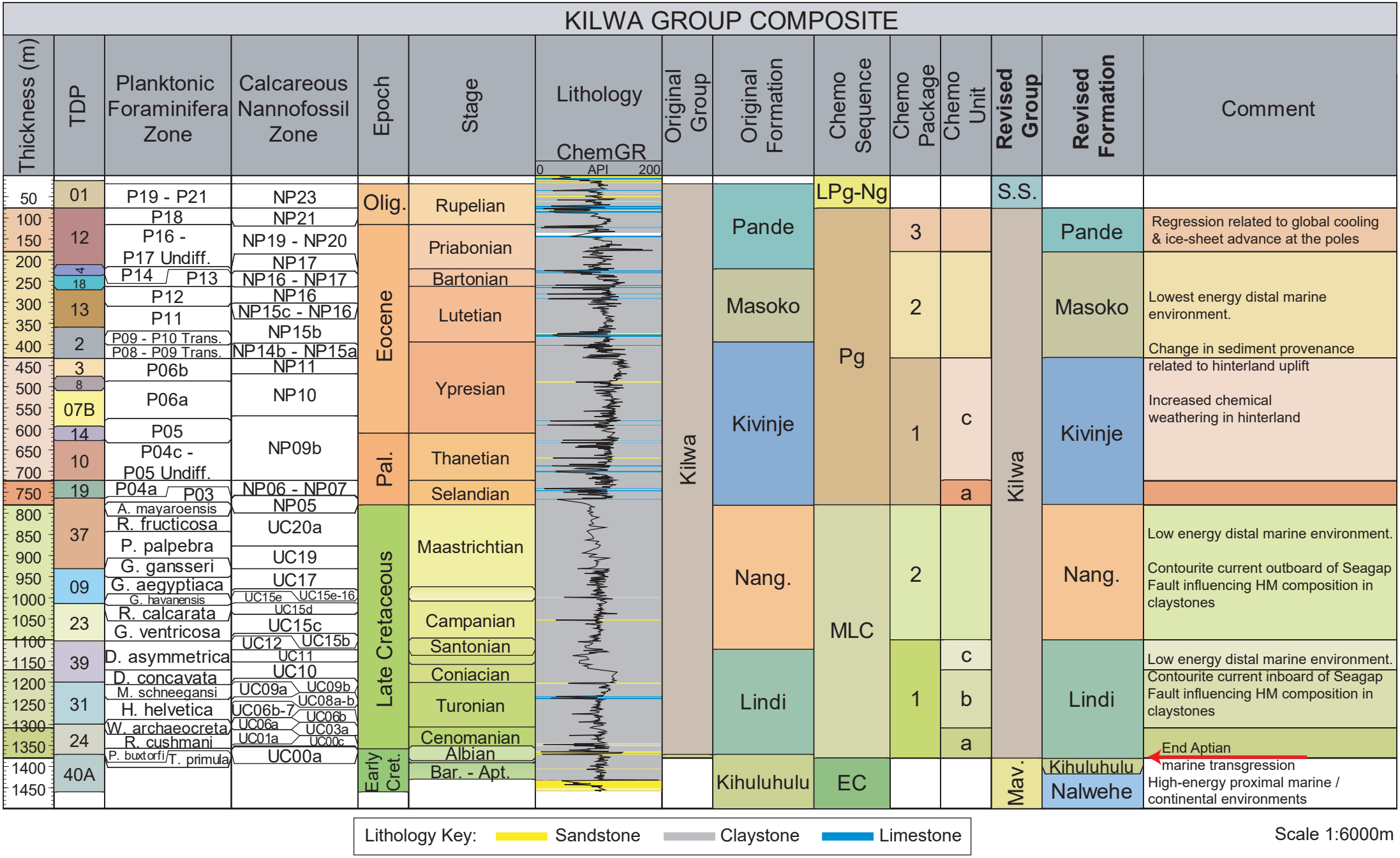

Figure 15

Click here to access/download;Figure;Figure 15 - 2 Column Image.pdf

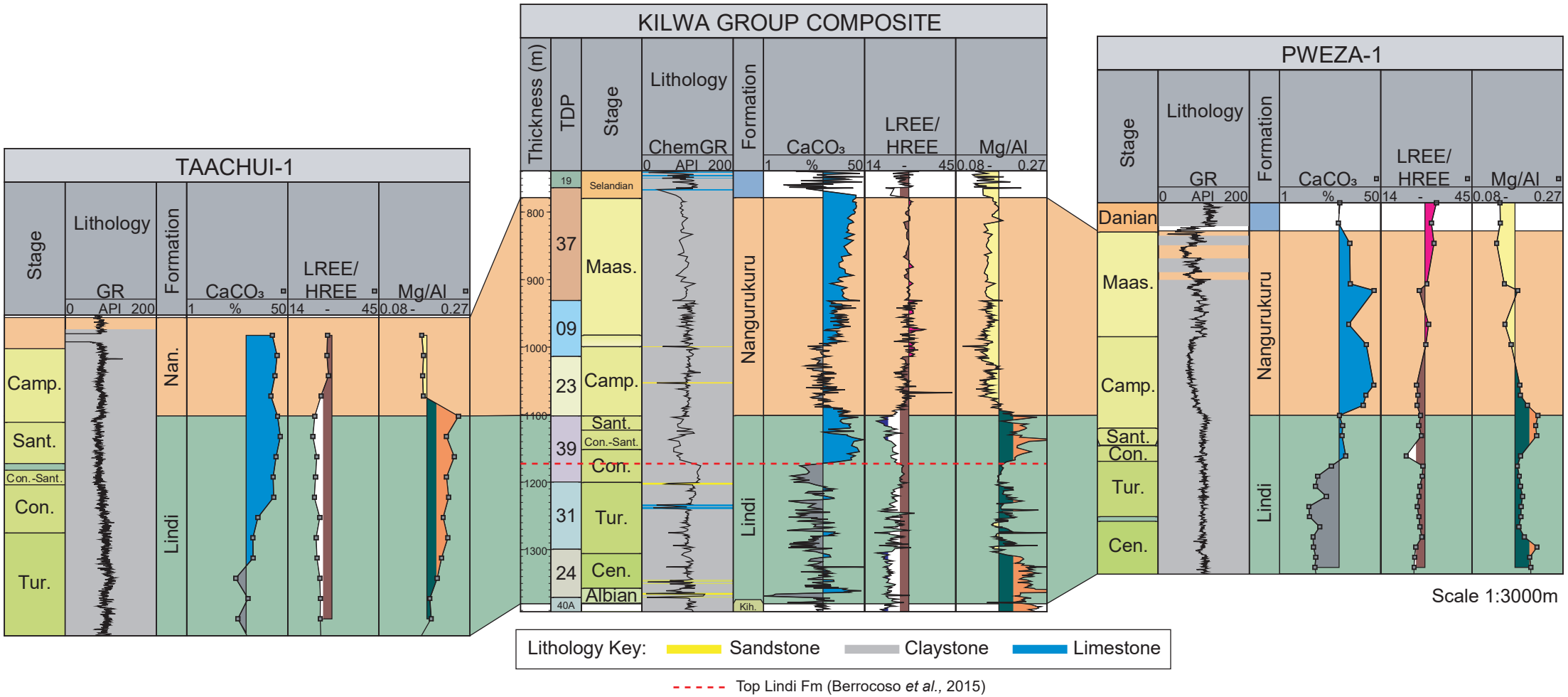

Title page

Chemostratigraphic and Mineralogical Examination of the Kilwa Group Claystones, Coastal Tanzania: An Alternative Approach to Refine the Lithostratigraphy

Ross McCabe, Christopher J. Nicholas, Bill Fitches, David Wray & Tim Pearce.

Declaration of interests

☒ The authors declare that they have no known competing financial interests or personal relationships that could have appeared to influence the work reported in this paper.

☐The authors declare the following financial interests/personal relationships which may be considered as potential competing interests: